sciendo

DOI: 10.2478/ata-2020-0001

Acta Technologica Agriculturae 1/2020 *Jana Galambošová et al.*

Acta Technologica Agriculturae 1
Nitra, Slovaca Universitas Agriculturae Nitriae, 2020, pp. 1–6

DETERMINING TRAFFICKED AREAS USING SOIL ELECTRICAL CONDUCTIVITY – A PILOT STUDY

Jana GALAMBOŠOVÁ[1]*, Miroslav MACÁK[1], Vladimír RATAJ[1], Marek BARÁT[1], Paula MISIEWICZ[2]

[1]Slovak University of Agriculture in Nitra, Slovak Republic
[2]Harper Adams University, United Kingdom

Increase in machinery size and its random traffic at fields cause soil compaction resulting in damage of soil structure and degradation of soil functions. Nowadays, rapid methods to detect soil compaction at fields are of high interest, especially proximal sensing methods such as electrical conductivity measurements. The aim of this work was to investigate whether electromagnetic induction (EMI) could be used to determine trafficked areas in silty clay soil. Results of randomized block experiment showed a high significant difference (p <0.01) in EMI data measured between compacted and non-compacted areas. EMI readings from compacted areas were, on average, 11% (shallow range) and 9% (deep range) higher than non-compacted areas, respectively. This difference was determined in both shallow and deep measuring ranges, indicating that the difference in soil compaction was detected in both topsoil and subsoil. Furthermore, the data was found to have a significant spatial variability, suggesting that, in order to detect the increase in EMI (which shows the increase in soil compaction), data within close surrounding area should be included in the analyses. Correlation coefficient of EMI and penetration resistance (average moisture content 32.5% and 30.8% for topsoil and subsoil) was found to be 0.66.

Keywords: EMI; CTF; proximal sensing; soil compaction

Soil compaction caused by vehicular traffic adversely affects the key soil functions and ecosystem services that soils provide (Keller et al., 2019). It has been shown that an increase in stress levels with higher bulk density and mechanical penetration resistance, and a decrease in soil hydraulic conductivity resulted in decreased root elongation rates and consequently prolonged the time required for roots to reach a certain soil depth. Soil compaction caused by machinery traffic needs to be: (a) either removed by costly subsoiling; or (b) avoided by implementation of technologies, such as wide span gantry technologies (Chamen, 2015; Bulgakov et al., 2018). Recently, controlled traffic farming (CTF) and its modifications show potential benefits worldwide (Godwin et al., 2015; Chamen, 2015; Gutu et al., 2015; Galambošová et al., 2017; Latsch and Anken, 2019; Antille et al., 2019; Masola et al., 2020). In order to conduct the aforementioned management steps, areas which were exposed to traffic should be spatially targeted. As soil compaction is defined as a change in the soil density, the most exact estimate can be obtained by measuring the soil density (Rataj et al., 2014). However, for practical reasons, traditional methods that rely on undisturbed soil samples are progressively being replaced by methods of proximal sensing. Proximal sensing comprises rapid methods, which enable measuring soil properties and producing soil maps with high resolution (Gebbers, 2019). Gebbers (2019) concluded that penetrometers and draft force sensors can be used for this purpose as direct methods. In terms of indirect methods, measuring the electrical conductivity of soil (ECa) has been employed in soil mapping recently. This is measured by two methods, galvanic couple electric resistivity (GCER) and electromagnetic induction (EMI). Heil and Schmidhalter (2017) reviewed the applications of ECa and concluded that not many studies have been conducted on determining the soil compaction using ECa. However, several studies (Krajčo, 2007; Alaoui and Diserens, 2018; Romero-Ruiz et al., 2019) show the potential of soil compaction targeting at field. So far, the most complex study was published by Krajčo (2007), who compared the Conductometer (GCEM) and the EMI measurement with favourable results for the former. On the basis of presented data, this latter study claims that the EMI was less sensitive in terms of distinguishing the compacted areas above 0.3 m.

Based on this, it is clear that there is still a lack of evidence in terms of direct assessment of this methods for targeting field trafficked/compacted areas. On the contrary, there is a need to examine these problems as current trends in precision agriculture are aimed at using soil proximal sensing, e.g. use of Topsoil Mapper (Geoprospectors GmbH, Austria). Furthermore, there are attempts to use such data for online variable tillage treatment. Therefore, the aim of this work was to examine the ability of soil electrical conductivity to detect soil compaction caused by field traffic using electromagnetic induction measurements.

Contact address: Jana Galambošová, Slovak University of Agriculture in Nitra, Faculty of Engineering, Tr. Andreja Hlinku 2, 949 76, Nitra, Slovak Republic, e-mail: jana.galambosova@uniag.sk

Material and methods

As soil proximal sensing method, the apparent electrical conductivity (ECa) of the soil was measured by a non-contact method using the electromagnetic induction (EMI) with an EM38-MK2 device (Geonics Limited, Canada). When using EMI, the transmitter coil creates primary magnetic field in the soil, which reacts by establishing a secondary field. The superposition of these two fields results in a bulk magnetic field, which is measured using a receiver coil (Gebbers, 2019). The EM38-MK2 device was used in a horizontal mode; this means that the depth range of measurement was 0–0.38 m and 0–0.75 m for shallow and deep measurements, respectively.

Experimental site

Experiment was conducted at a research area of the Slovak University of Agriculture in Nitra (48° 18' 07.4" N, 18° 05' 52.8" E). Soil texture analyses showed uniform soil texture across the site with a silty clay soil. The representation of the different fractions is provided in Table 1. Soil moisture content (MC) was measured in two depths (0.10–0.15 m and 0.25–0.3 m) at each of the locations using disturbed samples (sampled with a soil auger) that were analysed using the gravimetric method (Reynolds, 1970). Measurement of EMI was conducted (a) before trafficking the experiment (on 29th April 2019) and then (b) after trafficking to document the differences in compaction levels (on 30th April 2019).

Experimental layout

The experiment was a randomised block design with three blocks and four plots each block (two trafficked and two non-trafficked), as shown in Fig. 1. Soil compaction was produced by 'multi-trafficking' of the area with a John Deere 8230 tractor (11,406 kg, front tyres: 600/70 R30, 0.25 MPa, rear: 650/85 R38, 0.25 MPa) wheel by wheel and, as a result of that, the site comprised two variants:

1. Trafficked areas – Compacted plots;
2. Non-trafficked areas – Non-compacted plots (Control).

To document the difference between the variants in soil compaction, penetration resistance was measured using a Penetrologger (model P1.52, Eijlkelkamp Soil & Water, Giesbeek, The Netherlands) with ten insertions (n = 10) at each of the 12 plots following the ASABE standard no EP 541 (ASABE, 1999).

Software and statistical methods

Statistical analyses were undertaken using Statistica (StatSoft Inc., 2013). These involved descriptive statistics followed by an analysis of variance (ANOVA) and the least significant differences (*LSD*) to compare the means using probability levels of 95% and 99%.

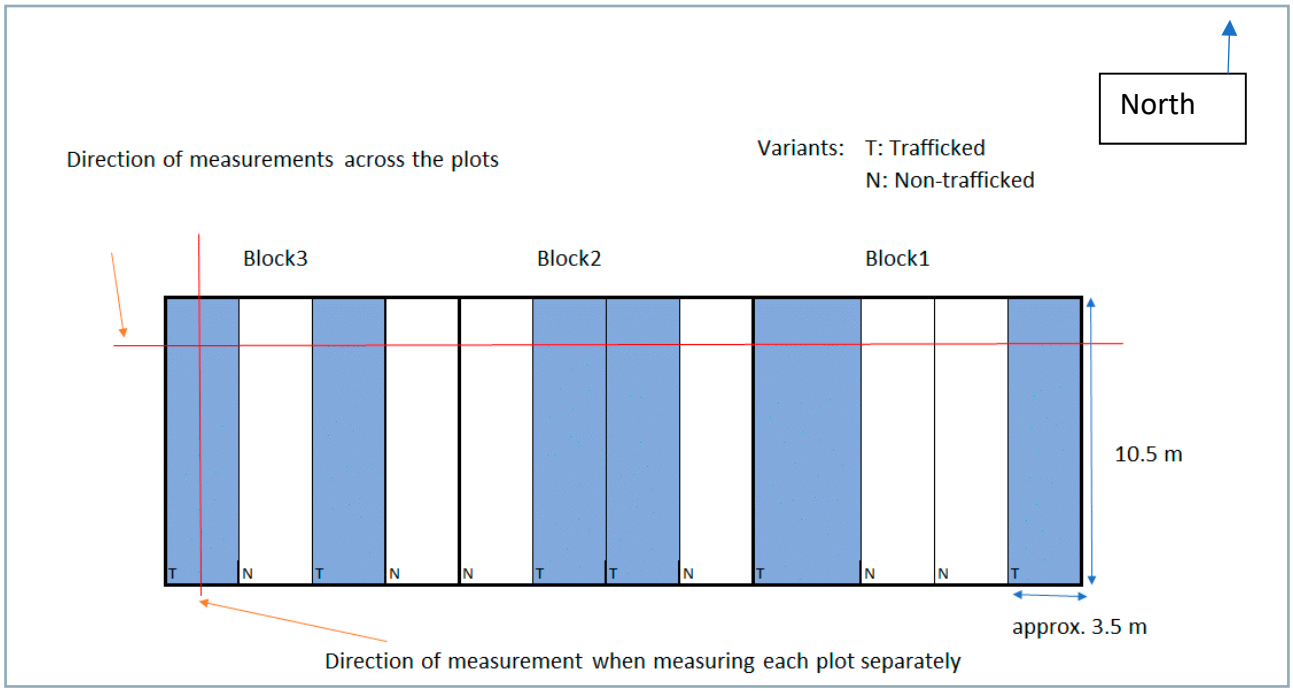

Fig. 1 Layout of the randomised block design experiment for soil electrical conductivity assessment

Table 1 Representation of different soil texture fractions at the experimental location

Depth (cm)	% of whole particles				
	>0.25	0.25–0.05	0.05–0.01	0.01–0.001	<0.001
0–30	1.75	4.35	14.85	38.72	40.31
30–60	2.71	1.05	14.26	36.08	45.88

The tests were conducted as one-factor analyses, which included the compaction level (of compacted and non-compacted areas). The same statistical approach was applied to investigate the effect of compaction, as well as spatial position (blocks), using ANOVA with two factors.

Spatial variability was displayed using ArcGIS (ESRI) and the spatial interpolation was performed by means of the Universal Kriging method for EMI values and IDW method for moisture content data. Correlation analysis was conducted as well.

Results and discussion

Before the wheel traffic was applied, the moisture content of the soil was 35.04% for the topsoil and 31.6% for the subsoil on average, with its spatial variability shown in Fig. 2. Further, the EMI was measured and the results of the scans before the trafficking are given in Fig. 3. These results indicate lower moisture content in subsoil in Block one and two and higher EMI values in deep horizon.

After trafficking was applied, soil strength was measured using a cone penetrometer (ASABE, 1999). The results shown in Fig. 4 (Left) were analysed using the ANOVA and showed a significant difference in the entire soil profile (p <0.01), with the greatest difference in the topsoil (depth up to 0.1 m). The actual soil MC measured from the soil samples

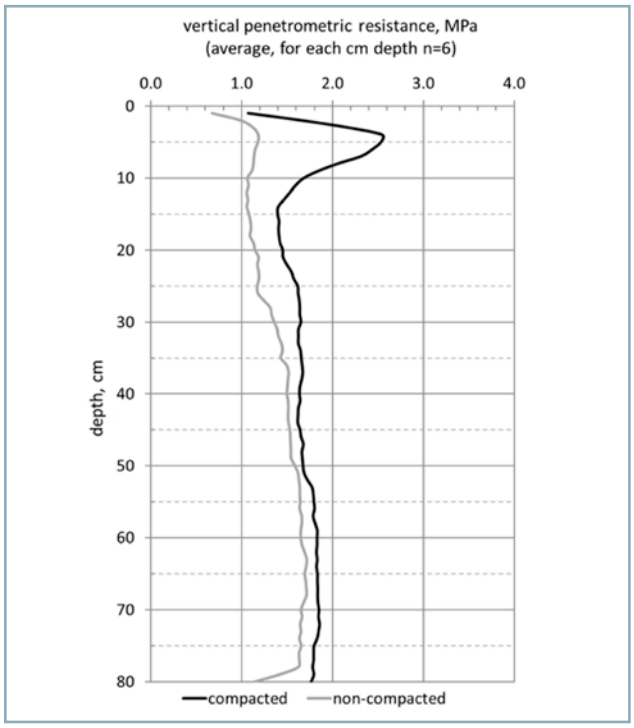

Fig. 4 Soil penetration resistance – average values for compacted and non-compacted plots (statistically significant difference at p <0.01 in whole depth)

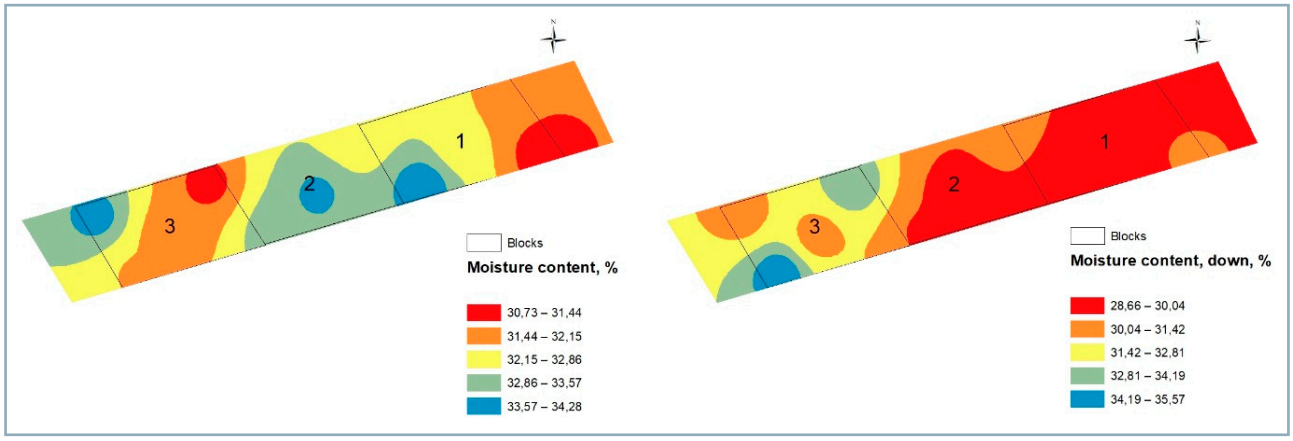

Fig. 2 Soil moisture content in the topsoil (Left) and subsoil (Right)

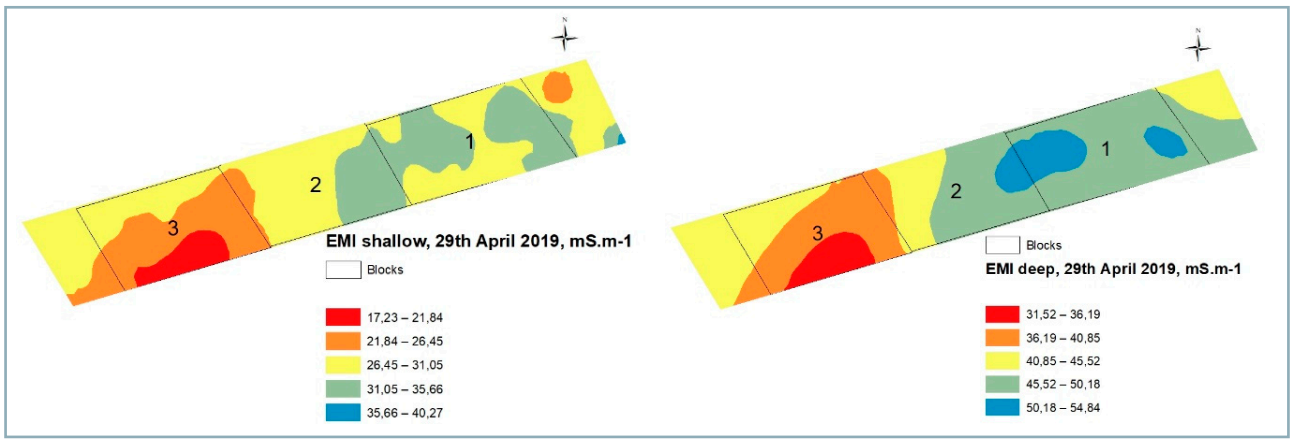

Fig. 3 Electromagnetic induction measured before the experiment in the shallow horizon (Left) and in the deep horizon (Right)

Table 2 Average values of EMI determined in trafficked and non-trafficked areas measured in the shallow and deep horizons

Depth horizon of EMI measurement	EMI (mS·m^{-1}) (mean ± SD)	
	trafficked areas	non-trafficked areas
Shallow (0–0.38 m)	47.72 ±5.08[a]	42.88 ±4.3[b]
Deep (0–0.75 m)	45.10 ±6.76[a]	41.2 ±5.78[b]

a, b – significantly different at p <0.01 when comparing the trafficked and non-trafficked areas at selected depths

analysed by gravimetric method was on average 30.8% for the topsoil and 32.5% for the subsoil.

The experimental site was observed using EM38-MK2 in two directions, as indicated in Fig. 1 (red lines). The device was handheld at an approximate distance of 100 mm above the ground. The results of a one-way ANOVA, in which all the three blocks were included, showed a highly significant difference in the EMI data at p <0.01; results are given in Table 2. The compacted areas were found to be characterised with higher mean values of EMI. Furthermore, the values for the shallow horizon were higher than with the results obtained in the deep horizon for both compacted and non-compacted variants.

Subsequently, the EMI was measured across the plots to simulate the movement of a machine on the field across compacted zones. The results are shown in Fig. 5 and the spatial variability of data is shown in Fig. 6. The data were interpolated using the Universal Kriging function. As it is clear from Fig. 5, the general trend is that the values decrease from the east to the west direction. The differences between Block three and the rest of the experimental site in values of EMI were present before and after trafficking. Therefore, blocks were used as an indicator of spatial location. The two-factorial ANOVA was applied to data to observe the effect of both block (spatial location) and field traffic and the results are shown in Fig. 7.

The EMI results were found to be highly significantly different (p <0.01) for the compacted and non-compacted areas in all the three blocks. This is valid for both the shallow and deep depth ranges – topsoil and subsoil, respectively. These findings bring a novel knowledge, since Krajčo (2007) did not find any significant difference between compacted and non-compacted areas in the topsoil in a randomized block design also using the EM38-MK2 device.

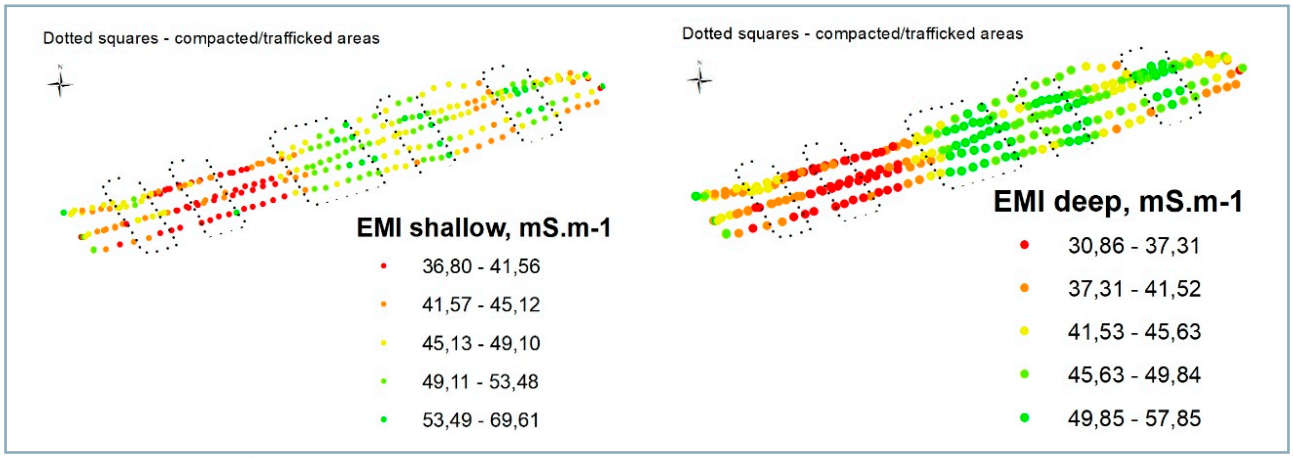

Fig. 5 EMI data (mS·m^{-1}) across the compacted and non-compacted areas at the shallow (Left) and deep depth range (Right)

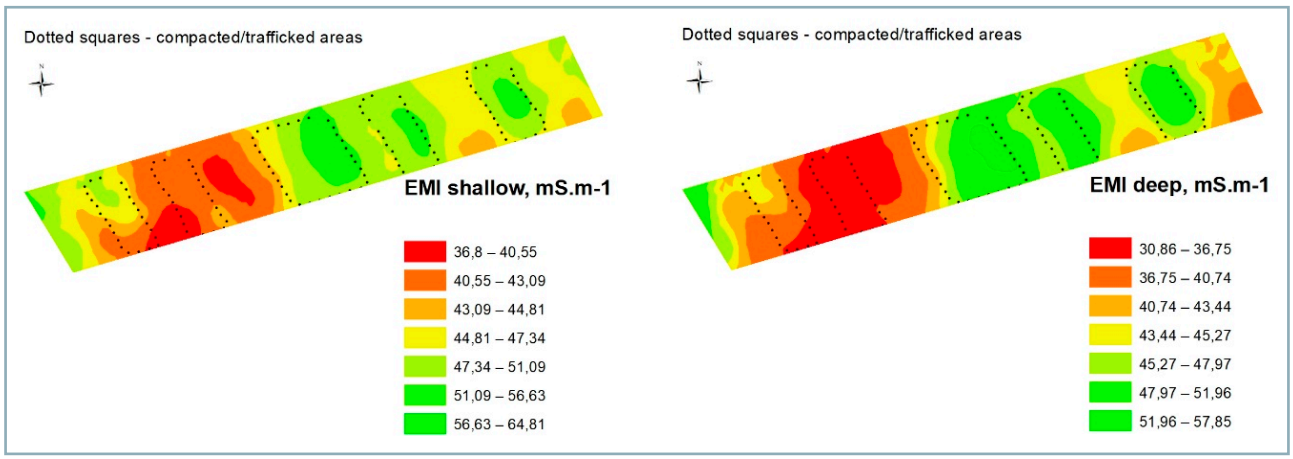

Fig. 6 Spatial variability of EMI for the compacted and non-compacted areas in the shallow (Left) and deep (Right) depth ranges

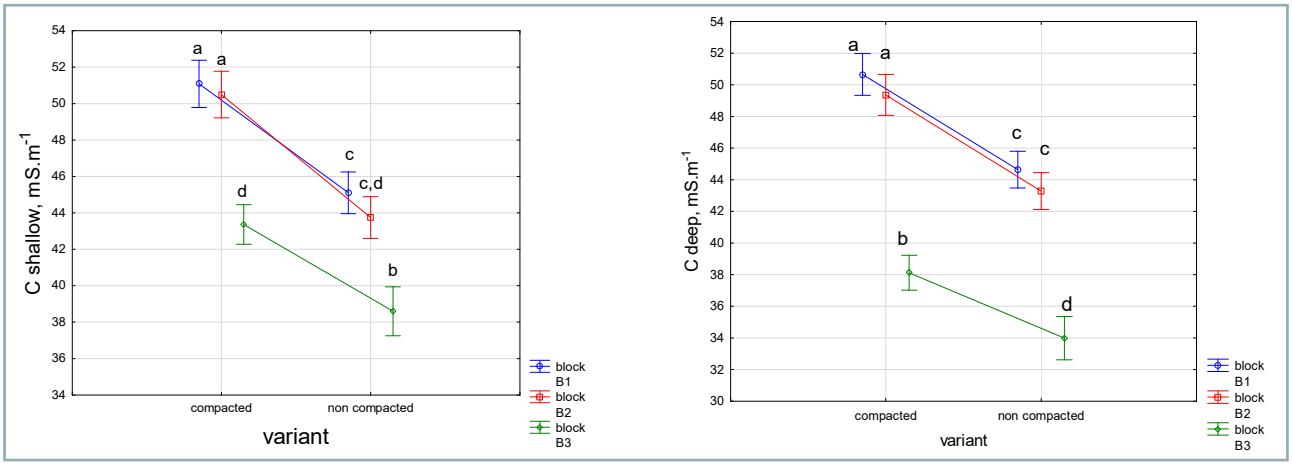

Fig. 7 Mean EMI values for the shallow (Left) and deep (Right) depth ranges for compacted and non-compacted plots/areas in three blocks (a, b, c, d letters indicate the statistically different groups based on the *LSD* analyses)

For both depth ranges measured (shallow and deep), Block 3 was found to have significantly lower EMI values compared to Blocks 1 and 2, which were not significantly different from each other. This significant spatial variability within such a small distance (42 m), between Block 3 and the rest of the experimental site, can be explained by the variability in MC (Fig. 1 Right). From a practical point of view, it suggests that the values of EMI need to be compared with data on very close surroundings if the increase should be detected. Furthermore, incorporating spatially dense data on moisture content would be beneficial in terms of data interpretation. This agrees with Heil and Schmidhalter (2017), who stressed that the interpretation and utility of ECa readings are highly location- and soil-specific; the soil properties contributing to ECa measurements must be clearly understood.

Further, the EMI data were correlated with the measured penetration resistance and a statistically significant correlation coefficient of EMI to penetration resistance was found to be equal to 0.69 at p <0.01 for the shallow measurement depth (depth range up to 0.38 m). Similar findings were published by Al-Gaadi (2012) for sandy soils, where the correlation coefficient was 0.69 at 8% soil MC. Hoefer et al. (2010) found similar relationship of penetrometer resistance and ECa at depth 0.30–0.40 m in loess-derived homogenous soil.

There is a potential that these data could be used to predict soil compaction caused by vehicular traffic. Further increase in precision could come from combination of EMI data with crop yield and other proximal sensing methods.

Conclusion

The results of the pilot study on the silty clay soil showed a potential of the EMI method to detect the trafficked areas of the field. Overall, a highly significant difference (p <0.01) in EMI values between compacted and non-compacted areas with an average increase by 11% for compacted areas of the shallow soil horizon and by 9% for compacted areas of the deep soil horizon was found. A significant spatial variability of the data within the 42 m distance, was found (Blocks 1and 2 significantly differed from Block 3); however, within each block, significant differences in compacted and non-compacted plots were still identified.

On the basis of the results, it can be recommended that EMI method can be used to determine the compacted areas in silty clay soil; however, data related to close surrounding area should be taken into account in the analysis.

Acknowledgments

This article was prepared in the framework of a research project funded by the European Union entitled ITEPAg: Application of Information Technologies to Increase the Environmental and Economic Efficiency of Production Agro-System (ITMS 26220220014, www.itepag.uniag.sk) and project Building the Research Centre AgroBioTech' (ITMS no. 26220220180).

Authors would like to thank to the management of the Botanical Garden of the Slovak University of Agriculture in Nitra for providing the experimental site.

References

ANTILLE, D. L. – PEETS, S. – GALAMBOŠOVÁ, J. – BOTTA, G. F. – RATAJ, V. – MACÁK, M. – TULLBERG, J. N. – CHAMEN, W. C. T. – WHITE, D. R. – MISIEWICZ, P. A. – HARGREAVES, P. R. – BIENVENIDO, J. F. – GODWIN, R. J. 2019. Review: Soil compaction and controlled traffic farming in arable and grass cropping systems. In Agronomy Research, vol. 17, no. 3, pp. 653–682.

ASABE EP542: 1999. Procedures for Using and Reporting Data Obtained with the Soil Cone Penetrometer.

ALAOUI, A. – DISERENS, E. 2018. Mapping soil compaction – A review. In Current Opinion in Environmental Science & Health, vol. 5, pp. 60–66.

AL-GAADI, K. A. 2012. Employing electromagnetic induction technique for the assessment of soil compaction. In American Journal of Agricultural and Biological Sciences, vol. 7, no. 4, pp. 425–434.

BULGAKOV, V. – KUVACHOV, V. – NOZDROVICKÝ, L. – FINDURA, P. – SMOLINSKYI, S. – IHNATIEV, Y. 2018.The study of movement of the wide span tractor-based field machine unit with power method of its control. In Acta Technologica Agriculturae, vol. 21, no. 4, pp. 160–165.

GALAMBOŠOVÁ, J. – MACÁK, M. – RATAJ, V. – ANTILLE, D. L. – GODWIN, R. J. – CHAMEN, W. C. T. – ŽITNÁK, M. – VITÁZKOVÁ, B. – DUDÁK, J. – CHLPÍK, J. 2017. Field evaluation of controlled traffic farming in Central Europe using commercially available machinery. In Transactions of the ASABE, vol. 60, no. 3, pp. 657–669.

GEBBERS, R. 2019. Proximal soil surveying and monitoring techniques. In STAFFORD, J. Precision Agriculture for Sustainability. UK : Burgleigh Dodds.

GODWIN, R. – MISIEWICZ, P. – WHITE, D. – SMITH, E. – CHAMEN, T. – GALAMBOŠOVÁ, J. – STOBART, R. 2015. Results from recent traffic systems research and the implications for future work. In Acta Technologica Agriculturae, vol. 18, no. 3, pp. 57–63.

GUTU, D. – HŮLA, J. – KROULÍK, M. 2015. Evaluation of soil physical properties in system with permanent traffic lanes practised in 10 ha field. In Acta Technologica Agriculturae, vol. 18, no. 3, pp. 92–96.

HEIL, K. – SCHMIDHALTER, U. 2017. The application of EM38: Determination of soil parameters, selection of soil sampling points and use in agriculture and archaeology. In Sensors, vol. 17, no. 11, p. 2540.

HOEFER, G. – BACHMANN, J. – HARTGE, K. H. 2010. Can the EM38 Probe Detect Spatial Patterns of Subsoil Compaction? In VISCARRA ROSSEL, R.A. et al. (eds.). Proximal Soil Sensing, Progress in Soil Science 1, 265, C Springer Science+Business Media B.V.

CHAMEN, T. 2015. Controlled traffic farming – from worldwide research to adoption in Europe and its future prospects. In Acta Technologica Agriculturae, vol. 18, no. 3, pp. 64–73.

KELLER, T. – SANDINA, M. – COLOMBIA, T. – HORND, R. – ORE, D. 2019. Historical increase in agricultural machinery weights enhanced soil stress levels and adversely affected soil functioning. In Soil and Tillage Research, vol. 194, p. 104293.

KRAJČO, J. 2007. Detection of Soil Compaction Using Soil Electrical Conductivity. MSc. Thesis, Cranfield University, Cranfield, UK.

LATSCH, A. – ANKEN, T. 2019. Soil and crop responses to a "light" version of Controlled Traffic Farming in Switzerland. In Soil and Tillage Research, vol. 194, p. 104310.

MASOLA, M. J. – ALESSO, C. A. – CARRIZO, M. E. – BERHONGARAY, G. – BOTTA, G. F. – HORN, R. – IMHOFF, S. 2020. Advantages of the one-wheeled tramline for multiple machinery widths method on sunflower (*Helianthus annus* L.) and maize (*Zea mays* L.) responses in the Argentinean Flat Pampas. In Soil and Tillage Research, vol. 196, p. 104462.

RATAJ, V. – GALAMBOŠOVÁ, J. – MACÁK, M. – NOZDROVICKÝ, L. 2014. Precision Agriculture – System, Machines, Experiences. Nitra : Profi Press. (In Slovak: Presné poľnohospodárstvo – Systém, stroje, skúsenosti).

REYNOLDS, S. G. 1970. The gravimetric method of soil moisture determination: Part I. A study of equipment, and methodological problems. In Journal of Hydrology, vol. 11, no. 3, pp. 258–273.

ROMERO-LUIZ, A. – LINDE, N. – KELLER, N. – ORE, D. 2019. A review of geophysical methods for soil structure characterization. In Reviews of Geophysics, vol. 56, pp. 672–697.

sciendo

DOI: 10.2478/ata-2020-0002

Acta Technologica Agriculturae 1/2020 *Jiří Votava et al.*

Acta Technologica Agriculturae 1
Nitra, Slovaca Universitas Agriculturae Nitriae, 2020, pp. 7–11

CHANGE OF MECHANICAL PROPERTIES OF ZINC COATINGS AFTER HEAT TREATMENT

Jiří VOTAVA*, Vojtěch KUMBÁR, Adam POLCAR, Martin FAJMAN

Mendel University in Brno, Czech Republic

Hot-dip galvanized coatings represent a protection based on passivation of the single zinc layer. It is one of the most commonly used surface treatments of steel. However, pure zinc forms merely an insignificant upper layer. Coating crosscut is formed by intermetallic phases that can cause decrease in the level of anticorrosion protection. This results from an iron diffusion from the base material. Goal of this paper is to analyse the changes in the mechanical properties of these phases in relation to zinc coating heat treatment. For the experiment, annealing temperatures of 200 °C and 300 °C were used, and the staying time was set at 1, 3 and 5 hours. Furthermore, samples without any heat treatment were subjected to comparison as well. Moreover, following tests were conducted: bending test in compliance with the ČSN EN ISO 1519 standard, and tearing test (in accordance with the ČSN EN ISO 4624 standard). On the basis of performed tests, the changes in mechanical properties of the zinc coating after heat treatment could be analysed.

Keywords: annealing; structure; mechanical degradation; hot-dip galvanizing

Use of anticorrosion protection requires the knowledge of the basic principles of corrosion processes and the mechanics of individual corrosion types, as well as anticorrosion protection. Chemical reaction with the elements from the corrosive environment turns metal into a solution identical or similar to the one it was originally produced from. For this reason, anticorrosion protection is indispensable (Trethewey and Chamberlain, 1995; Tulka, 2005).

General emphasis aimed at corrosion prevention has been constantly rising. Such a trend can be seen especially in surface treatments of steelworks in civil engineering, agriculture and machinery industry. Zinc coating of individual steelworks has a long tradition. These steelworks are assembled together; therefore, the zinc coating forms the only corrosion prevention of the entire assembly. In order to improve the corrosion prevention, paint can be used (Čičo et al., 2011; Votava and Kumbár, 2017). A properly used paint system does not only improve the corrosion prevention, but also modifies the visual appearance of the entire assembly. Drawback of such surface measures is that the upper layer can crack and peel because of bad paint fixation to the zinc coating.

Cracks in the paint system hold in air humidity which condensates on the zinc coating surface, which results in a chemical reaction generating $ZnCO_3$. Duplex corrosion protection of welded joints is thus highly relevant for this. In case of corrosion protection failure, the weld is always a potential place for initiation of a corrosion macrosegment (Čičo et al., 2006; Poláková and Dostál, 2019).

Zinc coatings may become subjects of mechanical degradation during and after their heat treatment. One of the reasons for inclusion of heat treatment to the production process lies in elimination of H2 from the base material. Hydrogen comes to the base material by diffusion in the process of preliminary treatment, such as staining, degreasing. Therefore, heat treatment prevents hydrogen brittleness. The dominant layer in the anchoring profile is formed by phases Gamma and Gamma-1, which are both very hard and fragile at the same time, which can cause the occurrence of coating delamination even under a low mechanical stress.

Individual intermetallic phases grow into a whole coating profile not only during the targeted heat treatment of zinc anticorrosion coating but also during everyday service heat stress. As a result, the ratio of the pure zinc decreases at the expense of massive growth of Zeta phases, thereby mechanical and anticorrosion properties of the whole coating may be reduced. However, the base material to which the zinc coating is applied also plays a significant role (Votava et al., 2018).

The anticorrosion capacity of the whole system may be harmed due to heat treatment of anticorrosion zinc coatings. The reason for heat treatment is the possibility of "dehydrogenation" of the base material (Fiala et al., 2003; Machek, 2013), which results in elimination of potential cracks originating in subsurface layers of the steel part.

Contact address: Jiří Votava, Mendel University in Brno, Faculty of AgriSciences, Department of Technology and Automobile Transport, Zemědělská 1, 613 00 Brno, Czech Republic, e-mail: Jiri.Votava@mendelu.cz

Material and methods

The experiment was executed on specimens made of steel sheet of the quality S235JRG1; the sheet size was 160 × 65 mm and the sheet thickness was 1 mm. Before the zinc dipping, the samples were degreased and steeped.

Tested samples were hot-dip galvanised under the laboratory zinc plating conditions. Degreasing of samples was performed in aqueous solution of HCl, the bath temperature was 50 ±2 °C and samples were dipped for 120 s. The zinc coating was composed of $ZnCl_2$ and NH_4Cl. The temperature of the galvanising bath was 450 ±5 °C. In order to improve foundering performance, the galvanising zinc bath was alloyed by 2% of pure aluminium. Such aluminium ratio is considered to improve the coating anticorrosion properties (Votava, 2014). Pure zinc formed 98% of the bath. The galvanizing bath was made of graphite.

After removing from the galvanising bath, samples were gradually cooled in air. The thickness of the zinc coating substrate is highly dependent on the time during which the component remained in the zinc bath. According to the experimental measurements, the period of 120 s results in coating thickness of approx. 65 µm.

Subsequently, the specimens were heat treated in a muffle furnace MP-05 at the temperatures of 200 and 300 °C for 1, 3 and 5 hours; the speed of run-up temperature was lower than 30 minutes. There were always six samples in each group. These samples were subjected to metallographic analysis and the changes of intermetallic phases were observed.

Tests were processed in compliance with the following standards:

– ČSN EN ISO 1519 Bend test (cylindrical mandrel);
– ČSN EN ISO 4624 Pull-off test for adhesion.

Results and discussion

Measuring the zinc-coat thickness

The zinc coat layer thickness was measured non-destructively by means of Permascope device, operating on the principle of contacting measurement; the thickness of the upper deposited layer on the original material was determined digitally. Average values of zinc coat thickness are listed in Table 1. The measurement accuracy of the metallographic specimen was checked using the computer programme analysis, metallographic microscope with 500 times magnification. Metallographic specimen is shown in Fig. 1.

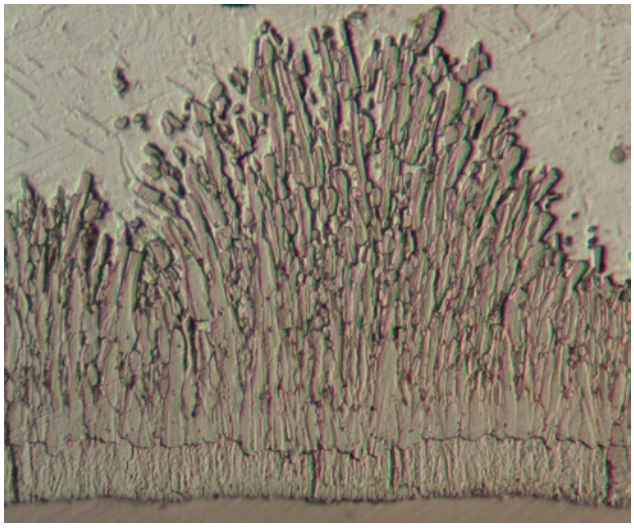

Fig. 1 Cross-section of the zinc layer with marked measured values

On the basis of metallographic observations, it can be concluded that the upper layer is formed by pure zinc. However, the zinc layer is uneven, yet the connections of intermetallic phases with the surface are just isolated.

As it is apparent from Fig. 1, pure zinc forms c. 10 µm of the upper layer of the anticorrosion coating. The Fig. 1 also nicely shows the phase Zeta ($FeZn_{13}$), for which long monoclinic crystals are typical. These crystals are visible after a slight etch of the surface.

Measuring the microhardness of intermetallic phases of the zinc coat

Using the HV method, the microhardness was measured by means of Hanneman's microhardness tester, with the connection with Neophot 21 microscope. The indentor with top angle of 136° was pressed to the material at the pressure of 0.1 N (Skálová et al., 1995). There were tested not only the heat-treated specimens but also those with no heat treatment (Fig. 2) for the purposes of comparison of potential differences. From among the heat-treated samples for both temperatures, three samples with 5-hour heat exposition (maximal phases growth) were analysed. Measured values are listed in Table 2.

On the basis of measurement results, it can be concluded that the bigger and/or longer the heat treatment, the higher the microhardness (Table 3). Changes in mechanical properties can be caused by diffusion of ferrum from the base material to the zinc coating (Zmrzlý et al., 2005). However, the disadvantage of this process lies in lowering of the anticorrosion protection of the inorganic coating. Under

Table 1 Average thickness values of zinc coatings (µm)

Group of specimens	Annealing time			Average zinc-coat thickness (µm)
Annealing temperature	1 hour	3 hours	5 hours	
200 °C	54.25	53.16	54.24	53.88
300 °C	55.18	55.45	54.29	54.97
Samples without heat treatment were measured in three sets				53.15

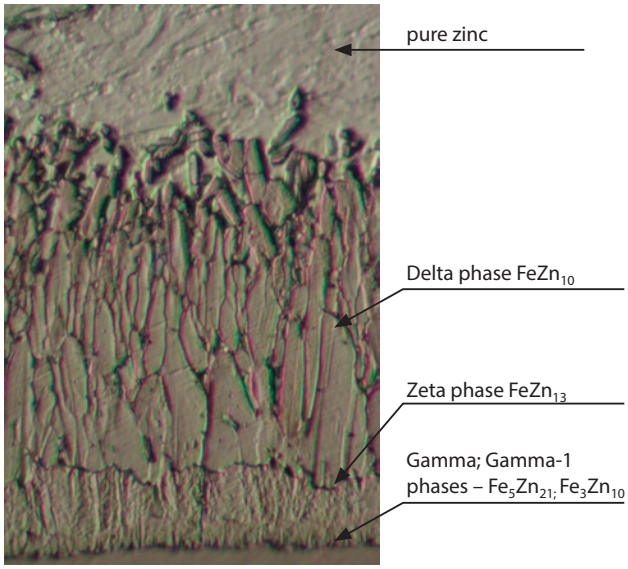

Fig. 2 Intermetallic phases in a zinc coating

corrosion stress, one can assume that zinc ions will be drawn faster, resulting in more rapid occurrence of red corrosion (Popov, 2015).

Bending test

Bending experiment was conducted in compliance with the ČSN EN ISO 1519 standard and carried out utilizing the Elcometer 1506 cylindrical mandrel bend tester. There were taken two mandrels; the first had 10 mm in diameter and represented a severe bending load. The second bending pin had 32 mm in diameter and simulated a low bending load. The results presented in Table 4 are after 5-hour heat treatment.

According to Kuklík and Kudláček (2014), it is possible to identify cracks and further delamination of zinc coating in the phases Gamma and Gamma-1. Considering the tests performed, this hypothesis can be also stated that the massive crack growth can be seen after a 3-hour heat treatment. Such a short time is sufficient for initiation of the diffusion process. According to Adelmann et

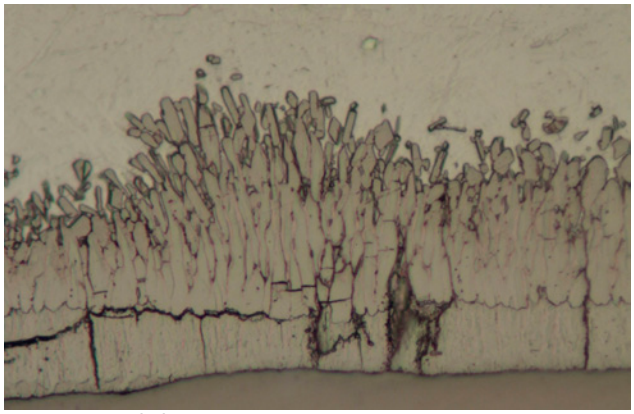

200 °C, mandrel 32 mm

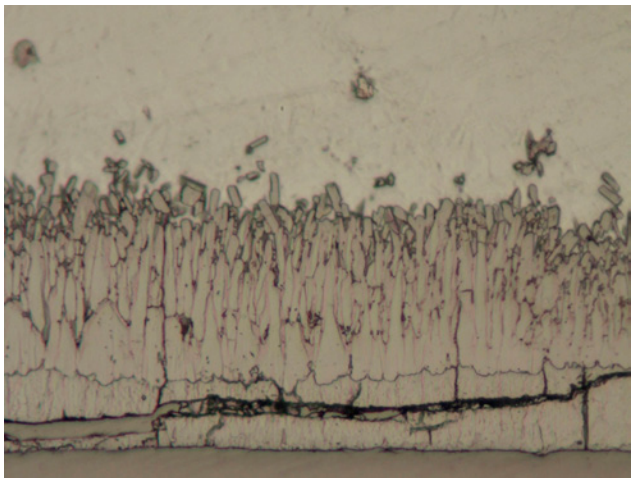

300 °C, mandrel 32 mm

Fig. 3 Cracks in the zinc coating originating from the bending test according to ČSN EN ISO 8401

Table 2 Microhardness of intermetallic phases of the zinc coat (HV) without heat treatment

	1	2	3	Average ($HV_{0.1}$)	Standard deviation ($HV_{0.1}$)	Variation coefficient (%)
Gamma	*	*	*	*	*	*
Delta	364	378	397	379.67	13.52	3.56
Zeta	222	201	236	219.67	14.38	6.55
Zinc	67	60	61	62.67	3.09	4.93

* By using this kind of measuring method, it was impossible to measure the microhardness for the Gamma and Gamma-1 phases. These phases can only be measured by a nanoindentor and using electron microscopy. It can be concluded that these phases showed higher microhardness than the Delta-phases

Table 3 Change in microhardness of phases Delta and Zeta depending on heat treatment

Heat treatment (°C)	Phase	1	2	3	Average ($HV_{0.1}$)	Standard deviation ($HV_{0.1}$)	Variation coefficient (%)
200	Delta	376	357	381	371.33	10.34	2.78
	Zeta	222	201	241	221.33	16.34	7.38
300	Delta	440	455	450	448.33	6.24	1.39
	Zeta	265	270	294	276.33	12.66	4.58

Table 4 Results of bending experiment

Heat treatment	Mandrel diameter 10 mm	Mandrel diameter 32 mm
Zero heat treatment	– the samples showed cracks of an average width of 18 µm	– there were no cracks caused by the bending test
200 °C	– the average width of cracks was 23 µm	– small cracks of approx. 5 µm were shown
300 °C	– specimens annealed at temperature exceeding 200 °C showed significant changes in mechanical properties, there were severe defects. The average width of cracks was 45 µm	– there were shown microcracks of 10–15 µm (see Fig. 3) in the coating due to the minimal mechanical stress (mandrel 32 mm)

Table 5 Pull-off test according to ČSN EN ISO 4624 standard

Heat treatment	Time (hour)	Measurement			Average (MPa)	Standard deviation (MPa)	Variation coefficient (%)
		no. 1 (MPa)	no. 2 (MPa)	no. 3 (MPa)			
200 °C	1	12.9	12.8	12.7	12.80	0.082	0.64
	3	12.5	12.9	12.4	12.60	0.216	1.71
	5	12.4	12.9	12.1	12.47	0.330	2.65
300 °C	1	13.5	13.6	13.6	13.57	0.047	0.35
	3	13.4	13.7	13.4	13.50	0.141	1.05
	5	14.2	14.1	14.5	14.27	0.170	1.19
Zero heat treatment laboratory temperature		12.5	13.4	13.8	13.23	0.544	4.12

al. (2010), the zinc coating may be peeled off. However, this was not proven true. The test implies that the limit border temperature is 200 °C.

As it is apparent from Fig. 3, the cracks may expand both in vertical and horizontal levels. Even though the anticorrosion coating belongs to cathodic protection of base metals, microcracks in the coating significantly lower its service life. Microcracks due to higher heat treatment can be eliminated by specific chemical composition of the zinc bath (Körber et al., 2012).

Pull-off test

The ability of the anticorrosion system to withstand dynamic and static stress is one of the criteria for the quality evaluation of protective coatings. In this respect, one of the most important characteristics is the adhesion between the anchoring profile of the base material and the coating substrate (Votava et al., 2016).

Anticorrosion system adhesion was determined according to the ČSN EN ISO 4624 standard. This standard establishes the procedure for pull-off testing in single-layered and multi-layered coating systems. Test result is determined by the tension in pulling required to damage the weakest boundary (adhesive failure) or the weakest component (cohesive failure) of the tested object. Adhesion analysis of individual anticorrosion systems was preformed immediately after complete drying of the anticorrosion coating. The delay was set at 48 hours. Test results are shown in Table 5.

On the basis of pull-off test results (Table 5), higher firmness of the coating after heat treatment was confirmed. The highest firmness values were reached by samples annealed at the temperature of 300 °C for 5 hours. Despite the higher material firmness thanks to the higher temperature of the heat treatment, there can occur microcracks, which lead to degradation of the coating as shown in the bending test.

Conclusion

The objective of this article was an assessment of deterioration of mechanical characteristics depending on heat-treating process of the upper zinc layer. Temperatures of 200 and 300 °C and annealing times of 1, 3 and 5 hours were observed in this experiment in terms of changes in microhardness of the phases in regards to both exposure time and temperature.

Emphasis should be given to the fact that fragile Gamma-phase grew in samples with 3- and 5-hour annealing time (Gamma-phase as such is the origin of cracks caused by mechanical stress). This proposition was confirmed during the bending test according to the ČSN EN ISO 1519. Furthermore, on the basis of results of the other tests, it can be stated that heat treatment of zinc coatings results in higher firmness, yet in lower tenacity at the same time as well.

The Gamma-phase detachment from the original surface can be easily seen during the metallographic observations. The Gamma and Gamma-1 phases always occur during the heat treatment; therefore, it is necessary to focus on their elimination. According to the scientific literature, the elimination of fragile phases is quite difficult. The basis is the chemical composition of galvanized steel. Heat treatment of hot-dip galvanized zinc coatings can be recommended for machine parts, in which it is necessary to dehydrogenize the base material. Dehydrogenization is a process eliminating hydrogen brittleness and the origin of cracks in the base

material. However, the annealing temperature should not exceed 200 °C. Exceeding this temperature increases the risk of horizontal and vertical cracks in the anticorrosion coating. Due to this, the individual parts should not be subjected to increased dynamic stress. On the other hand, it is not recommended for parts which could be subject to temperature exceeding 200 °C.

Acknowledgment

This contribution was created with the contribution of the project ZETOR (EG15_019/0004799 – ZETOR TRACTORS a.s.) – Optimal aggregation of machines with a tractor.

References

ADELMANN, J. – KÖRBER, D. – LANDGREBE, R. – BERGER, C. 2010. A new test procedure to investigate the cracking behaviour of hot-dip galvanised steel. In Material Prüefung, vol. 52, no. 9, pp. 578–587.

ČIČO, P. – KALINCOVÁ, D. – KOTUS, M. 2011. Influence of the welding method on microstructural creation of welded joints. In Research in Agricultural Engineering, vol. 57, special issue, pp. 50–56.

ČIČO, P. – TOLNAI, R. – KOTUS, M. 2006. Weld quality in pulse and non-pulse welding by synergic weld power supply. In Acta Technologica Agriculturae, vol. 9, no. 1, pp. 3–6. (In Slovak: Kvalita návaru pri impulznom a bezimpulznom naváraní synergickým zváracím zdrojom)

ČSN EN ISO 1519: 2011. Bend test (cylindrical mandrel). Praha : Český normalizační institut.

ČSN EN ISO 4624: 2016. Pull-off test for adhesion. Praha : Český normalizační institut.

FIALA, J. – ŠUTTA, P. – MENTL, M. 2003. Material Structure and Properties. 1st ed. Praha: Academia, 572 pp. ISBN 8020012230. (In Czech: Struktura a vlastnosti materiálů)

KÖRBER, D. – LANDGREBE, R. – ADELMANN, J. – HOCHE, H. – OECHSNER, M. 2012. Liquid metal induced crack formation in molten zinc – A damage mechanism driven by diffusion and stress. In Praktische Metallographie, vol. 49, no. 11, pp. 698–707.

KUKLÍK, V. – KUDLÁČEK, J. 2014. Hot Dip Galvanizing. Asociace českých a slovenských zinkoven, 208 pp. ISBN 9788090529823. (In Czech: Žárové zinkování)

MACHEK, V. 2013. Metal Materials I: Structures of Metal Materials. 1st ed. Praha: České vysoké učení technické, 168 pp. ISBN 9788001052488. (In Czech: Kovové materiály I: struktury kovových materiálů)

POLÁKOVÁ, N. – DOSTÁL, P. 2019. Titanium and stainless steel MIG LSC welding. In Acta Technologica Agriculturae, vol. 22, no. 2, pp. 56–59.

POPOV, B. N. 2015. Corrosion Engineering: Principles and Solved Problems. Oxford : Elsevier, 792 pp. ISBN 9780444627223.

SKÁLOVÁ, J. – BENEDIKT, V. – KOVAŘÍK, R. 1995. Basic Proves of Metal Materials. 2nd ed. Plzeň: Západočeská univerzita, 175 pp. ISBN 8070820217. (In Czech: Základní zkoušky kovových materiálů)

TRETHEWEY, K. R. – CHAMBERLAIN, J. 1995. Corrosion: For Science and Engineering. 2nd ed. Addison: Wesley Longman, 466 pp. ISBN 0582238692.

TULKA, J. 2005. Surface Treatments of Materials. 1st ed. Brno, VUT : Fakulta chemická, 136 pp. ISBN 8021430621. (In Czech: Povrchové úpravy materiálů)

VOTAVA, J. 2014. Corrosion resistance of zinc coatings with aluminium additive. In Acta Technologica Agriculturae, vol. 17, no. 2, pp. 49–52.

VOTAVA, J. – JUKL, M. – POLCAR, A. – KUMBÁR, V. – DOSTÁL, P. 2018. Anti-corrosion systems in vehicles for the transportation and application of fertilizers. In Metallic Materials, vol. 56, no. 2, pp. 131–136.

VOTAVA, J. – KUMBÁR, V. 2017. Usage of waterborne acrylate anticorrosion systems for ecological environment. In Manufacturing Technology, vol. 17, no. 1, pp. 103–110.

VOTAVA, J. – KUMBÁR, V. – POLCAR, A. 2016. Degradation processes in anticorrosive coatings for machinery designed for fertiliser application. In Acta Universitatis Agriculturae et Silviculturae Mendelianae Brunensis, vol. 64, no. 4, pp. 1257–1265.

ZMRZLÝ, M. – FIALA, J. – SCHNEEWEISS, O. – HOUBAERT, Y. 2005. Structure of intermetallic phases in al-free galvannealed zinc coatings. In Czechoslovak Journal of Physics, vol. 55, no. 7, pp. 923–931.

Acta Technologica Agriculturae 1
Nitra, Slovaca Universitas Agriculturae Nitriae, 2020, pp. 12–17

MICROSTRUCTURES AND ELEMENTAL DISTRIBUTION OF MAGNETIC FIELD PRE-TREATED FLUTED PUMPKIN LEAF

Michael Mayokun ODEWOLE*[1], Ayoola Patrick OLALUSI[2], Ajiboye Solomon OYERINDE[2], Olufunmilayo Sade OMOBA[2]

[1]University of Ilorin, Nigeria
[2]Federal University of Technology Akure, Nigeria

There is a scarcity of studies on the use of magnetic field for food pretreatment, especially in relation to a knowledge on the pretreatment at the level of microstructures and elemental distribution of food. Therefore, the effect of magnetic field pretreatment on the microstructures and elemental distribution (Na, K, Ca, Mg and Fe) of fluted pumpkin leaf was studied. Three types of magnetic field (static, pulse and alternating) in combination with varying magnetic field strength (5–30 mT) and pretreatment time (5–25 min) were used as variable factors. Fresh (untreated) and blanched samples were used for experiment control. After the pretreatment, all samples were dried at 50 °C and analysed in terms of microstructure and elemental distribution using scanning electron machine. Results showed that fresh and blanched samples of fluted pumpkin leaf exhibited microstructural features that were clearly different from samples pretreated by magnetic field. Pretreated samples showed contents of: 1.3–4.35% sodium; 1.20–3.42% potassium; 1.19–6.10% calcium; 0–5.10% magnesium and 1.22–6.62% iron. Changes in microstructures of samples caused by magnetic field pretreatment led consequently to better retention/improvement in elemental distribution in contrast to blanched and fresh samples in majority of cases.

Keywords: non-thermal processing; vegetables; effect; electromagnetism; thermal processing

Fluted pumpkin leaf (*Telfairia occidentalis*) is a leafy vegetable that has high nutritional and medicinal values (Ndor et al., 2013). It is referred to as "ugu" among the Igbo ethnic group of Nigeria (Odewole et al., 2015) and the name has been popularly adopted for use across most parts of Nigeria. Fluted pumpkin leaf can improve haematological parameters, has anti-inflammatory and anticholesterolemic properties (Obeagu et al., 2014). The leaf has microstructures just like any other vegetables (Verboven et al., 2018b).

Food microstructure is the organization and interaction of food constituents resulting in a particular microscopically visible spatial partition of different material phases (Verboven et al., 2018a). Rejaul et al. (2018) defined the food microstructure as the arrangement of its architectural elements into organized structures either naturally or through processing. Food microstructure was also reported as the architectural view of food at submicroscopic levels; and it helps to better understand the internal behaviour of processed food, as well as when new products are to be developed and during quality control operations (Rejaul et al., 2018).

Foods nutrients are ingested in the form of microstructures that can be as small as nanometres and up to a few millimetres in size (Troncoso and Aguilera, 2009). Microstructural studies help in the establishment of the relationship that exists in composition, processing and final properties of many food products (Heertje, 1993).

Food pretreatment involves taking necessary steps in order to maintain the desired properties or nature of food for as long as possible and to ensure the consumption of food with high nutritional values (Rahman and Perera, 2007). Both processing and pretreatment affect the food microstructures either by destroying the original food structures or creating new ones. Pretreatment as one of the unit operations in food processing has the tendency of modifying the microstructures and elemental composition of food. With the use of SEM (scanning electron machine), Vodal et al. (2012) reported that blanching pretreatment did not affect the pore size distribution of freeze-dried winter carrot. Dhawi et al. (2009) pretreated the seedlings of date palm with static magnetic field (SMF) of strength from 10 mT to 100 mT for 30–360 min. Elemental analysis of the date palm leaf with inductive couple plasma (ICP) spectroscopy showed increase in the concentrations of Ca, Mg, Mn, Fe, Na, K, and Zn; however, phosphorus (P) concentration dropped with increase in SMF strengths and exposure duration. Antonio et al. (2008) used SEM to confirm the formation of pores within the microstructure (tissue) of sweet potato treated with osmotic dehydration. Starodubtseva et al. (2018) pretreated winter wheat seeds with pulsed electric field of up to 2,500 $V \cdot m^{-1}$ field intensity, 50 µs pulse duration and 600 Hz pulse frequency; finally, it was observed that the seed moisture content increased from 10% to 13.5% with corresponding mass

Contact address: Michael Mayokun Odewole, University of Ilorin, Faculty of Engineering and Technology, Department of Food Engineering, Nigeria, e-mail: odewole2005@yahoo.com

increase of approx. 23.8%. Moreover, Otero et al. (2000) used histological technique to evaluate modifications in the microstructures of peach and mango. The results showed that both products maintained their original tissue structures to a great extent. Askari et al. (2004) investigated the effect of hot air drying and microwave drying methods on microstructural changes of apple slices as further processing steps to osmotic pretreatment in sucrose solution (60% w/w). The microstructure revealed resistance of microstructures to damage and increase in porosity of the products. Food pretreatment/processing methods can be broadly classified as conventional and non-conventional (Neetoo and Chen, 2014); both methods have thermal and non-thermal examples. Conventional methods include those that are commonly used, such as: blanching, salting, thermal pasteurization and sterilization. Non-conventional methods are scarcely used and referred to as novel or emerging methods in food processing. Some typical examples include: high hydrostatic pressure, pulsed electric field, microwave heating, ohmic heating, sous vide method, irradiation, pulsed light (Neetoo and Chen, 2014) and magnetic field (Barbosa-Canovas et al., 2005). Emerging non-thermal technologies focus on the production of higher quality food in contrast to heat-treatment methods as well as on decrease in the processing costs and value addition to the product (Barbosa-Canovas et al., 2005).

A magnetic field is defined as a region of space in which a magnetic body is capable of inducing the surrounding bodies (Barbosa-Canovas et al., 2005) either with permanent magnet or temporary magnet (electromagnet). Magnetic fields are classified as of low or high intensity according to their relative strength; as homogeneous or non-homogeneous according to the variation of intensity over space; as static or pulsed according to time interval (Kovacs et al., 1997). Use of magnetic fields as a non-thermal food processing method was first proposed in 1985 (Barbosa-Canovas et al., 2005). Electromagnetic technologies in food processing have attracted increased industrial interest, because they represent a potential replacement of certain thermal food processing methods and can enhance other beneficial factors for food processing (Rahman and Perera, 2007). It was reported in ICNRIP (2009) that all the studies conducted so far did not give convincing evidence of the harmful effects of magnetic fields on living things. However, these guidelines suggest the acceptable exposure limit for different parts of human body: 2–8 T for head, torso and limbs, and 400 mT for any other part of the body.

Basic theory governing the use of magnetic field for food pretreatment could be adapted or assumed from the submission of Dhawi et al. (2009) stating that living cells have charges exerted by ions or free radicals which act as endogenous (internal) magnets; these can be affected by exogenous magnet or an external magnetic field from either permanent magnet or electromagnet. This interaction would cause the naturally unpaired electrons (or scattered ions) present in the internal parts of food materials to be rearranged in uniform manner. Similarly, Ordonez and Berrio (2011) came to conclusion that biological membranes exhibited a strong orientation in magnetic field (MF) and the ions in them were responsible for the transmission of the effects of the MF treatments to various parts of the materials. Vegetables are living things, and hence contain cells; when harvested, their cells do not die immediately. These cells (which contain ions in them) would interact with an external magnetic field, resulting in the assumed modification of the microstructures leading to different responses of elements (minerals) present in the food product after exposure for a certain period of time. Several researchers (Hayder et al., 2015; Lipiec et al., 2004; Ordonez and Berrio 2011; Jia et al., 2015; Kyle, 2015; Ibara et al., 2015) have used magnetic field to carry out food processing. Few research works on the use of magnetic field to pretreat/process food are available and there has seemed to be a scarcity of information on the microstructures of food processed with magnetic field, and relationship between food microstructures and their elemental distribution. Therefore, the objective of this study was to investigate the effect of three types of magnetic fields (static magnetic field (SMF); pulse magnetic field (PMF); and alternating magnetic field (AMF)), varying magnetic field strength (5–30 mT) and various pretreatment times (5–25 min) on the microstructures and elemental distribution of fluted pumpkin leaf. The outcome of this research is a relevant reference point for future similar studies.

Material and methods

The following materials and equipment were used: a magnetic field (MF) pretreatment device; electronic weighing balance (OHAUS, Model 201, China); laboratory oven (Model SM9053, England); desiccator; scanning electron machine (JEOL, JSM-7600F, Japan); and fresh samples of fluted pumpkin leaf (FPL).

Fresh samples of FPL were procured, sorted, washed, cut, measured with the electronic weighing balance and pretreated using the MF device. Three types of magnetic fields (SMF, PMF and AMF) were used in combination with magnetic field strengths within the range (5–30 mT) and at pretreatment time (5–25 min). Fresh and water blanched samples of FPL were used for control purposes. After the pretreatment operation, all samples were immediately dried at 50 °C inside the laboratory oven for approx. 1 hour to an average moisture content of approx. 10% (db) and were taken for microstructural and elemental distribution analyses with the use of SEM. The experiment was conducted at the Food Engineering Laboratory of University of Ilorin, Nigeria in December 2018. The average laboratory temperature and average laboratory relative humidity during the drying process were 31 °C and 61%, respectively.

Results and discussion

Microstructures of MF pretreated fluted pumpkin leaf

Figs. 1(a–h) show the microstructures of FPL samples pretreated with SMF, PMF and AMF, as well as fresh and blanched samples. As it can be observed from the figures, fresh and blanched FPL samples (Figs. 1 h and g) exhibited microstructural features that are clearly different from MF pretreated samples (Figs. 1 a–f). This is an early indication

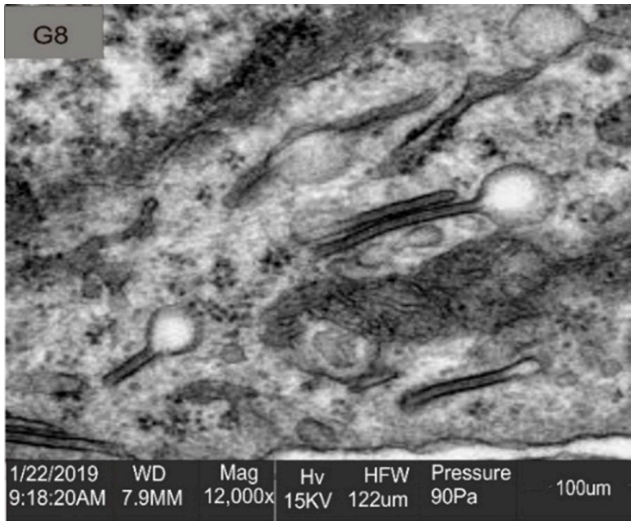

Fig. 1a (i) Microstructure of FPL at SMF (8 mT and 5 min)

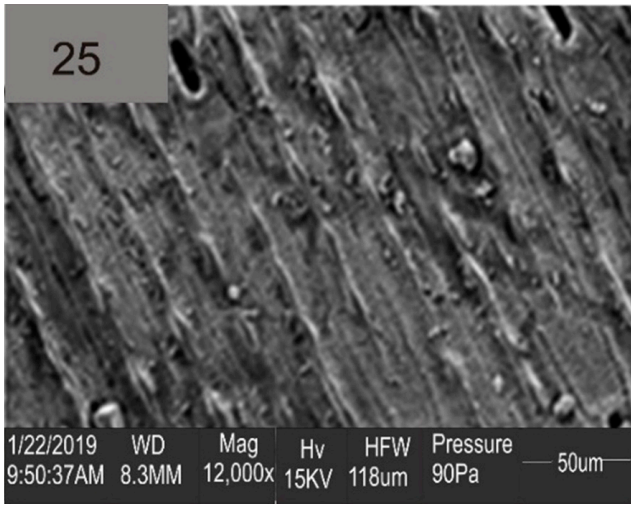

Fig. 1a (ii) Microstructure of FPL at PMF (8 mT and 5 min)

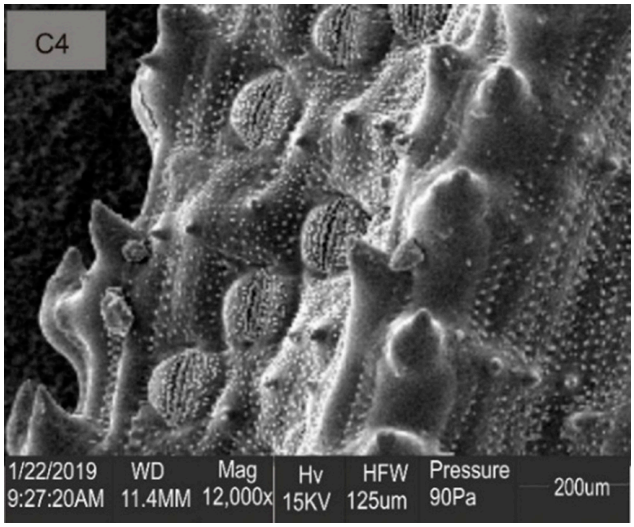

Fig. 1b (i) Microstructure of FPL at SMF (19 mT and 15 min)

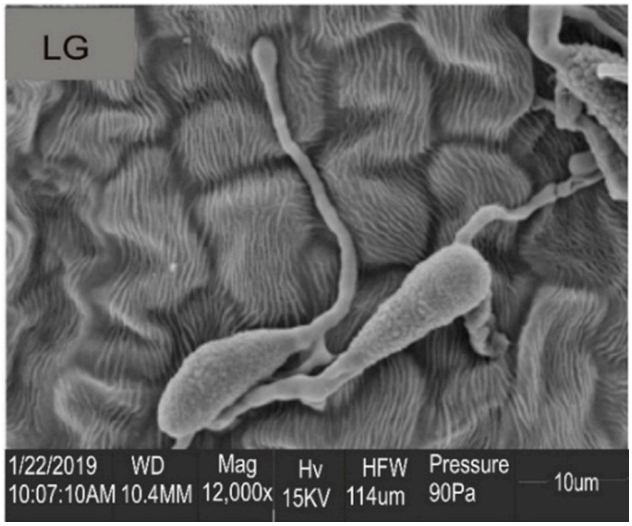

Fig. 1b (ii) Microstructure of FPL at PMF (19 mT and 15 min)

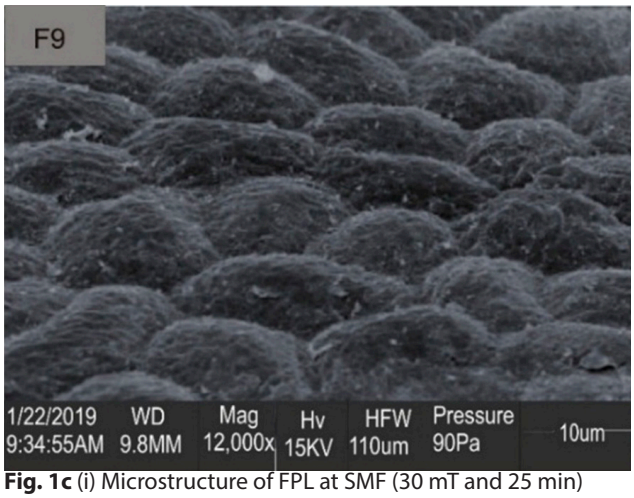

Fig. 1c (i) Microstructure of FPL at SMF (30 mT and 25 min)

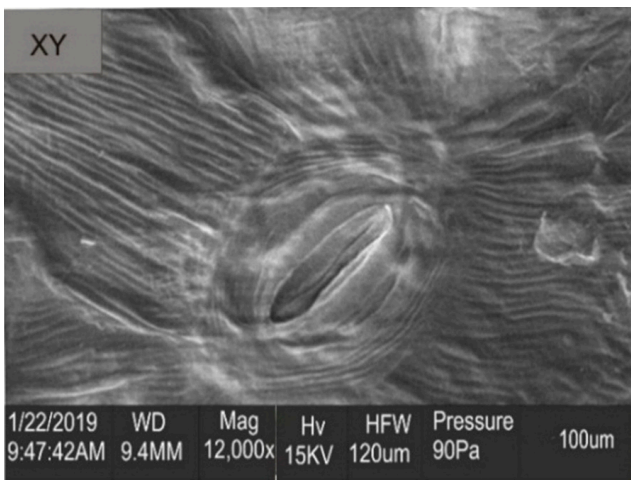

Fig. 1c (ii) Microstructure of FPL at PMF (30 mT and 25 min)

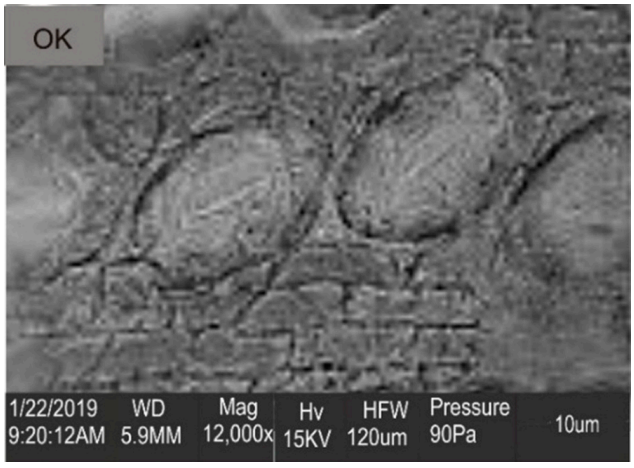

Fig. 1d Microstructure of FPL at AMF (5 mT and 5 min)

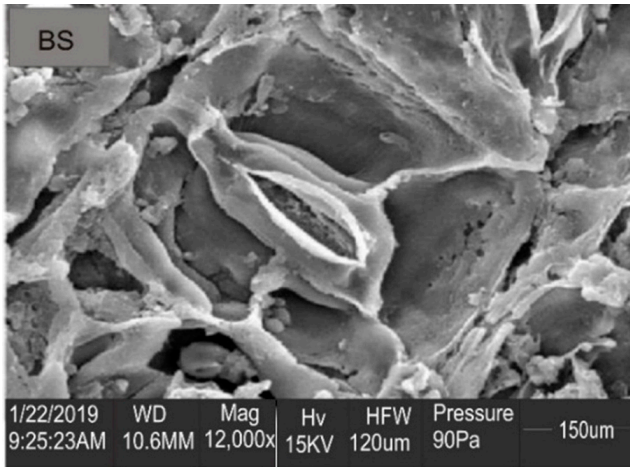

Fig. 1e Microstructure of FPL at AMF (9.5 mT and 15 min)

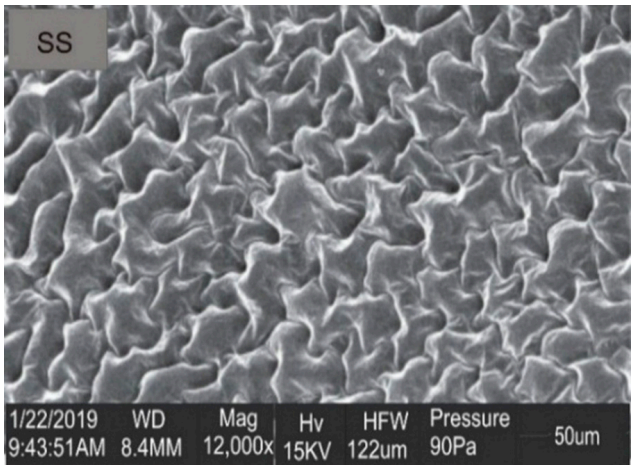

Fig. 1f Microstructure of FPL at AMF (14 mT and 25 min)

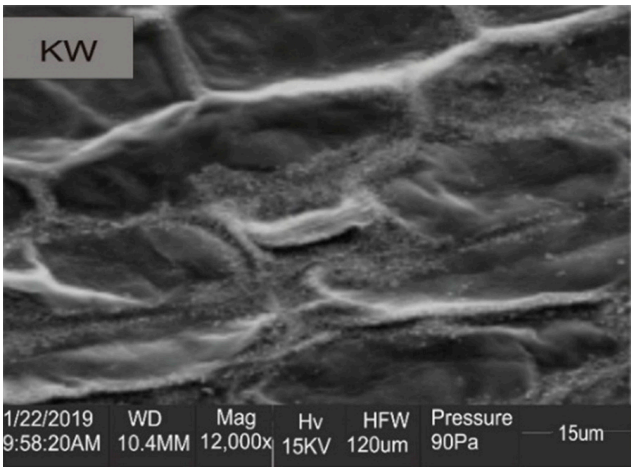

Fig. 1g Microstructure of FPL for blanched

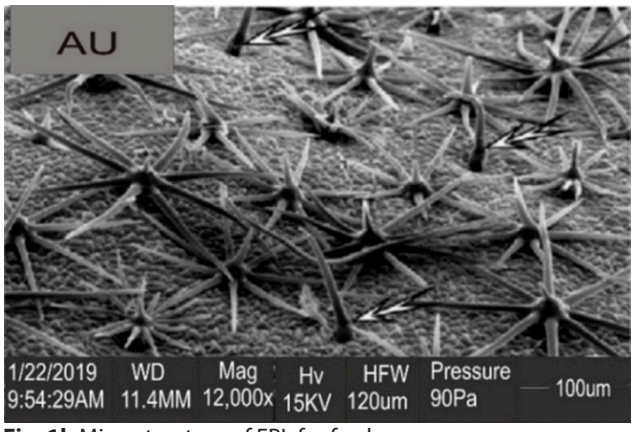

Fig. 1h Microstructure of FPL for fresh

that the three types of magnetic field used for pretreating the products caused different effects on their microstructures. These observations might be due to the fact that SMF, PMF and AMF have different wave patterns and characteristics. SMF is generated with full rectification of alternating current (AC) and its wave pattern is an approximated unidirectional straight line along the positive *x*-axis of voltage (V) versus time (t) graph. PMF is achieved with partial rectification of AC; it is also unidirectional along the positive x-axis with formation of distinct ripples. On the other hand, the AMF is generated when the raw alternating current is flowing; it has the frequency with sinusoidal wave pattern (Bird, 2010); hence, it is non-unidirectional, that is, its wave moves across both the positive and negative horizontal axes of the voltage-time graph.

The microstructures obtained for the MF pretreated FPL samples could be described as puffy: SMF (30 mT and 25 min) – Fig. 1c (i); partially serrated: SMF (19 mT and 15 min) – Fig. 1b (i); with wood bark pattern: PMF – (8 mT and 5 min) – Fig. 1a (ii); with collapsed interlocks: (14 mT and 25 min) – Fig. 1f; with burst puff: AMF (9.5 mT and 15 min) – Fig. 1e; and other patterns that cannot be easily described with high level of certainty. The fresh sample (Fig. 1h) showed multiple clusters of visible spikes, and this pattern did not occur in any of the SMF, PMF, AMF pretreatment combinations, nor the blanched samples (Fig. 1g). Antonio et al. (2008) used SEM to confirm the formation of pores within the microstructure (tissue) of sweet potato; this was achieved when a study on osmotic dehydration and high temperature short time (HTST) pretreatment of sweet potato together with convective drying was conducted. Furthermore, Vodal et al. (2012) reported that blanching process was unable to affect the pore size

Table 1 Elemental distribution of MF pretreated, blanched and fresh FPL samples

Magnetic field types	Na (%)	K (%)	Ca (%)	Mg (%)	Fe (%)
SMF (8 mT and 5 min)	1.30	2.70	5.20	3.70	3.90
PMF (8 mT and 5 min)	2.70	1.30	2.40	5.10	2.00
SMF (19 mT and 15 min)	2.80	2.15	1.61	3.24	3.20
PMF (19 mT and 15 min)	2.00	1.20	1.20	–	2.00
SMF (30 mT and 25 min)	2.96	2.77	2.10	2.80	6.62
PMF (30 mT and 25 min)	3.65	1.95	1.19	–	2.40
AMF (5 mT and 5 min)	4.35	2.17	1.60	3.25	1.22
AMF(9.5 mT and 15 min)	3.09	3.42	2.28	1.90	1.43
AMF (14 mT and 25 min)	2.20	1.40	6.10	2.10	6.00
Blanched	5.10	2.17	3.60	1.25	6.20
Fresh	2.90	1.70	4.40	0.80	2.60

SMF – Static magnetic field; PMF – Pulse magnetic field; AMF – Alternating magnetic field

distribution of freeze-dried winter carrot utilizing the SEM. Moreover, it was reported that no damage was inflicted to the microstructures of apple slices pretreated with osmotic sucrose solution coupled with drying; however, an increase in porosity was observed (Askari et al., 2004).

Elemental distribution of MF pretreated fluted pumpkin leaf

Table 1 presents the elemental distribution in samples at different combinations of the MF pretreatment and comparison of these samples with control samples (blanched and fresh samples). There are variations in the elements in the product at different MF pretreatment combinations. Each MF pretreatment combination led to different values of elements obtained in contrast to other MF pretreatments, as well as to blanched and fresh samples. This observation might be a result of different characteristics of the three types of magnetic field used (Bird, 2010); it is possible that different structures and forms, in which each element naturally exists within the vegetable, have influenced their behaviour in the MF pretreatment; however, the true reason for this might yet to be identified.

Furthermore, from the table, sodium (Na), potassium (K), calcium (Ca), magnesium (Mg) and iron (Fe) were observed to have the lowest and highest respective values: 1.2–4.35% (fresh – 2.9% and blanched – 5.10%); 1.30–3.42% (fresh – 1.70% and blanched – 2.17%); 1.19–6.10% (fresh – 4.40% and blanched – 3.60%); 0–5.10% (fresh – 0.80% and blanched – 1.25%) and 1.22–6.62% (fresh – 2.60% and blanched – 6.20%). The lowest and highest values of elements in the stated ranges for the MF pretreatment were obtained at SMF (8 mT and 5 min) and AMF (5 mT and 5 min) for Na; PMF (19 mT and 15 min) and AMF (9.5 mT and 15 min) for K; PMF (30 mT and 25 min) and AMF (14 mT and 25 min) for Ca; PMF (19/30 mT and 15/25 min) and PMF (8 mT and 5 min) for Mg and AMF (5 mT and 5 min) and SMF (30 mT and 25 min) for Fe. Dhawi et al. (2009) pretreated the seedlings of date palm with static magnetic field (SMF) of strength from 10 mT to 100 mT for 30–360 min. Date palm leaf elemental analysis utilizing inductive couple plasma (ICP) spectroscopy showed increase in the concentrations of Ca, Mg, Mn, Fe, Na, K, and Zn; however, phosphorus (P) concentration dropped with increase in SMF strength and exposure time.

Conclusion

Non-thermal magnetic field pretreatment caused various changes in the microstructures of fluted pumpkin leaf. In majority of cases, this consequently led to better retention/improvement of elements (minerals) present in fluted pumpkin leaf in comparison to blanched and fresh samples. The magnetic field pretreatment caused the fluted pumpkin leaf to have 1.3–4.35% sodium (Na); 1.20–3.42% potassium (K); 1.19–6.10% calcium (Ca); 0–5.10% magnesium (Mg) and 1.22–6.62% iron (Fe). Therefore, magnetic field is a possible non-thermal pretreatment alternative that can be explored for the replacement of blanching (a thermal pretreatment). For future research works, shelf life studies of the processed products using different packaging materials and storage conditions, as well as optimization of the process for selection of the best combination of magnetic field pretreatment factors are recommended.

References

ANTONIO, G. C. – ALVES, D. G. – AZOUBEL, P. M. – MURR, F. E. X. – PARK, K. J. 2008. Influence of osmotic dehydration and high temperature short time processes on dried sweet potato (*Ipomea batata* lam). In Journal of Food Engineering, vol. 84, no. 2008, pp. 375–382.

ASKARI, G. R. – EMAM-JOMEH, Z. – MOUSAVI, M. 2004. Effect of drying method on microstructural changes of apple slices. In Proceedings of the 14th International Drying Symposium (IDS 2004) São Paulo, Brazil, vol. B, pp. 1435–1441.

BARBOSA-CANOVAS, G. V. – SWANSON, B. G. – SAN MARTIN, M. F. – HARTE, F. 2005. Novel Food Processing Technologies: Use of Magnetic Fields as a Non-Thermal Technology. New York : CRC Press, pp. 443–451.

BIRD, J. 2010. Electrical Circuit Theory and Technology. 4th ed. United Kingdom : Elsevier Ltd., pp. 178–179.

DHAWI, F. – AL-KHAYRI, J. M. – HASSAN, E. 2009. Static magnetic field influence on elements composition in date palm (*Phoenix dactylifera* L.). In Research Journal of Agriculture and Biological Sciences, vol. 5, no. 2, pp. 161–166.

HAYDER, I. A. – ASAAD, R. S. A. – AMIR, K. A. 2015. The effect of magnetic field treatment on the characteristics and yield of Iraqi local white cheese. In IOSR Journal of Agriculture and Veterinary Science (IOSR-JAVS), vol. 8, no. 9, pp. 63–69.

HEERTJE, I. 1993. Microstructural studies in fat research. In Food Structure, vol.12, no. 1, pp. 77–94.

IBARA, I. S. – RODRIGUEZ, J. A. – GALAN-VIDAL, C. A. – CEPEDA, A. – MIRANDA, J. M. 2015. Magnetic solid phase extraction applied to food analysis. In Journal of Chemistry, vol. 15, no. 919414, pp. 1–13.

ICNRIP. 2009. Guidelines on limits of exposure of static magnetic field. In Health Physics, vol. 96, no. 4, pp. 504–514.

JIA, J. – WANG, X. – LV, J. – GAO, S. – WANG, G. 2015. Alternating magnetic field prior to cutting reduces wound responses and maintains fruit quality of cut *Cucumis melo* L. cv Hetao. In The Open Biotechnology Journal, vol. 9, no. 230, pp. 230–235.

KOVACS, P. E. – VALENTINE, R. L. – ALVAREZ, P. J. J. 1997. The effect of static magnetic fields on biological systems: Implications for enhanced biodegradation. In Critical Reviews in Environmental Science and Technology, vol. 27, no. 4, pp. 319–382.

KYLE, C. 2015. Influence of magnetic field exposure and clay mineral addition on the fractionation of Greek yogurt whey components. M.Sc. Thesis, Kansas State University, Manhattan, Kansas, USA, pp. 1–96.

LIPIEC, J. – JANAS, P. – BARABASZ, W. 2004. Effect of oscillating magnetic field pulses on the survival of selected microorganisms. In International Agrophysics, vol. 18, pp. 325–328.

NDOR, E. – DAUDA, S. N. – GARBA, M. N. 2013. Growth and yield performances of fluted pumpkin (*Telfairia occidentalis* Hook F.) under organic and inorganic fertilizer on ultisols of North Central Nigeria. In International Journal of Plant and Soil Science, vol. 2, no. 2, pp. 212–221.

NEETOO, H. – CHEN, H. 2004. Alternative Food Processing Technologies. Food Processing: Principles and Applications. 2nd ed., Eds: Stephanie Clark, Stephanie Jung and Buddhi Lamsal. John Wiley and Sons Ltd, pp. 137–169.

OBEAGU, E. I. – CHIKELU, I. F. – OBAREZI, T. N. – OGBUABOR, B. N. – ANAEBO, Q. B. 2014. Haematological effects of fluted pumpkin (*Telfairia occidentalis*) leaves in rats. In International Journal of Life Sciences, Biotechnology and Pharma Research, vol. 3, no.1, pp. 1–11.

ODEWOLE, M. M. – ADESOYE, O. A. – SHADARE, O. A. 2015. Determination of some mechanical properties of ugu seed (*Telfairia occidentalis*) in relation to the design of cracking machine. In Science, Technology and Arts Research (STAR) Journal, vol. 4, no. 3, pp. 187–191.

ORDONEZ, V. M. G. – BERRIO, L. F. 2011. Effect of ultrasound, and magnetic fields on pH and texture (TPA) in beef loin tuna (*Thunnus albacares*). In The 11th International Congress on Engineering and Food, 22–26 May 2011, Greece. Food Materials Science, no. FMS900. Available at: http://www.icef11.org/content/papers/fms/FMS900.pdf

OTERO, L. – MARTINO, M. – ZARITZKY, N. – SOLAS, M. – SANZ, P. 2000. Preservation of microstructure in peach and mango during high-pressure-shift freezing. In Journal of Food Science, vol. 65, no. 3, pp. 466–470.

RAHMAN, M. S. – PERERA, C. O. 2007. Drying and food preservation: In Rahman, M. S. (2nd ed.), Handbook of Food Preservation. Boca Raton, Florida : CRC PRESS, pp. 403–432.

REJAUL, H. B. – WADIKAR, D. D. – SEMAL, A. D. – SHARMA, G. K. 2018. Food microstructure: An instrumental journey into food interior. In Indian Food Industry Magazine, vol. 37, no. 1, pp. 26–32.

STARODUBTSEVA, G. P. – LIVINSKIY, S. A. – GABRIYELYAN, S. Z. – LUBAYA, S. I. – AFANACEV, M. A. 2018. Process control of pre-sowing seed treatment by pulsed electric field. In Acta Technologica Agriculturae, vol. 21, no. 1, pp. 28–32.

TRONCOSO, E. – AGUILERA, J. M. 2009. Food microstructure and digestion. In Food Science and Technology, vol. 23 no. 4, pp. 30–32.

VERBOVEN, P. – DEFRAEYE, T. – NICOLAI, B. 2018a. Food microstructure and its relationship with quality and stability. In Devahastin, S. (1st ed.), Woodhead Publishing Series in Food Science, Technology and Nutrition. Elsevier Ltd., pp. 3–283.

VERBOVEN, P. – DEFRAEYE, T. – NICOLAI, B. 2018b. Measurement and visualization of food microstructure: Fundamentals and recent advances. In Devahastin, S. (ed.), Woodhead Publishing Series in Food Science, Technology, and Nutrition. Food Microstructure and its Relationship with Quality and Stability. Elsevier Ltd., pp. 3–28. https://doi.org/10.1016/B978-0-08-100764-8.00001-0

VODAL, A. – HOMAN, N. – WITEK, M. – DUIJSTER, A. – VAN DALEN, G. – VAN DER SAM, R. – NIJSSE, J. – VAN VLIET, L. – VAN AS, H. – VAN DUYNHOVEN, J. 2012. The impact of freeze-drying on microstructure and rehydration properties of carrot. In Food Research International, vol. 49, pp. 687–693.

Acta Technologica Agriculturae 1
Nitra, Slovaca Universitas Agriculturae Nitriae, 2020, pp. 18–23

THE EFFECTS OF TILLAGE AND FERTILIZERS ON GROWTH CHARACTERISTICS OF KABULI CHICKPEA UNDER MEDITERRANEAN CONDITIONS

Mojtaba NOURAEIN[1]*, Hasan KOUCHAK-KHANI[1], Mohsen JANMOHAMMADI[1], Maryam MOHAMADZADEH[1], Viorel ION[2]

[1]University of Maragheh, Faculty of Agriculture, Iran
[2]University of Agronomic Sciences and Veterinary Medicine of Bucharest, Romania

Mediterranean semi-arid region is sensitive to physical, chemical and biological soil disturbances related to intensive tillage. Presented field experiment was conducted at Razan district, Hamedan, located in central west zone, Iran during the 2017–2018 growing season. It dealt with the effects of different tillage methods and treatments on growth, yield and yield contributing characters of spring Kabuli chickpea (*Cicer arietinum* L.) under irrigated condition. Effects of two tillage methods – inversion tillage (mouldboard ploughing – T1) and non-inversion tillage (chisel ploughing – T2) – in combination with five different fertilization treatments (C: complete fertilizer; 20FYM: 20 Mg·ha^{-1} farmyard manure; 40FYM: 40 Mg·ha^{-1} farmyard manure; NPK: nitrogen, phosphorus, and potassium at 2-1-1 ratio; 0: no fertilizer for the control purposes) were studied. The experiment was carried out in split block design with three replications. Results showed that application of 40FYM under T1 condition significantly decreased the number of days to seedling emergence. The highest number of days to flowering was recorded for plants cultivated with inorganic fertilization and reduced tillage. Application of large amounts of FYM significantly increased the ground cover and canopy width for both tillage methods. The highest number of secondary branches was recorded for combination 40FYM – T1, which was followed by C – T2. The pod number per plant was considerably sensitive to different combination of treatments and the best results were recorded for combinations 40FYM – T2; 20FYM – T2; and 40FYM – T1. A similar trend was also recorded for the total dry matter. The heaviest seeds were observed in cases with the application of high levels of FYM. The highest seed yield was observed for plants cultivated using 40FYM – T2. Furthermore, the highest harvest index was recorded for 40FYM – T2, and C – T2. The results indicate that non-inversion tillage together with high- level FYM application can significantly affect the yield levels.

Keywords: reduced cultivation of chickpea; plant growth; soil organic matter; chemical fertilizer; seed yield

Soil degradation represents one of the most significant issues in terms of maintaining the soil quality and ensuring of food production in the years to come. Soils contain the largest terrestrial carbon pool that is sensitive to climatic changes, as well as changes in utilization of land and agricultural management methods, such as tillage and fertilization (Haddaway et al., 2017). However, various types of human activity can significantly affect the soil organic matter (SOM) pool and thus may decrease the SOM contents and biological activity. If the organisms responsible for decomposition of SOM and binding of soil particles extinct in the soil, soil structure can be easily damaged by rain, wind, etc. This can lead to rainwater runoff and soil erosion, resulting in elimination of potential food for organisms, i.e. the topsoil organic matter (Bot and Benites, 2005).

Soil structure is defined as the manner in which the primary soil particles (sand, silt and clay) are combined and arranged with other solid soil components to form clumps or aggregates; one of the modifiers of soil structure is tillage practice (Shirani et al., 2002). Although soils are tilled principally to reduce weed population, the main aim of soil-manipulating activities lies in stabilization and improvement of crop production. Therefore, selection of the best tillage method, which would be consistent with the conditions, has always been of the greatest interest of agricultural researchers. Although the effects of different tillage intensity have been investigated in some semi-arid Mediterranean regions, its effects have not yet been fully interpreted. This is partly due to the fact that the type of tillage practice and its severity considerably affects other soil properties, such as soil moisture content, the availability of elements, etc. Hence, it is necessary to evaluate tillage methods in terms of different management conditions.

It has been examined that after green revolution, the rate intensity of SOM loss increased considerably. The most important factors affecting this issue include: replacement of mixed vegetation with monoculture of crops and pastures; high harvest index; use of bare fallow; burning of natural vegetation and crop residues; overgrazing; removal of crop residues; drainage and increased amount of fertilizer and pesticide application (Said-Pullicino et al., 2016). Tillage treatments directly or indirectly influence soil hydraulic

Contact address: Mojtaba Nouraein, University of Maragheh, Faculty of Agriculture, Department of Plant Genetics and Production, P. O. Box 55181-83111, Iran, e-mail: mojtabanouraein@yahoo.com

properties, such as water infiltration, etc., which determine the ability of the soil to capture and store water through precipitation or irrigation (Blanco-Canqui et al., 2017; Abbaspour-Gilandeh et al., 2018).

Application of farmyard manure and mulching are considered effective management for semi-arid region and crop cultivation (Kihanda et al., 2007). Organic manure, such as farmyard manure, municipal solid waste, etc., has been utilized as a source of nutrients and organic matter for plants suitable for enhancement of fertility conditions of agricultural lands for a long time (Dao and Cavigelli, 2003). It has been shown that its rational application enhances the water infiltration, water retention, soil water contents, grain yield, and rainfall use efficiency (Cui et al., 2014; Wang et al., 2016). All in all, the improvement in the physical, chemical, and biological properties was achieved by incorporated manures into soils. Multiple studies have shown the beneficial effects of animal manure on soil structural quality, including reduced bulk density, increased porosity, increased water absorption rate, saturated hydraulic conductivity and, etc. (Hati et al., 2006; Fares et al., 2008).

Current tillage methods utilized in semi-arid region of Iran can be divided into two broad groups: inversion tillage and non-inversion tillage. The former is considered a conventional tillage whereby a sequence of operations is applied to make ready a seedling growth zone including complete soil inversion to bury or incorporate crop residues and is usually accompanied by additional mouldboard ploughing (Cooper et al., 2016). The latter is also known as reduced tillage practice (RT), which minimizes the soil disturbance with targeted and appropriate soil disturbance on the basis of specific field needs, meaning that it is necessary to exercise fewer passes in contrast to conventional tillage, but it incorporates the crop residues into the surface (upper 0.1 m) whilst still leaving at least 30% of crop residues on the soil surface (Davies and Finney, 2002). RT methods have the potential to highly improve the soil quality and to reduce soil loss by providing protective crop residues on soil surface, as well as to improve water conservation by decreasing evaporation losses (Morris et al., 2010).

Understanding the changes in plant growth properties under conditions of different tillage methods and fertilizers is important to soil water content and soil nutrient management (Günal et al., 2018). However, lack of data on interactions of soil tillage and fertilizers effects limits the recognition of the efficiency of tillage method on plant growth parameters. Therefore, this information is particularly necessary in the regions with scarce SOM for the purpose of crop production and inappropriate soil conditions are one of the limiting factors for the crop cultivation. Due to the economic and social conditions of semi-arid regions, the use of long-term methods requires the awareness of farmers and their focus on the short-term benefits. The short-term effects of non-inversion tillage along with different fertilizer applications on chickpea performance have scarcely been studied in Iran. The objective of this study was to determine the effects of conventional and RT practices on chickpea yield in a clay loam soil under Mediterranean climate.

Material and methods

This study was conducted at a research farm in Razan, Hamedan province, Iran (latitude 35.39° N, longitude 49.03° E, altitude 1,803 m above sea level) during the 2017–2018 growing season. The location was in the west central part of Iran. The weather is cold and cooler in contrast to other cities in this province. However, summer weather was moderately cool with mean annual temperature 11 °C. The average city annual rainfall was estimated at 350 mm; this mountainous region is generally considered to be moderately cold. According to the Köppen climate classification, location climate is BSk – semi-arid moderate (Peel et al., 2007). The experimental design was a factorial arrangement in the form of randomized complete block design with three replications. Treatments included two tillage methods (T) (T1 is mouldboard ploughing with average depth of 0.3 m plus two repetitions of shallow disk harrowing as inversion tillage method; T2 is chisel ploughing with average depth of 0.15 m plus two repetitions of shallow disk harrowing as non-inversion tillage method) assigned to the main plot. Subplots were treated using five different fertilizers, i.e. C (10% N, 52% P, 10% K, 3.50% S, 0.12% Fe, 0.05% Zn, 0.03% Cu, 0.05% Mn, 0.03% B in recommended dose); 20FYM; 40FYM; NPK (provided from urea, triple superphosphate, potassium sulphate); 0. Six soil samples were prepared from specimens taken at standard depths ranging from 0 to 0.3 m and a composite sample was sent to the laboratory for chemical analysis after mixing. The soil from experimental site was a clay loam soil and it contained 21% sand, 36% silt and 43% clay. The soil showed low organic carbon content (0.41%) with a pH value of 7.54 and total nitrogen and $CaCO_3$ contents of 0.129% and 14%, respectively. Electrical conductivity (EC), as well as iron, manganese, copper, zinc, and potassium contents of the soil were measured at 1.38 $ds \cdot m^{-1}$, 0.79 ppm, 0.61 ppm, 0.41 ppm, 0.43 ppm, and 428 ppm, respectively. Chickpea (*Cicer arietinum* L.) seeds cv. "Arman" were planted on 30 April 2018 and harvested at full maturity stage. Each plot included sixteen rows, 4 m long and spaced at 0.25 m. Seeds were sown 0.05 m apart. Considering the land management, a wheat-chickpea-fallow rotation was applied as a common rotation system in the region. The field, as part of the entire farm, had been managed for 2 years as fallow. Tillage and manure application were performed in February. Planting was carried out one month after manure application. Sprinkler irrigation was applied in 3–7-day intervals. Two seeds were sown per hill and these were thinned to only one seedling per hill after germination. Throughout the entire experiment, pests or diseases did not attack the plants.

Weeds were eliminated by frequent hand weeding. In order to ensure uniform germination, the plot was immediately irrigated after planting. Subsequently, it was irrigated for four times during the growth period. Phenological growth phases were monitored at 1–2-day intervals throughout the season and time to 50% flowering, number of days of vegetative growth period, and number of days to maturity were recorded for each treatment. Canopy width was calculated by measuring the length and breadth of canopy surface for each plant, on the basis of which

the mean canopy width was computed and expressed in centimetre, assuming the canopy is rectangular in shape. Plant freshness and weight, biological yield per plant, seed yield, as well as harvest index were measured from a 2.0 m^2 harvest area from the central four rows of each plot when the crop reached the physiological maturity. Analysis of variance procedures with the statistical program SPSS 15.0 and *LSD* test applied for comparison of means were exploited for the purposes of data processing (Janmohammadi et al., 2017).

Results and discussion

The analysis of variance (ANOVA) showed that the two-way interaction effects of tillage × fertilizer were statistically significant for number of days to emergence. Application of T1 and FYM significantly increased the seedling emergence rate. However, plants cultivated with 0 and chemical fertilizers under T2 showed the highest number of days to emergence. Evaluation of other phenological parameters revealed that application of FYM under T1 significantly reduced the number of days to 50% flowering. The highest number of days to flowering was recorded for plants cultivated under T2 with C. To some extent, similar results were observed for the number of days to podding. In relation to both tillage methods, manure application reduced the necessary number of days to podding. However, plants cultivated with FYM started their podding stage much earlier than others. Despite the differences in reproductive stages, these were not significant in terms of the number of days to maturity; only specimens cultivated utilizing C under T1, and without any fertilizer under T1 showed early maturity in contrast to other treatments (Table 1).

Plant height assessment showed that the tallest plants were recorded for specimens cultivated with combinations of NPK – T1, and C – T2. However, no significant difference was observed between other combinations of tillage methods and fertilizers.

Ground cover percentage assessment showed that the highest value was achieved by application of 40FYM under both tillage conditions. Ground coverage by 20FYM and NPK was slightly lower.

Canopy width investigation showed that chemical fertilizer application under T2 was more efficient than under T1. However, the efficiency of FYM application on canopy width was more evident under T1. The highest number of secondary branches under T1 was related to plants cultivated with 40FYM, whereas the highest number of secondary branches under T2 was related to chemical fertilizers application (C and NPK). The first pod height from the ground level was sensitive to different fertilization treatments only under T1. Plants cultivated with 40FYM and C under T1 showed the highest first pod height. As one of the most important traits in determining the yield, the number of pods per plant was strongly influenced by tillage methods and fertilization treatments. The highest pod number per plant was recorded for plants cultivated with 40FYM under T2, which was followed by 20FYM – T2, and 40FYM – T1 (Fig. 1). A similar trend was also observed in

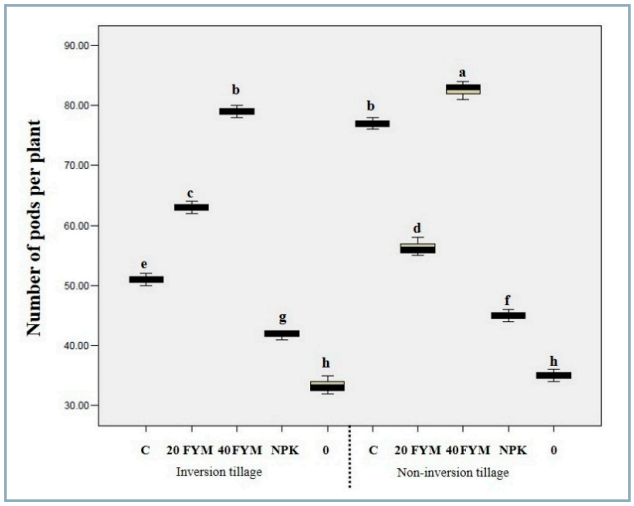

Fig. 1 Effects of different soil fertilizers on the number of pods per plant using different tillage methods; columns with different letters are statistically different at the 5% level

Table 1 Comparison of means of phenological stages and yield components of chickpea (*Cicer arietinum* L.) as affected by fertilizers and tillage methods

	DTE	DTF	DTP	DTM	PH	GC	CW	FPH	STY	HI
T1-C	12.00^{abc}	38.66^{bc}	50.00^{a}	75.66^{d}	27.00^{b}	83.33^{ef}	31.3^{c}	8.66^{a}	226.66^{f}	42.21^{de}
T1-20FYM	9.00^{de}	31.00^{e}	39.66^{e}	83.66^{bc}	30.66^{ab}	96.33^{abc}	43.33^{a}	7.33^{b}	267.00^{d}	43.18^{c}
T1-40FYM	7.33^{e}	29.66^{e}	37.66^{e}	81.00^{cd}	29.66^{ab}	99.33^{a}	44.00^{a}	9.33^{a}	312.00^{a}	44.54^{b}
T1-NPK	12.33^{ab}	39.00^{bc}	49.66^{a}	84.33^{bc}	30.66^{ab}	91.66^{cd}	41.00^{ab}	6.66^{bc}	191.00h	41.68^{fe}
T1-0	12.00^{abc}	38.33^{bc}	49.00^{ab}	80.33^{cd}	28.33^{b}	81.66^{f}g	37.33^{abc}	6.66^{bc}	142.66j	43.00^{c}
T2-C	13.00^{a}	42.00^{a}	50.00^{a}	93.66^{a}	33.00^{a}	94.33^{abcd}	44.00^{a}	6.66^{bc}	290.66^{c}	46.00^{aq}
T2-20FYM	11.00^{bc}	36.66^{cd}	45.00^{cd}	87.00^{b}	28.66^{ab}	92.66^{bcd}	42.00^{ab}	6.33^{c}	262.66^{e}	41.99^{de}
T2-40FYM	10.33^{cd}	34.33^{d}	42.66^{d}	87.00^{b}	26.66^{ab}	98.33^{ab}	40.33^{ab}	6.33^{c}	304.00^{b}	46.49^{a}
T2-NPK	12.66^{ab}	38.66^{bc}	46.66^{bc}	88.66^{ab}	29.33^{ab}	88.33^{de}	45.66^{a}	6.00^{c}	217.33g	51.11^{f}
T1-0	13.33^{a}	4.66^{ab}	49.66^{a}	83.66^{cd}	28.00^{b}	76.66g	33.33^{bc}	5.33^{d}	155.33i	42.53^{cd}

DTE – number of days to emergence, DTF – number of days to flowering, DTP – number of days to podding, DTM – number of days to maturity, PH – plant height, GC – ground cover by canopy, CW – canopy width, FPH – height of the first pod from the ground, STY – straw yield, HI – harvest index. Columns with different letters show statistically significant difference at the 5% level

terms of plant dry matter. Plants cultivated with 0 showed the lowest dry matter. Straw yield evaluation showed that application of high level of FYM (40 Mg·ha^{-1}) under T1 significantly increased the straw yield. The highest straw yield under T2 was shown by plants cultivated using NPK.

Furthermore, seed size (100 seed weight) was also affected by fertilization treatment. ANOVA showed that the two-way interaction effects of tillage × fertilizer application was statistically significant for this yield component. Plants cultivated with 40FYM under both tillage conditions showed larger seeds (Fig. 2). Considering the seed weight, results showed that the effectiveness of fertilizers under T2 was lower than under T1. Application of C and high levels of FYM significantly increased the number of full pods under both tillage conditions. However, the highest number of semi-filled pods and wrinkled seeds was observed in plants cultivated with NPK and without application of any fertilizer. Seed yield evaluation revealed that the best results were acquired with application of 40FYM and under non-inversion tillage condition. The lowest seed yield was recorded for plants cultivated under inversion tillage without fertilizer application (Fig. 3).

Regarding Fig. 4, the most prominent relations are: a strong positive association between seed yield, 100 seed weight, straw yield, plant dry matter, first pod height, canopy width, pod number per plant as indicated by the steep angles close to zero between their vectors (r = cos 0 = +1).

The cluster analysis of combined treatments based on similarity is shown in Fig. 5. Cluster II showed the lowest performance; it includes 0 under both tillage conditions. Cluster IV includes combined treatments that had the most positive effect on evaluated properties; it contains 40FYM – T2; C – T2; and 40FYM – T1.

Presented findings revealed that phenological development is affected by fertilizers and tillage methods. Plant development is also influenced by the availability of elements and other optimal conditions, such as soil moisture. Results showed that application of NPK and C had the most positive effects on phenological stages. This resulted from high availability and rapid supply of elements via chemical fertilizers for the plant. Moreover, effects of non-inversion tillage were more prominent than those of inversion tillage; this is partly due to the low soil disturbance and high soil moisture content, as well as reduced element leaching. Crop phenology is essential for prediction of physiological responses under varying field conditions. Specifically, in order to avoid confrontation of sensitive developmental stages with adverse seasonal conditions, selection and application of fertilizer and tillage method (changing conditions of the rhizosphere) must be taken into careful consideration in semi-arid regions (Janmohammadi et al., 2014). It is encouraging to compare the obtained results with Sharifi and Namvar (2016), who found that higher nutrient availability and favourable soil conditions can delay crop phenology due to organic source of N.

Furthermore, it was observed that tillage methods and fertilizer application have also impact on canopy height and transverse growth components, such as height and ground cover percentage. Plant growth is controlled by phytohormones ratio. Most stature growth was recorded for plants cultivated utilizing chemical fertilizers under

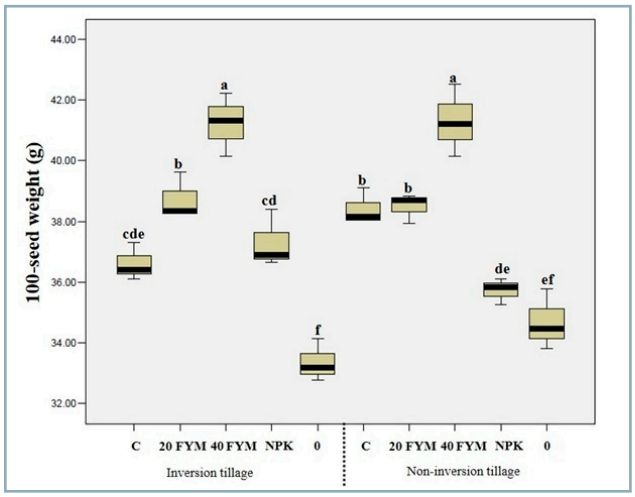

Fig. 2 Effects of different soil fertilization treatment on 100-seed weight under different tillage methods; columns with different letters are statistically different at the 5% level

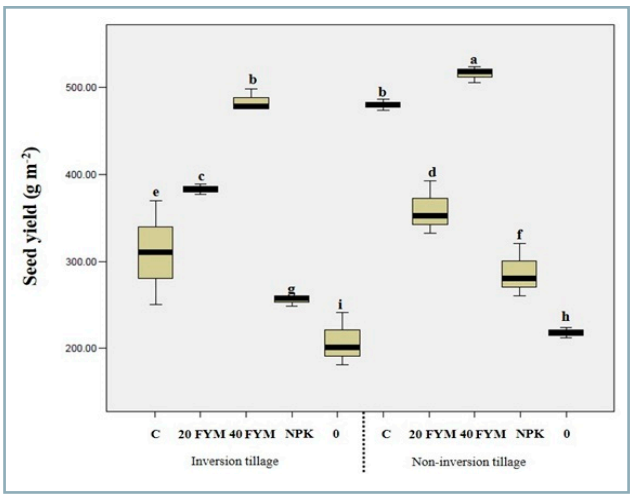

Fig. 3 Effects of different soil fertilization treatment on seed yield under different tillage methods; columns with different letters are statistically different at the 5% level

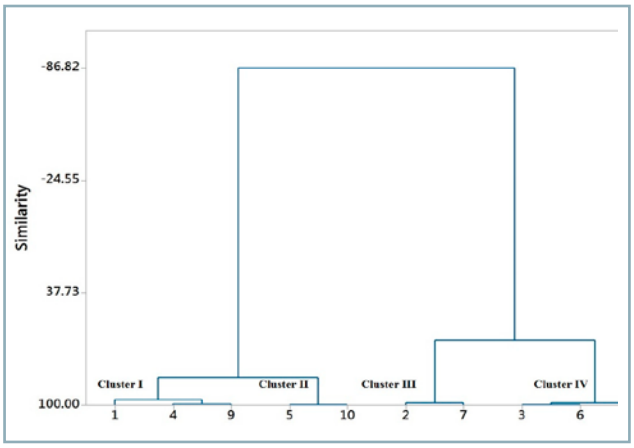

Fig. 4 Cluster analysis of different soil fertilization and tillage methods
1: C – T1; 2: 20FYM – T1; 3: 40FYM – T1; F4: NPK – T1; F5: 0 – T1; 6: C – T2; 2: 20FYM – T2; 3 – 40FYM – T2; F4: NPK – T2; F5: 0 – T2

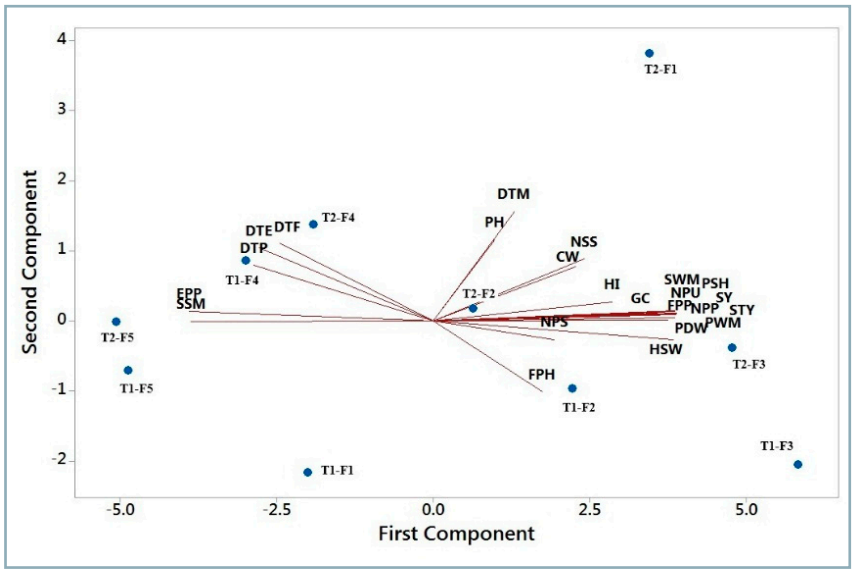

Fig. 5 PCA biplot: spatial distribution of different morpho-physiological traits of chickpea under different soil fertilization and tillage methods using the first two PCs; traits with smaller angles have a significant positive correlation
DTE – number of days to emergence, DTF – number of days to flowering, DTP – number of days to podding, DTM – number of days to maturity, PH – plant height, GC – ground cover by canopy, CW – canopy width, NPS – number of primary branches per plant, NSS – number of secondary branches per plant, FPH – the first pod height from the ground, NPP – number of pod per plant, NPU – pod number per m^2, PDW – plant dry matter per m^2, PWM – pod weight per m^2, SY – seed weight per m^2, STY – straw yield, PSH – pod shell weight, HSW – 100-seed weight, EPP – percentage of empty pods, HI – harvest index)

non-inversion tillage. Increase in plant height due to higher N concentration can be attributed to better vegetative development that resulted in increased mutual shading and intermodal extension. The results indicate that the application of chemical fertilizers has a more pronounced effect than FYM application due to rapid release of the elements in short term. Differences in impacts of tillage methods in question were not significant in this case. In addition to this, results suggest that the non-inversion tillage without application of FYM was not able to create a stable structure and there was not any positive effect on the physical soil properties. On the other hand, it seems that the soil deformation due to wetting and drying, rain and disintegration of soil aggregates was more prominent in cases when inorganic fertilizers were applied.

The results showed that the highest seed yield was acquired by application of high level of FYM under non-inversion tillage. Seed yield is affected by environmental, nutritional and soil conditions and this is more prominent in semi-arid region, where soil and moisture conditions are not so favourable.

Soil quality is affected by multiple external factors, such as utilization of land, soil and crop management, environmental interactions, human objectives, and various natural conditions. Soil organic matter (SOM) is a major indicator of soil quality and health and is strongly influenced by agricultural and fertilization managements. SOM is a major soil source of S, P, N, C; their mobilization, availability and accessibility are continuously changing due to microbial immobilization and mineralization. Furthermore, it improves soil physical properties, water conservation and nutrient availability, ultimately leading to higher biomass content and seed yield. However, the most important factor in semi-arid regions, such as the studied site, is that reduced tillage methods cannot be effective without application of large amounts of FYM. Considering the low rainfall in the studied area and minor return of plant residues to soil, the frequent use of FYM or its combined use with chemical fertilizers can improve performance via optimization of conditions. These results are consistent with Hati et al. (2006) and Naab et al. (2017) and suggest that manure application and reduced tillage improve the plant growth and seed yield in semi-arid regions by improving the soil properties, such as enhanced aggregation root proliferation, increased saturated hydraulic conductivity, reduced mechanical resistance and bulk density.

Selection of the most economical tillage method depends on a number of factors and varies from farm to farm (Epplin and Vitale, 2008; Garcia-Franco et al., 2018). However, since soil and management conditions in the area are relatively similar, experimental results can be generalized. Non-inversion tillage has the potential to conserve soil and water by reducing their loss relative to some form of conventional tillage. It can also reduce time and energy use for crop establishment and nonpoint pollution, as well as enhance the storage or retention of SOM and improve the soil quality at the soil surface. The latter is especially important because SOM preservation can improve the soil water storage and reduce the need for irrigation. In terms of economy and energy saving, there was shown a significant positive effect.

Moreover, it seems that fertilizers can significantly affect the crop nutritional quality. There was observed an increase in concentrations of proteins in cereals and pulses; oil in oilseed crops; starch in tubers; and of essential amino acids and vitamins in vegetables. However, excessive fertilizer application, especially N-based fertilizers, can result in undesirable changes, such as increase in nitrate, titratable acidity and acid-to-sugar ratio and decrease in concentrations of vitamin C, soluble sugar, soluble solids, and Mg and Ca in certain crops. Other agronomic measures, such as tillage and crop rotation, organic farming, soil moisture management, crop breeding and genetic engineering, can also have a large impact on food crop quality; however, potential benefits of these measures for improving the crop quality has not yet been fully explored.

Conclusion

The results revealed that the effects of fertilizers on the evaluated traits depend on applied tillage methods.

Experimental research showed that conservation tillage method without application of organic fertilizers does not have any significant effect on plant growth in short term. Due to the unfavourable soil conditions of semi-arid regions, non-inversion tillage alone is not sufficiently efficient and requires high levels of FYM. Enhancement of plant growth values was recorded for non-inversion tillage method with application of 40FYM fertilizer; this combination of tillage method and fertilizer can improve the physical soil properties and structural stability, minimizing the negative consequences of low water or air penetration on the lower soil layers.

Finally, findings showed that if the soil tillage method is changed, it is necessary to select an appropriate and suitable fertilizer management compatible with the tillage method.

Acknowledgements

Authors gratefully acknowledge all financial supports provided from University of Maragheh. Also, the authors would like to thank the experts of Central Laboratory (depended on Laboratory Network of Strategic Technologies) for their assistance in some analysis.

References

ABBASPOUR-GILANDEH, Y. – HASABKHANI-GHAVAM, F. – SHAHGOLI, G. – RASOOLI SHARABIAN, V. – ABBASPOUR-GILANDEH, M. 2018. Investigation of the effect of soil moisture content, contact surface material and soil texture on soil friction and soil adhesion coefficients. In Acta Technologica Agriculturae, vol. 21, no. 2, pp. 44–50.

BLANCO-CANQUI, H. – WIENHOLD, B. J. – JIN, V. L. – SCHMER, M. R. – KIBET, L. C. 2017. Long-term tillage impact on soil hydraulic properties. In Soil and Tillage Research, vol. 170, pp. 38–42.

BOT, A. – BENITES, J. 2005. The importance of soil organic matter: Key to drought-resistant soil and sustained food production (No. 80). Food and Agriculture Organization of the United Nations, Rome, Italy.

COOPER, J. – BARANSKI, M. – STEWART, G. – NOBEL-DE LANGE, M. – BÀRBERI, P. – FLIEßBACH, A. – PEIGNÉ, J. – BERNER, A. – BROCK, C. – CASAGRANDE, M. – CROWLEY, O. 2016. Shallow non-inversion tillage in organic farming maintains crop yields and increases soil C stocks: a meta-analysis. In Agronomy for Sustainable Development, vol. 36, no. 1, pp. 22–29.

CUI, H. Y. – WEI-CHENG, X. U. – SUN, Y. M. – NIU, J. Y. – FANG, Z. S. 2014. Effects of different organic manures application on soil moisture, yield and quality of oil flax. In Journal of Soil and Water Conservation, vol. 28, pp. 307–312.

DAO, T. H. – CAVIGELLIB, M. A. 2003. Mineralizable carbon, nitrogen, and water-extractable phosphorus release from stockpiled and composted manure and manure-amended soils. In Agronomy Journal, vol. 95, pp. 405–413.

DAVIES, D. B. – FINNEY, J. B. 2002. Reduced cultivations for cereals: research, development and advisory needs under changing economic circumstances. Kenilworth : Home Grown Cereals Authority. London.

EPPLIN, F. M. – VITALE, J. 2008. Chapter 6. Economics: No-till versus conventional tillage. In MALONE, J. No-till Cropping Systems in Oklahoma. Oklahoma State University, USA.

FARES, A. – ABBAS, F. – AHMAD, A. – DEENIK, J. L. – SAFEEQ, M. 2008. Response of selected soil physical and hydrologic properties to manure amendment rates, levels, and types. In Soil Sciences, vol. 173, pp. 522–533.

GARCIA-FRANCO, N. – HOBLEY, E. – HUBNER, R. – WIESMEIER, M. 2018. Chapter 23. Climate-smart soil management in semiarid regions. In MUNOZ, M. A. – ZORNOZA, R. 2017. Soil Management and Climate Change. Science Direct, Academic Press. ISBN 978-0-12-812128-3.

GÜNAL, E. – ERDEM, H. – ÇELIK, İ. 2018. Effects of three different biochars amendment on water retention of silty loam and loamy soils. In Agricultural Water Management, vol. 208, pp. 232–244.

HADDAWAY, N. R. – HEDLUND, K. – JACKSON, L. E. – KÄTTERER, T. – LUGATO, E. – THOMSEN, I. K. – LUGATO, E. – THOMSEN, I. K. – JØRGENSEN, H. B. – ISBERG, P. E. 2017. How does tillage intensity affect soil organic carbon? A systematic review. In Environmental Evidence, vol. 6, no. 1, pp. 30.

HATI, K. M. – MANDAL, K. G. – MISRA, A. K. – GHOSH, P. K. – BANDYOPADHYAY, K. K. 2006. Effect of inorganic fertilizer and farmyard manure on soil physical properties, root distribution, and water-use efficiency of soybean in vertisols of central India. In Bioresource Technology, vol. 97, no. 16, pp. 2182–2188.

JANMOHAMMADI, M. – NASIRI, Y. – ZANDI, H. – KOR-ABDALI, M. – SABAGHNIA, N. 2014. Effect of manure and foliar application of growth regulators on lentil (*Lens culinaris*) performance in semi-arid highland environment. In Botanica Lithuanica, vol. 20, no. 2, pp. 99–108.

JANMOHAMMADI, M. – JAVANMARD, A. – SABAGHNIA, N. – NASIRI, I. 2017. The effect of balanced nutrition and soil amendments on productivity of chickpea (*Cicer arietinum* L.). In The Agricultural Society of Thailand, vol. 5, no. 2, pp. 76–86.

KIHANDA, F. M. – WARREN, G. P. – MICHENI, A. N. 2007. Effects of manure application on crop yield and soil chemical properties in a long-term field trial in semi-arid Kenya. In Advances in Integrated Soil Fertility Management in Sub-Saharan Africa: Challenges and Opportunities. Dordrecht : Springer.

MORRIS, N. L. – MILLER, P. C. H. – ORSON, J. H. – FROUD-WILLIAMS, R. J. 2010. The adoption of non-inversion tillage systems in the United Kingdom and the agronomic impact on soil, crops and the environment – A review. In Soil and Tillage Research, vol. 108, no. 1–2, pp. 1–15.

NAAB, J. B. – MAHAMA, G. Y. – YAHAYA, I. – PRASAD, P. V. V. 2017. Conservation agriculture improves soil quality, crop yield, and incomes of smallholder farmers in North Western Ghana. In Frontiers in Plant Science, vol. 8, p. 996.

PEEL, M. C. – FINLAYSON, B. L. – MCMAHON, T. A. 2007. Updated world map of the Köppen-Geiger climate classification. In Hydrology and Earth System Sciences Discussions, vol. 4, pp. 439–473.

SAID-PULLICINO, D. – MINIOTTI, E. F. – SODANO, M. – BERTORA, C. – LERDA, C. – CHIARADIA, E. A. – ROMANI, M. – CESARI DE MARIA, S. – SACCO, D. – CELI, L. 2016. Linking dissolved organic carbon cycling to organic carbon fluxes in rice paddies under different water management practices. In Plant and Soil, vol. 401, no. 1–2, pp. 273–290.

SHARIFI, R. S. – NAMVAR, A. 2016. Effects of time and rate of nitrogen application on phenology and some agronomical traits of maize (*Zea mays* L.). In Biologija, vol. 62, No. 1. pp. 35–45.

SHIRANI, H. – HAJABBASI, M. A. – AFYUNI, M. – HEMMAT, A. 2002. Effects of farmyard manure and tillage systems on soil physical properties and corn yield in central Iran. In Soil and Tillage Research, vol. 68, no. 2, pp. 101–108.

WANG, X. – JIA, Z. – LIANG, L. – YANG, B. – DING, R. – NIE, J. – WANG, J. 2016. Impacts of manure application on soil environment, rainfall use efficiency and crop biomass under dryland farming. In Scientific Reports, vol. 6, p. 20994.

sciendo

DOI: 10.2478/ata-2020-0005

Acta Technologica Agriculturae 1
Nitra, Slovaca Universitas Agriculturae Nitriae, 2020, pp. 24–29

GYROSCOPIC EFFECT IN MACHINE WORKING ASSEMBLIES

Marcin ZASTEMPOWSKI*, Andrzej BOCHAT

UTP University of Science and Technology, Bydgoszcz, Poland

This paper discusses and calculates the impact of the gyroscopic effect on the increase in the agricultural machine working assemblies' load on bearings of the chaff cutter type. This effect occurs under natural field operational conditions of this type of machine either during the change in direction of its movement or moving over irregular surface and is caused by a sudden change in the axis direction of quickly rotating masses. In a form of graph, there is a presentation of a mathematical model and exemplary results of simulation calculations for selected parameter values related to the movement and operation of machines with a high-speed drum. Calculations were conducted on the basis of analysis of technical data of working machines of the chaff cutter type. Conducted analysis of the agricultural machine working assemblies' load on bearings showed that these loads may temporarily increase even by ten times in case of the machine turn and eight times in case of moving over irregular of surface, considerably influencing their lifetime.

Keywords: increased load on bearings; high-speed machine working assemblies; bearing load in cutting assemblies; bearing load in working machines; mathematical model

Working assemblies of many machines and devices comprise high-speed elements with a high moment of inertia, rotating around a dynamic symmetry creating the so-called gyroscope, their movement being called the gyroscopic proper motion.

When a gyroscope axis is motionless, machine bearings are loaded with interaction:

- working one, resulting from an operation performed by a rotating element;
- gravitational, resulting from interaction with gravitational field.

Gyroscopic effect occurs in cases when the axis of quickly rotating masses would change its direction.

Such a phenomenon occurs in working machines of either chaff cutter type or combine harvester type during turning or driving over irregular surfaces. Subsequently, there is an additional, quick-changing load on bearings in cutting drums of a chaff cutter or rotating bearings of threshing assemblies in combine harvesters, in which there is a tendency of changes in the direction of a gyroscope axis. This phenomenon also occurs in bearings of ship propulsion turbine during changing of course when it moves together with the vessel around the vertical axis or in case of strong swaying due to waves.

In contemporary literature, there is no detailed analysis of the gyroscopic effect impacts on the balance of forces load on the bearing elements. Subject area related to kinematics and dynamics of machine working assemblies' movement has already been discussed in a detailed manner; however, modelling of the working processes has never taken the gyroscopic effect into consideration. Flizikowski et al. (2015), Keska and Gierz (2011), Zastempowski and Bochat (2014, 2015, 2016) have dealt with this issue.

Multiple scientific studies (Ligaj and Szala, 2010; Strzelecki et al., 2016) have presented the issues related to design and analysis of construction resistance, rules for manufacturing execution system use, numerical and mathematical modelling, and construction optimization.

Vital issue, with which the designers must cope, lies in appropriate design of machines equipped with quick-rotating working assemblies. It is possible if all dependencies and relations resulting from the impacts of the gyroscopic effect on the bearing load are fully recognized and taken into account.

Due to universality of occurrence and availability of input data for simulation calculations, the analysis was conducted for a working machine of a self-propelled chaff cutter type. It was equipped with a high-speed drum cutting assembly located in the machine body. Special attention should be paid to this issue, as subject of cutting assemblies is very topical, since they represent the basic working assemblies in a large group of agricultural machines for crop harvesting for energetic purposes (biomass), fodder, as well as consumption.

The mathematical model developed in the article takes fully into consideration the cases of gyroscopic effect occurring as a result of the machine turning and running over irregular surface under field operational conditions.

Contact address: Marcin Zastempowski, UTP University of Science and Technology, Faculty of Mechanical Engineering, Al. Kaliskiego 7, 85-796 Bydgoszcz, Poland; e-mail: zastemp@utp.edu.pl

Material and methods

The gyroscopic effect during the turning of the chaff cutter

Fig. 1 presents a scheme of rotating chaff cutter drum [2] mounted on the shaft [3] with a determined coordinate system. The shaft with drum is located above the vehicle front axis and is mounted in points *A* and *B*. In the drum gravity centre [0], there is centred a dextrorotatory Cartesian coordinate system *xyz*, so that the system's axes follow the main drum's inertial axes. The mass moment of inertia towards these axes amounts to: J_x, J_y, J_z, respectively.

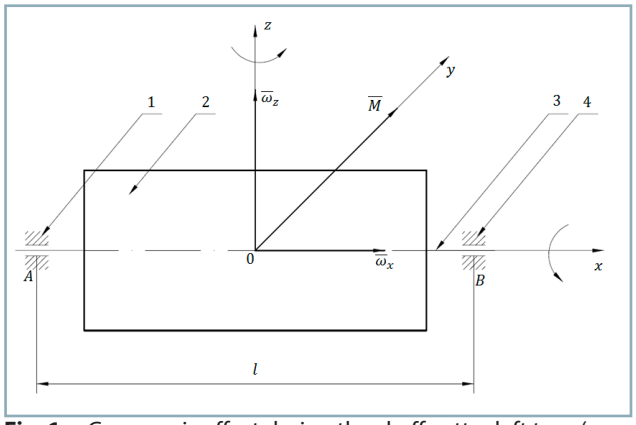

Fig. 1 Gyroscopic effect during the chaff cutter left turn (own study)
1 – place of the shaft support (left bearing A); 2 – rotating cutting drum; 3 – shaft; 4 – place of the shaft support (right bearing B)

The gyroscope is created by the drum rotating at an angular speed ω_x around the axis *x*. The axis *y* follows the direction of a vehicle rotation at the speed *v*. A case of turning the vehicle to the left, corresponding to the angular speed described with vector $\bar{\omega}_z$ in relation to axis *z*, will be analysed.

For any vector $\bar{H}$ at a momentary rotational momentum ω, the derivative of that vector will take the following in regard to time *t* (Landau and Lifszyc, 2012):

$$\frac{d\bar{H}}{dt} = \bar{\omega} \times \bar{H} \tag{1}$$

Therefore, by means of an analogy to the gyroscope angular momentum $\bar{K}$, the following expression (Eq. 2) was received:

$$\frac{d\bar{K}}{dt} = \bar{\omega}_z \times \bar{K} = \bar{\omega}_z \times \left(J_x \bar{\omega}_x + J_z \bar{\omega}_x\right) \tag{2}$$

Taking into account that $\bar{\omega}_z \times \bar{\omega}_z = 0$, and the fact that the derivative of the angular momentum after a time equals to the moment of external forces $\bar{M}$ acting on the gyroscope, the dependence describing the gyroscopic effect will have the following form:

$$\bar{M} = \bar{\omega}_z \times J_x \bar{\omega}_x \tag{3}$$

Analysing the chaff cutter movement during its turning to the left, the direction of the momentum vector $\bar{M}$ coincides with the axis *y*, and three vectors $\bar{\omega}_z$, $\bar{\omega}_x$, $\bar{M}$ form the dextrorotatory system. Thus, it is possible to describe the absolute value of the moment $M = |\bar{M}|$ by:

$$M = J_x \omega_x \omega_z \tag{4}$$

where:
ω_x – is described by the dependency $\omega_x = |\bar{\omega}_x|$
ω_z – is described by the dependency $\omega_z = |\bar{\omega}_z|$
M – is described by the dependency $M = |\bar{M}|$

The geometry scheme of the chaff cutter turning is presented in Fig. 2.

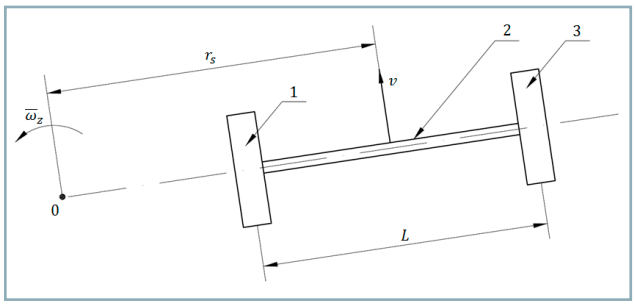

Fig. 2 Geometry scheme of the chaff cutter turning to the left (own study)
1 – vehicle left wheel; 2 – vehicle axis; 3 – vehicle right wheel

By analysis of this vehicle type movement at the speed ν around the point 0, the value of the angular speed ω_z at the turning radius r_s may be established as:

$$\omega_z = \frac{\nu}{r_s} \tag{5}$$

The mass moment of inertia J_x can be described with the following dependence:

$$J_x = r_b^2 m \tag{6}$$

where:
r_b – radius of gyration, i.e. the radius on which it is pointwise located, with mass equal to the mass of the drum
m – mass of the drum

The force of gravitational interaction G_g on a single bearing amounts to:

$$G_g = \frac{1}{2} mg \tag{7}$$

where:
g – gravitational acceleration

However, the effect of the gyroscopic interaction force Gż on the bearing can be described by the dependence:

$$G_{\dot{z}} = \frac{M}{l} \tag{8}$$

where:
M – moment described by Eq. 4
l – spacing of the drum bearings (Fig. 1)

Joining the dependences (Eqs. 5–8), the influence of the gyroscopic effect $G_{\dot{z}}$ on the bearing can be determined in relation to gravitational interactions G_g in the form of:

$$\frac{G_{\dot{z}}}{G_g} = \frac{\beta^2}{2\alpha}\frac{d}{l}\frac{d}{L}\frac{\omega_x \nu}{g} \tag{9}$$

The dimensionless parameter α in Eq. 9 describes the twist radius r_s dependent on the spacing of machine wheels L; the parameter β describes the mass distribution of the chaff cutter drum in accordance with Eqs. 10 and 11:

$$\alpha = \frac{r_s}{L} \tag{10}$$

$$\beta = \frac{2r_b}{d} \tag{11}$$

where:
d – drum diameter
β – number from the range (0; 1) describing the splitting of the drum mass

In such a manner, the quotient $\frac{G_{\dot{z}}}{G_g}$ will be calculated as a product of dimensionless expressions.

The gyroscopic effect during the movement of the chaff cutter over irregular surface

Fig. 3 presents the analogical mechanical system as Fig. 1. The drum mounted on the shaft rotates at the angular speed ω_x. The case of left wheel movement over irregular surface, which corresponds to the angular speed described with the vector $\bar{\omega}_y$ with direction of axis y, will be subjected to analysis.

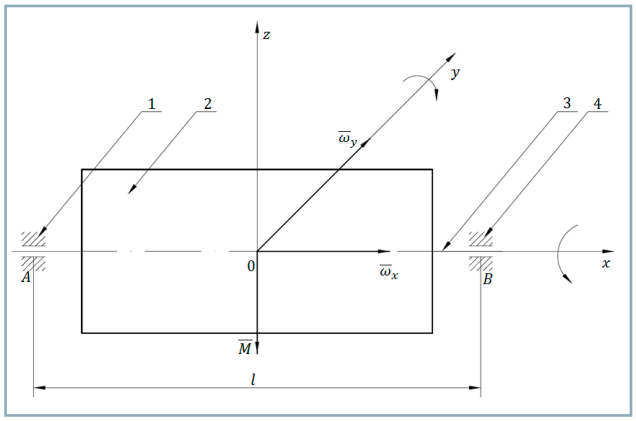

Fig. 3 Gyroscopic effect on the left wheel of the chaff cutter moving over irregular surface (own study)
1 – place of the shaft support (left bearing A); 2 – rotating cutting drum; 3 – shaft; 4 – place of the shaft support (right bearing B)

In this case, the angular momentum of gyroscope can be described as:

$$\bar{K} = J_x \bar{\omega}_x + J_y \bar{\omega}_y \tag{12}$$

The derivative of the moment of momentum in relation to the time amounts to:

$$\frac{d\bar{K}}{dt} = \bar{\omega}_y \times \left(J_x \bar{\omega}_x + J_y \bar{\omega}_y\right) = \bar{\omega}_y \times J_x \bar{\omega}_x + \bar{\omega}_y \times J_y \tag{13}$$

Since:

$$\bar{\omega}_y \times J_y \bar{\omega}_y = 0 \tag{14}$$

and

$$\frac{d\bar{K}}{dt} = \bar{M} \tag{15}$$

the gyroscopic effect on the wheel during movement over the irregular surface can be described by the following equation:

$$\bar{M} = \bar{\omega}_y \times J_x \bar{\omega}_x \tag{16}$$

Direction of the moment $\bar{M}$ of the left wheel during movement over irregular surface corresponds with the axis z. Three vectors $\bar{\omega}_x$, $\bar{\omega}_y$ and $\bar{M}$ form a dextrorotary system. Therefore, the absolute value of the moment $\bar{M} = |\bar{M}|$ can be described by dependence:

$$M = J_x \omega_x \omega_y \tag{17}$$

The value of angular speed ω_y can be determined by means of analysis of the movement process over irregular surface in accordance with Fig. 4.

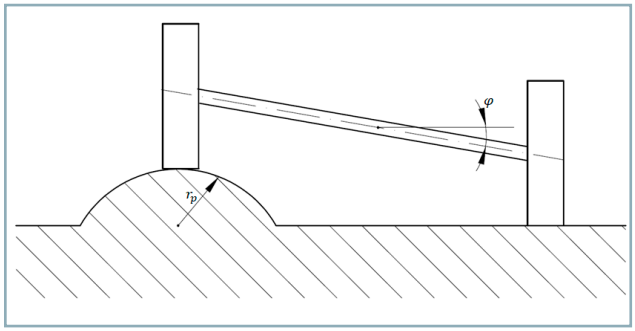

Fig. 4 General scheme of the chaff cutter left wheel movement over irregular surface with radius r_p (own study)

Half of the roller with a radius r_p has been assumed as the irregularity model. In the middle of the obstacle – point P – there was located the system of coordinates hs. The monitoring process (Fig. 5) of the wheel track with the radius r_k began in the moment of the wheel's contact with the obstacle in point A. Subsequently, there occurs a rapid raising of wheel from the ground, which can be described

with a derivative *dh*/*ds*. For a driving medium marked with point *K*, the coordinates *a*, *b* were assumed.

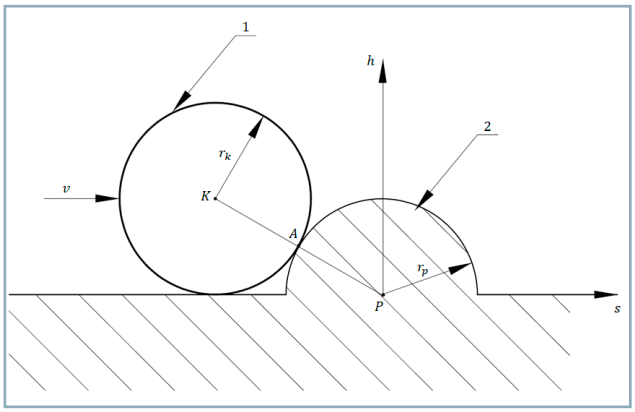

Fig. 5 Movement geometry of the left wheel over irregular surface (own study)
1 – machine wheel; 2 – surface irregularity

The coordinate *b* amounts to:

$$b = r_k \tag{18}$$

while the coordinate *a* is determined by the following equation:

$$a^2 + b^2 = (r_k + r_p)^2 \tag{19}$$

from which follows:

$$a = -\sqrt{2r_k r_p + r_p^2} \tag{20}$$

The inclination coefficient *k* of the segment *KP* was determined from the following dependence:

$$k = \frac{b}{a} \tag{21}$$

Since the tangent in point *A* is perpendicular to the section *KP*, it means that:

$$\frac{dh}{ds} = -\frac{1}{k} \tag{22}$$

Taking the Eqs. 18–21 into account, the derivative *dh*/*ds* can be written as:

$$\frac{dh}{ds} = \sqrt{2\frac{r_p}{r_k} + \left(\frac{r_p}{r_k}\right)^2} \tag{23}$$

For the purposes of the below analysis it has been assumed that the angular speed of the chaff cutter's axis is equal to the angular speed ω_y of the gyroscope axis.

Since:

$$\omega_y = \frac{d\varphi}{dt} \tag{24}$$

and the differential $d\varphi$ can be obtained with dependence:

$$d\varphi = \frac{1}{L} dh \tag{25}$$

Eq. 24 will be of the following form:

$$\omega_y = \frac{1}{L}\frac{dh}{dt} = \frac{1}{L}\frac{dh}{ds}\frac{ds}{dt} = \frac{dh}{ds}\frac{\nu}{L} \tag{26}$$

where:
ν – machine movement speed
L – machine wheel track

Taking the Eq. 23 into consideration, Eq. 26 can be written as follows:

$$\omega_y = \gamma \frac{\nu}{L} \tag{27}$$

where:
γ – coefficient of the surface irregularity described by the following dependence (Eq. 28):

$$\gamma = \sqrt{2\frac{r_p}{r_k} + \left(\frac{r_p}{r_k}\right)^2} \tag{28}$$

The surface irregularity coefficient γ is a function of the irregularity radius quotient r_p to the ground wheel radius r_k. Fig. 6 shows the curve describing this dependence.

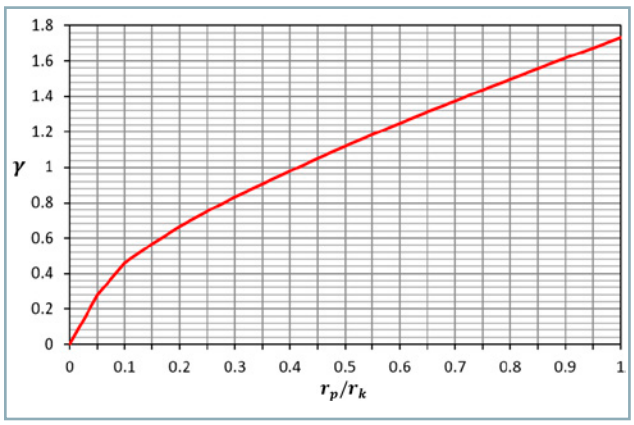

Fig. 6 Graph of the surface irregularity coefficient as a function of the irregularity radius quotient r_p and vehicle ground wheel radius r_k (own study)

Considering the Eq. 28, it is possible to determine the gyroscopic effect during movement over irregular surfaces on the basis of the following equation:

$$\frac{G_z}{G_g} = \frac{\gamma\beta^2}{2}\frac{d}{l}\frac{d}{L}\frac{\omega_x \upsilon}{g} \tag{29}$$

Results and discussion

For the purposes of simulation calculations, there were assumed the real constructional features and parameters of the following chaff cutters: New Holland FR Forage Cruiser; Claas Jaguar 900; and John Dear series 8000.

In regard to numerical calculations according to constructional and kinematic parameters of the selected working machines, the following was assumed:

a) dimensionless forms of constructional coefficients:

$$\beta = 0.7; \quad \frac{d}{l} = 0.7; \quad \frac{d}{L} = 0.2$$

and α in the interval $(0.5; \infty)$;

b) dimensionless forms of kinematic coefficients $\frac{\omega_x \upsilon}{g}$, for which the range of values was determined as $\frac{\omega_x \upsilon}{g} \in (10; 90)$.

Fig. 7 presents the graph showing the increase in the load on the cutting drum bearing elements during its turning in the form of relation of the gyroscopic effect $G_{\dot{z}}$ to the gravitational reaction G_g dependent on the machine movement speed for specific coefficients α according to Eq. 9. The value $\alpha = 0.5$ describes the smallest possible turning radius; the movement of the vehicle without turning occurs when $\alpha = \infty$.

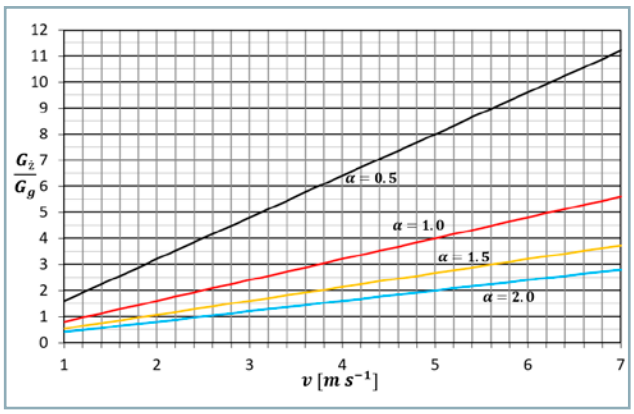

Fig. 7 Graph presenting the relation of the gyroscopic effect $G_{\dot{z}}$ to gravitational reaction G_g dependent on the machine movement speed during its turning (own study)

Analysing the results obtained from simulation calculations, it is possible to establish that the dimensionless parameter of kinematic values $\frac{\omega_x \upsilon}{g}$ and α the parameter a describing the turning radius (which equals half of the wheel track $r_s = \frac{L}{2}$), with a minimum value of $\alpha = 0.5$, have a significant impact on the value $\frac{G_{\dot{z}}}{G_g}$.

The force $G_{\dot{z}}$ occurring during the turning of this type of vehicle has a direction consistent with the gravitational force G_g. For the case presented in Fig. 1, the forces having an effect on the bearing *A* amount to:

$$G_A = G_{\dot{z}} - G_g$$

while forces having an effect on the bearing *B* amount to:

$$G_B = G_{\dot{z}} + G_g$$

Fig. 8 shows the diagram of increase in load on the chaff cutter bearings during moving of its wheels over the irregular surface under field operational conditions. The diagram is presented in the form of relationship of the gyroscopic effect $G_{\dot{z}}$ to gravitational force G_g dependent on the machine operational speed for the determined relations of the wheel radius r_k and the ground surface irregularity radius r_p. The lower the value of the expression $\frac{r_p}{r_k}$, the smaller the surface irregularities.

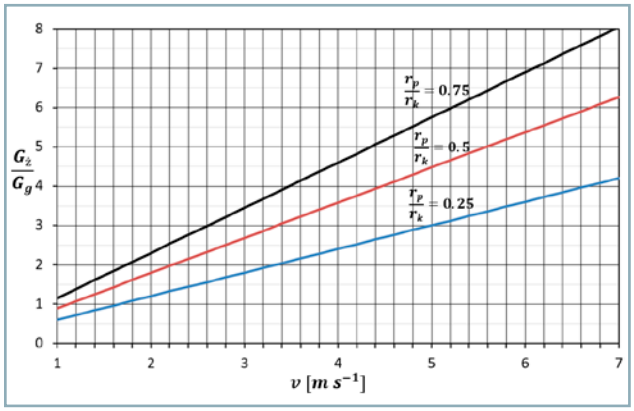

Fig. 8 Graph of the relation of the gyroscopic effect $G_{\dot{z}}$ to the gravitational fore G_g dependent on the machine movement speed during monitoring of its movement over irregular surface (own study)

The force $G_{\dot{z}}$ occurring during its moving over the surface irregularities is orthogonal to the force G_g. The resultant force *G* impacting the bearing amounts to:

$$G = \sqrt{G_{\dot{z}}^2 + G_g^2} \qquad (30)$$

Considering the known literature, authors do not deal with a detailed impact analysis of the gyroscopic effect on the balance of forces interacting on the fast-rotating machines bearings in motion working assemblies. The subject widely taken up by researchers is mainly related to the analysis and strategy of the agricultural machinery maintenance and repair (Pourdarbani, 2019), deformation and wear of working tools in agricultural and forestry machinery (Ťavodová et al., 2018), determination of operating parameters and functioning effectiveness (Moinfar and Shahgholi, 2018), and investigation of hydraulic systems in agricultural machinery (Tkáč et al., 2017) without analysis of additional load in the machinery working assemblies.

The gyroscopic effect increases the load on fast-rotating bearing elements, which can result in their faster wear or damage. That is a reason why it is necessary to take this phenomenon into account in terms of both design of working assemblies' bearings, and development of a preventive system for technical facilities exploitation, which has not been done so far and was presented by Knopik and Migawa (2017), and Knopik and Migawa (2018). The increased load on technical facilities may also result in their increased impact on the environment (Karwowska et al., 2013; Karwowska et al., 2014).

Conclusion

One can encounter the impacts of the gyroscopic effect during the everyday exploitation of the selected constructions of machines, making the subject matter quite topical.

The increased load on the bearing elements can result in adverse effect on the durability of machine working assemblies.

Considering the results of the analysis of simulation calculations conducted for the selected type of self-propelled chaff cutters, the gyroscopic effect can increase the bearing load by more than ten times in case of turning, and approximately by eight times in case of moving over irregular surface.

Analysing the results obtained from the simulation calculations, it may be found that, just like in the case of machine turning, the kinematic coefficient $\frac{\omega_x \upsilon}{g}$ and the coefficient γ connected to the irregularity of surface geometry have a decisive impact on the value $\frac{G_{\dot{z}}}{G_g}$.

Having the models presented in the paper at disposal, the designers of machines and equipment can more carefully and precisely design the bearings of rotating elements burdened with a gyroscopic effect. It will enable decreasing the failure rate of this machinery, which will be reflected in lowering of the costs for exploitation and maintenance.

References

FLIZIKOWSKI, J. – SADKIEWICZ, J. – TOMPOROWSKI, A. 2015. Functional characteristics of a six-roller mill for grainy or particle materials used in chemical and food industries. In Przemysl Chemiczny, vol. 94, no. 1, pp. 69–75.

KARWOWSKA, M, – MIKOLAJCZAK, J. – DOLATOWSKI, Z. – BOROWSKI, S. 2013. The effect of varying distances from the wind turbine on meat quality of growing finishing pigs. In Annals of Animal Science, vol. 15, no. 4, pp. 1043–1054.

KARWOWSKA, M. – MIKOLAJCZAK, J. – BOROWSKI, S. – DOLATOWSKI, Z. – MARC-PIENKOWSKA, J. – BUDZYNSKI, W. 2014. Effect of noise generated by the wind turbine on the quality of goose muscles and abdominal fat. In Annals of Animal Science, vol. 14, no. 2, pp. 441–451.

KESKA, W. – GIERZ, L. 2011. Mathematical modeling and computer simulation of sowing. In 69th International Conference on Agricultural Engineering Land Technik AgEng, Hannover, Germany, pp. 459–464.

KNOPIK, L. – MIGAWA, K. 2017. Optimal age-replacement policy for non-repairable technical objects with warranty. In Eksploatacja i Niezawodnosc – Maintenance and Reliability, vol. 19, no. 2, pp. 172–178.

KNOPIK, L. – MIGAWA, K. 2018. Multi-state model of maintenance policy. In Eksploatacja i Niezawodnosc – Maintenance and Reliability, vol. 20, no. 1, pp. 125–130.

LANDAU, L. D. – LIFSZYC, J. 2012. Mechanics. Warszawa : PWN publishing house. ISBN 9788301151522.

LIGAJ, B. – SZALA, G. 2010. Experimental verification of two-parametric models of fatigue characteristics by using the tests of S55J0 steel as an example. In Polish Maritime Research, vol. 17, no. 1, pp. 39–50.

MOINFAR, A. M. – SHAHGHOLI, G. 2018. Dimensional analysis of the tractor tractive efficiency parameters. In Acta Technologica Agriculturae, vol. 21, no. 3, pp. 94–99.

POURDARBANI, R. 2019. Choosing a proper maintenance and repair strategy for tractors (in Urmia). In Acta Technologica Agriculturae vol. 22, no. 1, pp. 12–16.

STRZELECKI, P. – TOMASZEWSKI, T. – SEMPRUCH, J. 2016. A method for determining a complete S-N curve using maximum likelihood. In 22nd International Conference on Engineering Mechanics, Svratka, Czech Republic, pp. 530–533.

ŤAVODOVÁ, M. – DŽUPON, M. – KALINCOVÁ, D. – HNILICOVÁ, M. 2018. Deformation of exposed tool parts for crushing of undesirable advance growth. In Acta Technologica Agriculturae, vol. 21, no. 4, pp. 166–173.

TKÁČ, Z. – ČORŇÁK, S. – CVIKLOVIČ, V. – KOSIBA, J. – GLOS, J. – JABLONICKÝ, J. – BERNÁT, R. 2017. Research of biodegradable fluid impacts on operation of tractor hydraulic system. In Acta Technologica Agriculturae, vol. 20, no. 2, pp. 42–45.

ZASTEMPOWSKI, M. – BOCHAT, A. 2014. Modeling of cutting process by the shear-finger cutting block. In ASABE Applied Engineering in Agriculture, vol. 30, no. 3, pp. 347–353.

ZASTEMPOWSKI, M. – BOCHAT, A. 2015. Mathematical modelling of elastic deflection of a tubular cross-section. In Polish Maritime Research, vol. 22, no. 2, pp. 93–100.

ZASTEMPOWSKI, M. – BOCHAT, A. 2016. Innovative constructions of cutting and grinding assemblies of agricultural machinery. In TAE 2016 – Proceedings of the 6th International Conference on Trends in Agricultural Engineering, pp. 726–735.

sciendo

DOI: 10.2478/ata-2020-0006

Acta Technologica Agriculturae 1
Nitra, Slovaca Universitas Agriculturae Nitriae, 2020, pp. 30–39

FACTORS AFFECTING THE ADOPTION OF AGRICULTURAL AUTOMATION USING DAVIS'S ACCEPTANCE MODEL (CASE STUDY: ARDABIL)

Mahdi SALIMI, Razieh POURDARBANI*, Bagher ASGARNEZHAD NOURI

University of Mohaghegh Ardabili, Ardabil, Iran

Taking into account that traditional agricultural methods reduce the farm performance and make agriculture economically ineffective, development of intelligent machinery is essential for improving the quality of crops and agricultural activities. The most important issue in development of agricultural technologies lies in users' willingness to adopt it. Therefore, the purpose of this study is to investigate the key factors of Davis's model in automation acceptance in agriculture. Presented paper describes an applied research with a survey approach through a questionnaire. Questionnaire data were collected from 378 people and respondents include university students, farmers and experts in a randomized sampling from the Ministry of Agriculture. Firstly, the questionnaire data were described in a form of statistical numerical characteristics. Secondly, in order to verify the data normality, the Kolmogorov-Smirnov test was calculated in SPSS and the relationship between the variables was investigated in the conceptual model. Subsequently, hypotheses were tested via appropriate statistical models using LISREL and SPSS software. The results showed that for all hypotheses, the *T*-test exceeds 1.96 and the significance level is less than 0.05. In such a manner, all hypotheses were confirmed at 95% level, and the path coefficients in the hypotheses H1, H2 and H6 were negative – indicating the negative effect of the independent variable on the dependent variable in the hypothesis. In the other hypotheses, these were positive – indicating the positive effect of the independent variable on dependent variable. By means of modelling, it was found that there was an inverse relationship between social and individual factors with perceived usefulness, as well as an inverse relationship between social factors with perceived ease-of-use, while there was a positive and significant relationship between other factors. According to a set of fitting indices, the research conceptual model was appropriate and Cronbach's coefficients for each factor were greater than 0.7, suggesting that the questionnaire was valid. On the basis of findings, the better a person understands the usefulness of automation, the more likely this person is to adopt it. Since the risk and issues related to it play an important role in farmers' decision making, it is recommended that future studies address the issue of risk in adopting precision farming technology.

Keywords: attitude; intention to use; LISREL; perceived usefulness

In Iran, agriculture is the largest economic sector after services, accounting for approx. 20% of gross national product and the major share of non-oil exports. Moreover, a large number of people is employed in agriculture; therefore, the sector growth largely determines the economic growth of the country (Ebrahimi et al., 2017).

According to the World Food and Agriculture Organization (FAO), the world's population is expected to reach 9.1 billion by 2050. Therefore, to feed this population, food production should increase by at least 70% and developing countries must double their food supply. Since this is not achievable by traditional agricultural methods, it is necessary to modernise the technologies in the agricultural sector (Sreekantha, 2016; Beloev, 2016). It is typical for developed economies that high technologies and innovative solutions associated with the progressing economy globalisation, as well as wider access to outlets play a vital role in their growth (Biały and Žarnovský, 2017).

One of the solutions that can mitigate or eliminate the damage caused by traditional agriculture is its automation; the lack of this technology is one of the most significant issues in the agricultural sector (Masoudi, 2016). The automation is in fact a software permanent management focused on all system processes (day-to-day), which is monitored and controlled by a central processor unit (Goodarzi and Sadeghi Fard, 2014). Machine automation allows these systems to perform their work efficiently, reliably, accurately and almost without any human intervention (Schueller, 2006) and automation utilization benefits in agriculture include increases in export and production, production quality improvement, time saving, production cost reduction, reduction of issues related to water losses in the agricultural system, boom in agriculture, conservation of biological resources, and decrease in the growth of urban migration.

Diversification of agricultural systems around the world makes it difficult to use automation and control. Many outdoor agricultural automation systems that may be exposed to a wide range of environmental and atmospheric conditions, such as high temperature, humidity, etc. cannot perform accurate automation. Considering the developing countries, one particular concern is associated to the lack of workforce due to automation, as well as the lack

Contact address: Razieh Pourdarbani, University of Mohaghegh Ardabili, Department of Biosystem Engineering, Ardabil, Iran, e-mail: r_pourdarbani@uma.ac.ir

of willingness to adopt the automation in a region due to the economic, social, cultural, technical and environmental conditions.

Due to population growth and rising costs in the coming years and demand for food, there should be strategies for higher production and less waste. Utilization of robots can be justified with higher production, waste reduction and reduction of current costs by means of more and more accurate monitoring (Torabi et al., 2014).

The first step in the development of agricultural automation is to identify consumer behaviour and factors affecting its acceptance. Therefore, this research was conducted with the aim of identifying the factors affecting the agricultural automation adoption in Ardabil and providing a model for automation acceptance in the agricultural sector. In this study, consumer behaviour was assessed on the bases of behavioural models – the most common conceptual models.

Development of hypotheses and conceptual model

1. Individual factors

There are multiple individual factors significantly affecting the consumer behaviour (Amen, 2010). In research, human capital measurements have been based on assessment of data on education, age, gender, and family size of the farmer (Keelan et al., 2014). The education level of a farmer increases their ability to understand presented ease aspects and usefulness of a new technology (Okunlola et al., 2011; Adebiyi and Ekonola, 2010). Studies on the adoption of microcomputers in agriculture (Putler and Zilberman, 1988), crop reduction and precision agriculture (Roberts et al., 2004) show a positive relationship between habitat and acceptance. Age is also one of the factors influencing the new technology acceptance. Older people have gained knowledge and experience over time and are more able to evaluate technical information in contrast to young farmers (Mignouna et al., 2011; Kariyasa and Dewi, 2011).

H1: Individual factors affect the perceived usefulness of the automation application in agriculture.

H2: Individual factors affect the perceived ease aspects of automation application in agriculture.

2 Social factors

Social norms represent one of the subcategories of social factors that affect technology adoption with an effect on attitude of the individual towards an object (Malte et al., 2008; Chong et al., 2010; Verma and Sinha, 2018).

H3: Social factors affect the perceived usefulness of the automation application in agriculture.

H4: Social factors affect the perceived ease aspects of the automation application in agriculture.

3. Organizational factors

Access to support services is also recognized as a key aspect of technology acceptance. Farmers are often informed on the existence and benefits of new technology via expanding agents. Many authors have reported a positive relationship between post-sales services and automation adoption (Bonabana-Wabbi, 2002; Sserunkuuma, 2005; Akudugu et al., 2012).

H5: Organizational factors affect the perceived usefulness of the automation application in agriculture.

H6: Organizational factors affect the perceived ease aspects of the automation application in agriculture.

4. Automation features

Tests that can be performed at a small scale before the full automation adoption represent another significant factor influencing the automation acceptance (Doss, 2003; Mignouna et al., 2011). These are necessary to introduce any new technology to farmers, so they can evaluate and understand suitability of tested technology under their own conditions (Karugia et al., 2004).

H7: Automation features affect the perceived usefulness of the automation application in agriculture.

H8: Automation features affect the perceived ease aspects of the automation application in agriculture.

5. Perceived usefulness (PU)

In regard to the numerous variables affecting the system utilization, perceived usefulness is considered a prerequisite for automation acceptance and behavioural intent (Kim et al., 2007; Callum et al., 2014; Park and Chen, 2007; Mansour et al., 2017; Shirmohammadi, 2004; Lotfi and Bakhsayeshi, 2010; Wafaei, 2009; Davis, 1989).

H9: Perceived usefulness affects the attitude towards the agricultural automation.

H10: Perceived usefulness affects the willingness to use the agricultural automation.

6. Perceived ease of use (PEOU)

Perceived ease of use is a degree to which every individual believes that particular system utilization will facilitate his work (Davis, 1989; Verkantesh et al., 2003). According to Venkatesh and Davis (2000); Liu et al. (2009); Saghafi et al. (2017), a positive relationship was found between PEOU and PU.

H11: Perceived ease of use affects the attitude towards the agricultural automation.

H12: Perceived ease of use affects the willingness to use agricultural automation.

7. Attitude (ATU)

Attitude can be expressed as one's view of the chosen act (Yadav and Pathak, 2016). Attitudes have a significant effect on the individual's behaviour, and this relationship becomes more intense when it is related to one's health.

H13: The attitude towards automation affects the intention to use the automation in agriculture.

8. Intention to use (IU)

The intention to use (IU) is a key factor for the actual use (Davis et al., 1989). In terms of the technology utilization, a decision to willingly use the technology in full extent is generally positive (Turner et al., 2010).

H14: The intention to use the automation affects the actual (AU) automation utilization in agriculture.

Based on aforementioned hypotheses, conceptual research model can be presented as follows:

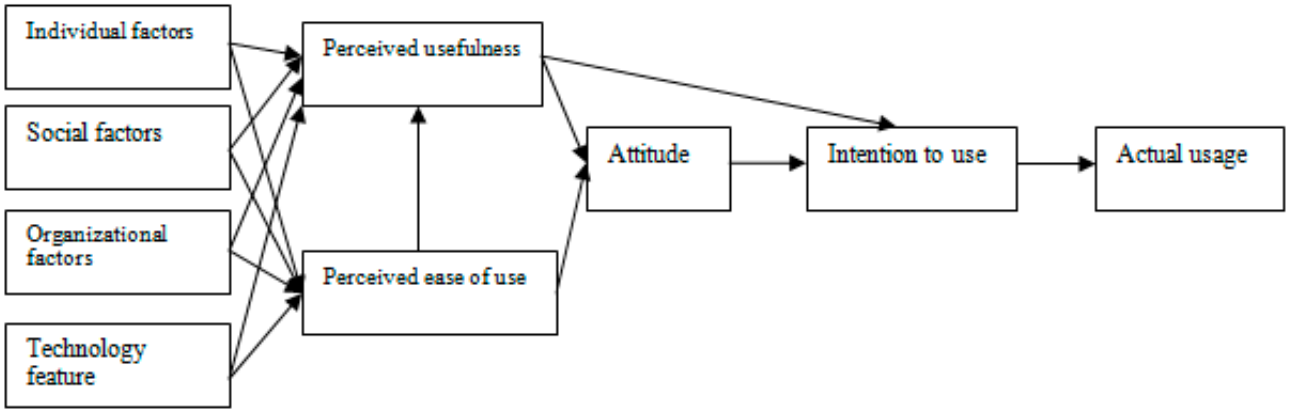

Fig. 1 Conceptual framework for research (source: author's research)

Material and methods

The purpose of this study was to investigate the factors affecting the automation adoption in agriculture in Ardabil. The statistical population of this research consisted of three academic circles, experts from the Ministry of Agriculture (Jahad) and farmers, 27,670 people in total. Randomized sampling method was used. On the basis of sample size set by Krejcie and Morgan (1970) and the Cochran formula utilization, 380 individuals were calculated as sample size:

$$n = \frac{\frac{z^2 pq}{d^2}}{1+\frac{1}{N}\left[\frac{z^2 pq}{d^2}-1\right]} = \frac{\frac{1.96^2 \times 0.5 \times 0.5}{0.5^2}}{1+\frac{1}{27{,}670}\left[\frac{1.96^2 \times 0.5 \times 0.5}{0.5^2}-1\right]} = 380 \quad (1)$$

where:
n – sample size
N – size of statistical population
z – acceptable random error
P – ratio of success
q – failure ratio
d – degree of accuracy

Considering the possibility that the questionnaires might not be filled out by all respondents, the questionnaires were distributed to 385 respondents. Finally, after deleting the invalid questionnaires, 378 questionnaires remained to be observed; therefore, study sample size was 378 individuals, indicating the response rate of 98.18%. Data collection was performed using library and field methods. The questionnaire was developed by the researcher based on Davis's model (Fig. 1). It consists of several main sections; the first to seventh sections are: organizational factors, individual factors, perceived usefulness, perceived ease of use, attitude, intention to use and actual usage. Using Bartlett test and confirmatory factor analysis, a number of questions was deleted in each section in order to lower the factor loading, and a final questionnaire with 80 questions was developed.

Factor analysis and Cronbach's alpha coefficient were used to determine the questionnaire validity and its reliability:

$$r_a = \frac{j}{j-1}\left(1-\frac{\sum_{j=1}^{n} s_j^2}{s^2}\right) \quad (2)$$

where:
j – number of questionnaire items
s_j^2 – variance of the subtest j
s^2 – variance of entire questionnaire or test

The data normalization assumption was performed by means of Kolmogorov-Smirnov test (K-S). Confirmatory factor analysis examines the relationship of items or questions with the structures; this process was carried out using the LISREL software. The *T*-test statistic is used to determine the significance of the relationship between the variables. Since the significance is checked at a level of 0.05, if the observed factor loading shows a *t*-value of less than 1.96, it is not significant.

Chi-squared test (X^2) was used to measure the correspondence between the experimental and theoretical curves. This test indicates the designed model is based on actual data. Finally, to test the research hypotheses, structural equation modelling was employed, which is a strong multivariate analysis technique from the family of multivariable regression.

Results and discussion

Evaluation of data normality and questionnaire validity and reliability

In order to verify the data normality, Kolmogorov-Smirnov test was calculated for the variables of individual, social and organizational

Table 1 Demographic characteristics of the respondents

Characteristic	Number of respondents	Level	Absolute frequency	Relative abundance
Gender	378	man	321	84.9
		woman	57	15.1
Age	378	less than 20 years old	7	1.8
		21–29 years old	148	39.2
		30–39 years old	111	29.4
		40–49 years old	87	23
		50–59 years old	23	6.1
		over 60 years old	2	0.5
Level of education	378	illiterate	61	16.1
		diploma and lower	85	22.5
		B.A/B.S	111	29.4
		M.A/M.S	81	21.4
		PhD and higher	40	10.6
Average monthly income	378	less than 1 million	144	38.2
		between 1 and 3 million	157	41.5
		between 3 and 5 million	36	9.5
		more than 5 million	41	10.8
Employment status	378	graduate student	94	24.9
		academic staff	37	9.8
		agricultural expert	75	19.8
		farmer	172	45.5
Experience of agricultural work	378	less than 5 years	92	24.3
		5 to 14 years old	155	41
		15 to 24 years old	105	27.8
		25 to 34 years old	19	5
		35 to 49 years old	7	1.9

factors, technology characteristics, perceived usefulness, perceived ease, attitude, intention to use and actual use by means of SPSS software (Table 2).

Based on the data shown in Table 2, the significance level for all components exceeds value 0.05, indicating that these variables have a normal distribution, and structural equations can be used to test the hypotheses in terms of parametric testing.

Confirmatory factor analysis results for each variable conducted via the LISREL software are presented in Table 4 for each variable separately. It should be emphasized that, in order to reduce the number of variables, the factor loading obtained should not exceed value 0.3 (Momeni and Qiyomi, 2017). However, before performing the factor analysis, the point that needed to be addressed first was to make sure that the number of data for the factor analysis is appropriate. For this purpose, Kaiser-Meyer-Olkin (KMO) index and Bartlett test were used (Table 3).

According to Table 3, the KMO index is 0.843, which is in the range above 0.6. Therefore, the research sample size is appropriate for factor analysis. Furthermore, the significance level of Bartlett test is less than 0.05, suggesting that the factor analysis is suitable for identifying the structure (factor model).

Therefore, a confirmatory factor analysis could be used to analyse the questionnaire. The *T*-test was used to test the significance of relationships between variables. Since the significance is checked at a level of 0.05, if the factor loading observed shows a *t*-value lower than 1.96, it is not significant. Each question with a factor loading less than 0.3 was deleted from the questionnaire.

Estimation of research conceptual model

Research model test was carried out using the structural equation modelling method (Figs. 2 and 3).
The hypotheses test results are summarized in Table 4.

Table 2 Kolmogorov-Smirnov test before and after normalization

Variable	Kolmogorov-Smirnov test before normalization		
	Statistics	Degrees of freedom	Significance level
Individual factors	4.05	378	0.000
Social factors	3.87	378	0.000
Organizational factors	3.11	378	0.000
Technology features	2.32	378	0.000
Perceived usefulness	4.87	378	0.000
Perceived ease of use	3.24	378	0.000
Attitude	5.62	378	0.000
Intention to use	3.36	378	0.000
Actual usage	4.52	378	0.000
Variable	**Kolmogorov-Smirnov test after normalization**		
	Statistics	**Degrees of freedom**	**Significance level**
Individual factors	0.11	378	0.09
Social factors	0.16	378	0.22
Organizational factors	0.07	378	0.45
Technology features	0.16	378	0.14
Perceived usefulness	0.17	378	0.13
Perceived ease of use	0.19	378	0.12
Attitude	0.20	378	0.12
Intention to use	0.13	378	0.11
Actual usage	0.12	378	0.15

Table 3 Bartlett test and KMO index for evaluated data

KMO index		0.843
Bartlett test	Chi-squared test	465.93
	Degree of freedom	1225
	The significance level	0.000

Table 4 Hypotheses test results

Hypothesis	Independent variable	Dependent variable	Path coefficient	T statistics
H1	individual factors	perceived usefulness	-0.41	-5.28
H2	social factors	perceived usefulness	-0.32	-4.38
H3	organizational factors	perceived usefulness	0.36	4.52
H4	technology features	perceived usefulness	0.34	4.45
H5	individual factors	perceived ease of use	0.92	13.55
H6	social factors	perceived ease of use	-0.43	-5.46
H7	organizational factors	perceived ease of use	0.62	11.20
H8	technology features	perceived ease of use	0.65	12.10
H9	perceived ease of use	perceived usefulness	0.52	8.80
H10	perceived usefulness	attitude	0.74	13.09
H11	perceived ease of use	attitude	0.41	5.30
H12	perceived usefulness	intention to use	0.97	14.44
H13	attitude	intention to use	0.50	8.72
H14	intention to use	actual usage	0.95	13.90

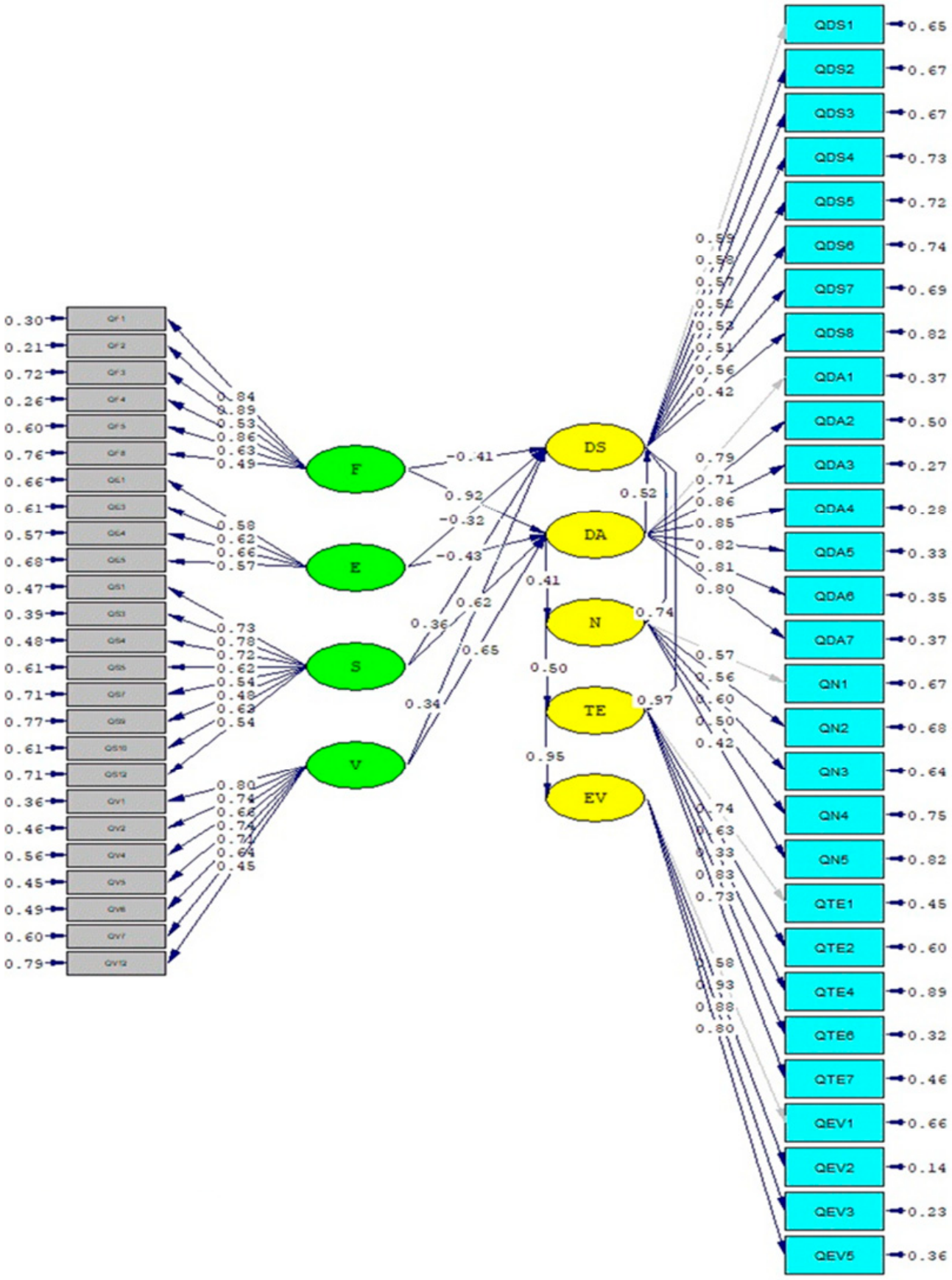

Fig. 2 Estimation of standard correlation coefficient in model
Chi-square = 3,735.17; *df* = 1,357; *P*-value = 0.00000; RMSEA = 0.068

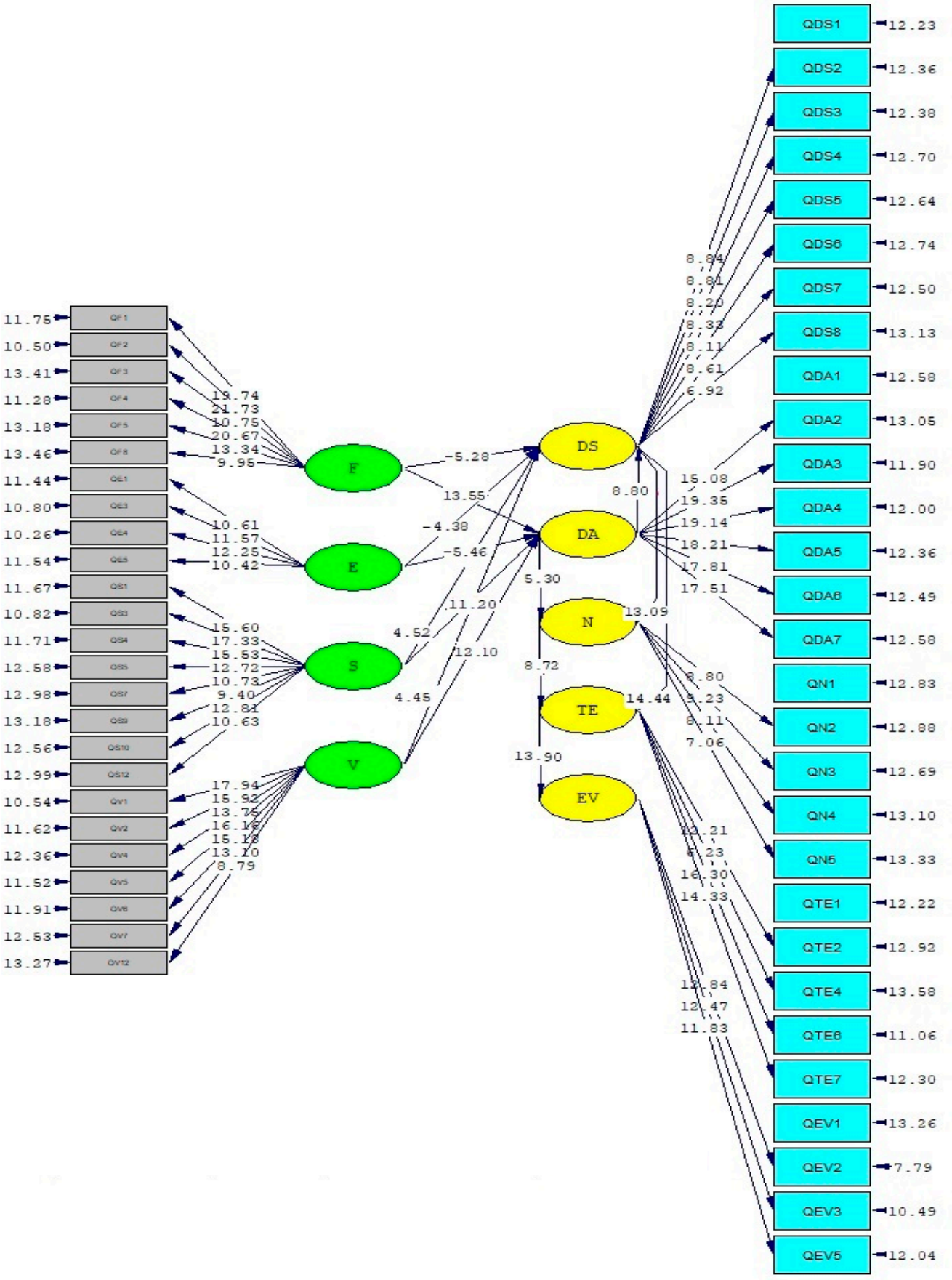

Fig. 3 Estimation of the t-statistic in the model
Chi-square = 3,735.17; *df* = 1,357; *P*-value = 0.00000; RMSEA = 0.068

Table 5 Model suitability indices

	Model fit indices	Acceptable range	The amount earned
Chi-square	Chi-square	–	3,735.17
Degree of freedom	*df*	–	1,357
The ratio of chi-square to the degree of freedom	x^2/df	3>	2.75
The root mean estimation of the approximation error variance	RMSEA	0.1>	0.060
The root mean square of the remainder	RMR	0.1>	0.060
Goodness of fit index	GFI	0.9<	0.954
Non-normalized fitting index	NNFI	0.9<	0.962
Comparative fitting index	CFI	0.9<	0.987

The results shown in Table 4 indicate that for all hypotheses, the *t*-test exceeds the value of 1.96 and the significance level is lower than 0.05. Therefore, all hypotheses were confirmed at 95% level, and the path coefficients in the hypotheses H1, H2 and H6 were negative, suggesting the negative effect of the independent variable on the dependent variable in the hypotheses. The other hypotheses are also positive, indicating the positive effect of the independent variable on dependent variable.

Structural equation modelling and significance indices

In general, to determine the fit of the estimated model, various indicators are used and the model fitness must be reasoned by more than one. Therefore, these indicators should be combined. The values of model fit indices are shown in Table 5.

According to Table 5, all model fit indices are acceptable. Therefore, on the basis of fitting indices, it can be concluded that the conceptual research model is appropriate and calculation results for relationships in the research model are valid and reliable.

Conclusion

Using the structural equation modelling results, it was determined that there is a significant relationship between individual factors and perceived usefulness. The correlation coefficient between the two variables was negative, indicating that with an increase in individual factors, the perceived usefulness decreases. This means that experience; prior knowledge; self-confidence; financial status; education level; land area; and the number of family labourers do not have positive impact on the productivity increasing. The reason for this was poor and unfavourable classes in knowledge creation.

There was observed a significant relationship between social factors and perceived usefulness. The correlation coefficient between the two variables was negative, indicating that with an increase in social factors, perceived usefulness decreases. This means that social factors, such as mental norm; trust in friends; and classes, played a significant and positive role in farmers' understanding of technology usefulness. Therefore, these classes should be presented in a more specialized and practical way.

There was also a significant relationship between organizational factors and perceived usefulness. The correlation coefficient between the two variables was positive, suggesting that with an increase in the organizational factors, there is an increase in the perceived usefulness and vice versa. In general, this means that membership in the rural cooperative; advertising; behaviour of the host companies; sponsor organization availability; support services; justification training; low interest loans; long-term repayment deadlines; and timely funding can effectively provide new technology utilization.

The positive correlation coefficient between automation and perceived usefulness means that the automation features, such as relative advantages; compatibility; low complexity; visibility; testability; no need for further labour; optional adoption, can make the technology more useful.

The positive correlation coefficient between individual factors and perceived ease means that farmers' experience, knowledge and confidence; education level and good financial status make it easier to use the automation.

There was also a significant relationship between the automation features and perceived ease. The correlation coefficient between the two variables was positive, suggesting that with an increase in automation features, there is an increase in perceived ease. Therefore, it seems that relative advantages; compatibility; low complexity; the lower need for workforce; optional adoption; low start-up costs; etc. make it easier to understand the ease of use of technology.

There was a significant relationship between perceived usefulness and attitude. The correlation coefficient between the two variables was positive and indicated that with an increase in perceived usefulness, the attitude increases. In other words, the more people understand the benefits of automation, the better their attitude toward using it. These findings are consistent with the results presented by Siregar et al. (2017).

A significant relationship between perceived usefulness and the intention to use the automation was also observed. The correlation coefficient between the two variables was positive, indicating that with an increase in perceived usefulness, the intention to use also increases. In other words, when farmers consider the automation utilization to be useful, they tend to use it more.

A significant relationship between attitude and intention to use was also shown. The correlation coefficient between the two variables was positive and indicated that with an increase in attitude, the intention to use is also increased.

There was observed a significant relationship between the intent to use the technology and its actual usage. The correlation coefficient between the two variables was positive, indicating that with an increase in the intent to use the technology, its actual usage increases. This means that, when using automation, the person will actually use it in agriculture.

In general, based on the model fit indices obtained in the research, it seems that Davis's technology acceptance model is suitable for investigating effective factors in agricultural automation in Ardabil.

References

ADEBIYI, S. – EKONOLA, J. 2010. Factors affecting adoption of cocoa rehabilitation techniques in Oyo State of Nigeria. In World Journal of Agricultural Sciences, vol. 9, no. 3, pp. 258–265.

AKUDUGU, M. – GUO, E. – DADZIE, S. 2012. Adoption of modern agricultural production technologies by farm households in Ghana: What factors influence their decisions? In Journal of Biology, Agriculture and Healthcare, vol. 2, no. 3.

AMEN, U. 2010. Consumer attitude towards mobile advertising. In Interdisciplinary Journal of Contemporary Research in Business, vol. 70, no. 3, pp. 75–104.

BELOEV, I. H. 2016. A review on current and emerging application possibilities for unmanned aerial vehicle. In Acta Technologica Agriculturae, vol. 19, no. 3, pp. 70–76.

BIAŁY, W. – ŽARNOVSKÝ, J. 2017. Acquiring EU funds for the development of research potential of enterprises as a method for developing smart specialisations. In Acta Technologica Agriculturae, vol. 20, no. 2, pp. 46–51.

BONABANA-WABBI, J. 2002. Assessing Factors Affecting Adoption of Agricultural Technologies: The Case of Integrated Pest Management (IPM) in Kumi District. MSc. Thesis, Eastern Uganda. Available at: http://hdl.handle.net/10919/36266

CALLUM, K. M. – JEFFREY, L. – KINSHUK. 2014. Comparing the role of ICT literacy and anxiety in the adoption of mobile learning. In Computers in Human Behavior, vol. 39, pp. 8–19.

CHONG, A. – OOI, K. – TAN, B. 2010. Online banking adoption: an empirical analysis. In International Journal of Bank Marketing, vol. 28, pp. 267–287.

DAVIS, F. D. 1989. Perceived usefulness, perceived ease of use, and user acceptance of information technology. In MIS Quarterly, vol. 13, no. 3, pp. 319–340.

DOSS, C. R. 2003. Understanding Farm Level Technology Adoption: Lessons Learned from CIMMYT's Microsurveysin Eastern Africa. CIMMYT Economics Working Paper 03–07. Mexico, D.F.: CIMMYT.

EBRAHIMI, A. – BIZHNI, M. – SEDIGHI, H. 2017. Acceptance of nuclear technology in the field of agriculture: Application of DTBP and UTAUT theories. In The Second National Congress on the Development and Promotion of Iranian Agricultural Engineering and Soil Science, May 27, Tehran, Iran. (In Farsi)

GOODARZI, A – SADEGHI FARD, S. 2014. Intelligence and the place of industrial automation in agriculture. In The Second National Agricultural and Sustainable Natural Resources Conference, July, Tehran, Iran. (In Farsi)

KARIYASA, K. – DEWI, A. 2011. Analysis of factors affecting adoption of integrated crop management farmer. In International Journal of Food and Agricultural Economics, vol. 1, no. 2, pp. 29–38.

KARUGIA, S. – BALTENWECK, I. – WAITHAKA, M. – MIANO, M. – NYIKAL, R. – ROMNEY, D. 2004. Perception of technology and its impact on technology uptake: The case of fodder legume in central Kenya highlands. In The Role of Social Scientists Proceedings of the Inaugural Symposium, 6–8 December, Grand Regency Hotel, Nairobi, Kenya.

KEELAN, C. – THORNE, F. – FLANAFAN, P. – NEWMAN, C. 2014. Predicted willingness of Irish farmers to adopt GM. In Journal of Economics and Sustainable Development, vol. 12, pp. 208–216. KREJCIE, R. V. – MORGAN, D. W. 1970. Determining sample size for research activities. In Educational and Psychological Measurement, vol. 30, pp. 607–610. Available at: https://doi.org/10.1177/001316447003000308

KIM, H. W. – CHAN, H. C. – GUPTA, S. 2007. Value-based adoption of mobile internet: an empirical investigation. In Decision Support System, vol. 43, pp. 111–126.

LOTFI, A. – BAKHSHAYESHI, M. 2010. Investigating the factors affecting e-library acceptance. In Fifth National Conference and Second International Conference on E-Learning and Education, Tehran.

LIU, S. – LIAO, H. – PRATT, J. A. 2009. Impact of media richness and flow on e-learning technology acceptance. In Computers & Education, vol. 52, pp. 599–607.

MALTE, N. – ROSSI, M. – TUUNIAINEN, V. – OORNI, A. 2008. An empirical investigation of mobile ticketing service adoption in public transportation. In Personal and Ubiquitous Computing, vol. 12, pp. 57–65.

MANSOUR, I. H. – ELJELLY, A. M. – ABDULLAH, A. M., 2017. Consumers' attitude towards e-banking services in Islamic banks: the case of Sudan. In Review of International Business and Strategy, vol. 26, no. 2, pp. 244–260.

MASOUDI, H. 2016. A new ground for innovating and developing entrepreneurship in the animal husbandry. In Entrepreneurship Journal in Agriculture, vol. 2, no. 3, pp. 256–273. (In Farsi).

MIGNOUNA, B. – MANYONG, M. – RUSIKE, J. – MUTABAZI, S. – SENKONDO, M. 2011. Determinants of adopting imazapyr-resistant maize technology and its impact on household income in western Kenya. In AgBioforum, vol. 14, no. 3, pp. 158–163.

MOMENI, M. – QIYOMI, A. 2017. Statistical Analysis Using SPSS. Negarandedanesh publication.

OKUNLOLA, O. – OLUDARO, O. – AKINWAERE, B. 2011. Adoption of new technologies by fish farmers in Akure, Ondo. In Journal of Agricultural Technology, vol. 7, no. 6, pp. 1539–1548.

PARK, Y. – CHEN, J. V. 2007. Acceptance and adoption of the innovative use of smartphone. In Industrial Management & Data Systems Information, vol. 107, no. 9, pp. 1349–1365.

PUTLER, D. S. – ZILBERMAN, D. 1988. Computer Use in Agriculture: Evidence from Tulare County, California.

ROBERTS, K. – ENGLISH, B. – LARSON, J. – COCHRAN, R. – GOODMAN, W. – LARKIN, S. – MARRA, M. – MARTIN, S. – SHURLEY, W. – REEVES, M. 2004. Adoption of site-specific information and variable-rate technologies in cotton precision farming. In Journal of Agricultural and Applied Economics, vol. 36. no. 1, pp. 143–158.

SAGHAFI, F. – MOGHADDAM, E. N. – ASLANI, A. 2017. Examining effective factors in initial acceptance of high-tech localized technologies: Xamin, Iranian localized operating system. In Technological Forecasting and Social Change, vol. 122, pp. 275–288.

SCHUELLER, J. K. 2006. Applied machine vision of plants: a review with implications for field deployment in automated farming operations. In Intelligent Service Robotics, vol. 3, no. 4, pp. 209–217.

SHIRMOHAMMADI, M. 2004. Development of Technology Acceptance Model (TAM) and its Testing at the Ministry of the Interior. MSc. thesis, Tehran University (In Farsi).

SIREGAR, J. J. – PUSPOKUSUMO, R. A. W. – RAHAYU, A. 2017. Analysis of affecting factors technology acceptance model in the application of knowledge management for small medium enterprises in industry creative. In Procedia Computer Science, vol. 116, pp. 500–508.

SREEKANTHA, D. K. 2016. Automation in agriculture. In International Journal of Engineering Science Invention Research & Development, vol. 2, no. 6, pp. 458–472.

SSERUNKUUMA, D. 2005. The adoption and impact of improved maize and land management technologies in Uganda. In The Electronic Journal of Agricultural and Development Economics, Food and Agriculture Organization of the United Nations, vol. 2, no. 1, pp. 67–84.

TORABI, A. – MALEKI, A. – ISHAG BEIGI, A. 2014. The importance and position of the robot in the modern agriculture. In The Second National Conference on Agricultural Engineering, Environment and Sustainable Natural Resources, March 20, Tehran, Iran (In Farsi).

TURNER, M. – KICHENHAM, B. – BRERETON, P. – CHARTERS, S. – BUDGEN, D. 2010. Does the technology acceptance model predict actual use? A systematic literature review. In Information and Software Technology, vol. 52, no. 5, pp. 463–479.

VENKATESH, V. – DAVIS, F. D. 2000. A theoretical extension of the technology acceptance model: Four longitudinal field studies. In Management Science, vol. 46, no. 2, pp. 186–204.

VERKANTESH, V. – MORRIS, M. G. – DAVIS, G. B. – DAVIS, F. D. 2003. User acceptance of information technology: Toward a unified view. In MIS Quarterly, vol. 27, no. 3, pp. 425–478.

VERMA, P. – SINHA, N. 2018. Integrating perceived economic wellbeing to technology acceptance model: The case of mobile based agricultural extension service. In Technological Forecasting and Social Change, vol. 126, pp. 207–216.

WAFAEI, N. 2009. Identifying and Prioritizing Factors Affecting Adoption of Mobile Banking from the Point of View of Customers (Case Study: National Bank of Iran Branches in Tehran). MSc. thesis, Tarbiat Modares University, Tehran (In Farsi).

YADAV, R. – PATHAK, G. 2016. Determinants of consumers' green purchase behavior in a developing nation: Applying and extending the theory of planned behavior. In Ecological Economics, vol. 134. pp. 114–122.

sciendo

DOI: 10.2478/ata-2020-0007

Acta Technologica Agriculturae 1
Nitra, Slovaca Universitas Agriculturae Nitriae, 2020, pp. 40–45

INFLUENCE OF THE PLOUGH WITH TEKRONE MOULDBOARDS AND LANDSIDES ON PLOUGHING PARAMETERS

Volodymyr NADYKTO[1]*, Volodymyr KYURCHEV[1], Volodymyr BULGAKOV[2], Pavol FINDURA[3], Olexander KARAIEV[1]

[1]Tavria State Agrotechnological University, Ukraine
[2]National University of Life and Environmental Sciences of Ukraine, Ukraine
[3]Slovak University of Agriculture in Nitra, Slovak Republic

This paper is dedicated to Tekrone composite material utilization in agricultural machinery. In terms of its technical properties, tekrone is very similar to steel 60 that is used for production of plough mouldboards and landsides. However, Tekrone shows more preferable characteristics, because its friction coefficient (k_f) is 2.6 times lower in contrast to steel 60. This fact indicates that the draft resistance can be decreased by replacing the plough mouldboards and landsides made of steel 60 with their counterparts made of Tekrone. This science hypothesis was confirmed by experimental investigation results. Analyses showed that utilization of plough with Tekrone mouldboards and landsides instead of steel ones significantly reduces their sticking to the wet soil. This results in a "soil moves over plough mouldboard surface" process instead of a "soil moves over soil" process. The plough draft resistance was decreased by 13.6% after replacement of the steel equipment with Tekrone one. Simultaneously, the performance of new tractor-plough aggregate was increased by 12.6%, the specific fuel consumption was reduced by 11.8%, and the preserving probability of the agrotechnological ploughing depth tolerance (±2 cm) was increased from 88% to 93%.

Keywords: ploughing; friction coefficient; draft resistance; soil sticking

Ploughing is one of the most frequently utilized tillage processes. In practice, ploughs are responsible for performance of this process. Although the history of their appearance and development is quite long, plough construction was fundamentally modified only. The majority of these were aimed at the plough draft resistance reduction, since even today, ploughing is the most energy-intensive tillage operation.

The task of the plough draft resistance reduction has been dealt with by different methods, e.g. Araya and Kawanishi (1985) supplied compressed air into the working zone of the ploughshare via special nozzles. As a result, the significant horizontal cracks were formed, which crumbled the soil and reduced the draft resistance of the soil tillage implement. Other researchers (Loveykin and Dyachenko, 2012; Niyamapa and Salokhe, 2000) used a mechanical vibration of the plough bottoms in a horizontal plane. For this purpose, they used hydraulic vibrators that oscillated the plough bottoms at a frequency of 6–8 Hz.

Furthermore, Romanuk et al. (2016) also investigated the influence of the plough vibrations on the horizontal plane on its draft resistance. Such plough oscillations were provided by polygonal support wheels. As a result, the plough produced oscillations with a frequency of 6–7 Hz, resulting in the draft resistance reduction.

In addition to this, Lukashok and Kornev (2009) mounted the rollers into the three-bottom plough mouldboards. This reduced the soil frictional force acting on the plough mouldboards and the draft power necessary for its movement was reduced by 3 kW.

Belousov and Trubilin (2013) tried to decrease the draft resistance by mounting additional flat ploughshares – these were mounted on the left of the main ploughshares and crumbled the soil, which was being tilled during the next working pass. As a result, the plough draft resistance was reduced.

Searching for methods for the plough draft resistance reduction has led to designing of the plough disk variant (Nkakini and Akor, 2012). There were attempts to reduce the plough draft resistance by changing the parameters of its mouldboards and shares (Bulgakov et al., 2019; Godwin, 2007; Shmulevich et al., 2007). However, these ploughs are not widely applicable, because they mix the upper and lower layers of arable soil horizon, which is undesirable.

Discover of the electro-hydraulic effect allowed creation of a complex of electro-hydraulic ploughs (Utkin, 1986). Utilization of these tillage implements allowed decreasing their draft resistance and promoting the assimilation of plants with different chemical elements. Primarily, the amount of dissolved forms of nitrogen increased in the soil due to electro-hydraulic influence. However, such tillage implements were and are very expensive.

Other researchers (Pavlyuk and Sotnikov, 2014) tried to decrease the plough draft resistance by using

Contact address: Volodymyr Nadykto, Tavria State Agrotechnological University, Ukraine, e-mail: volodymyr.nadykto@tsatu.edu.ua

Fig. 1 Tekrone plough mouldboards and landsides

electric osmosis, ultrasound, and magnetic field. In spite of a significant decrease in draft resistance of tillage implements, these technical decisions are not used due to their difficult implementation and high cost.

There is a cheaper option to reduce the plough draft resistance – specifically by replacing the steel surface of the mouldboard with a material that shows a lower soil friction coefficient.

Attempts to use the Teflon mouldboards were already patented in 1959 (Owen et al., 1959). Good results were obtained with the mouldboards made of polyethylene 211-07 (Kiryukhin et al., 1974). The researchers experimentally found that the draft resistance in sucha plough showed a decrease, provided its performance increased by 11% and the fuel consumptionwas reduced by 6% at minimum.

This paper presents the results of practical implementation of another method for the plough draft resistance reduction. It is essentially based on replacing of steel plough mouldboards and landsides with equipment made of Tekrone (Fig. 1).

Material and methods

Tekrone is a thermoplastic-based composite material created in Belgium. Comparison of its main physical-technical characteristics with steel 60, which is traditionally used for manufacturing of the plough mouldboards and landsides, is presented in Table 1.

Table 1 Tekrone physical-technical characteristics in comparison to steel 60

Item	Value	
	Tekrone	Steel 60
Bulk density (kg·m^{-3})	930	7800
Normalized hardness	60 (by Shor)	217 (HB)
Tensile modulus (MPa)	720	920
Tensile creep modulus (MPa)	460	590
Tensile yield strength (MPa)	17	17
Relative tensile strain (%)	20	19
Static friction coefficient (k_f)	0.20	0.52

The bulk density represents the very first indicator in which these materials significantly differ: steel 60 shows at least 8 times higher bulk density than Tekrone and thanks to this fact, steel 60 shows higher normalized hardness (see Table 1). Simultaneously, data analysis shown in Table 1 indicates that the rest of compared indicators are the same.

Aforementioned physical-technical properties of Tekrone mainly characterize the durability and reliability of the products made of it. Considering the decreasing of the plough draft resistance, the Tekrone friction coefficient (k_f) is of higher significance. The (k_f) value for new material is lower by 2.6 times than that for steel 60 (Table 1). This is largely due to the fact that Tekrone is characterised by rather low adhesion. In terms of interaction of a body with a surface of low adhesion, the friction is minimal (Abbaspour-Gilandeh et al., 2018; Poláková and Dostál, 2019). In addition to this, Tekrone shows high hydrophobic properties, which are very important during the soil ploughing with moisture of 20% and less.

All in all, this fact suggests that the plough with Tekrone mouldboards and landsides shows lower draft resistance.

In order to determine the influence of material of the mouldboards and landsides on the plough draft resistance, a strain-measuring method was utilized (Fig. 2).

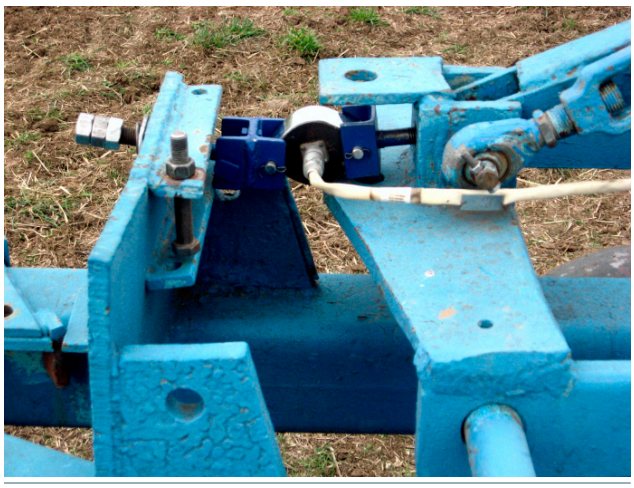

Fig. 2 Strain-measuring method applied to plough with Tekrone mouldboards and landsides

The electrical signal from the strain-measuring plough was transferred to an analogue-to-digital converter and

Fig. 3 Tractor XTZ-170 during strain measurement

then to computer. This test was conducted on a XTZ-170 series tractor equipped with an engine YMZ-236 (Fig. 3).

The strain-measuring plough was adjusted to the ploughing depth of 25 cm. The measurement quantity of this parameter was equal to 100 and the step of these measurements was equal to 0.2 m.

To determine the width of the tractor-plough set before its passage from the furrow wall at a distance *L* (during field tests, this distance equalled to 2 m), 200 pegs were installed with 1 m steps. After the tractor-plough set passed from each peg to the wall of newly laid furrow, the distances (h_i) were measured (Fig. 4).

The working width of the tractor-plough set (B_p) was calculated on the basis of the following expression:

$$B_p = L - h_i \quad (1)$$

For estimation of an inner nature of the ploughing width and depth oscillations, the normalized correlation functions and spectral density were used.

The tractor with plough moved on the same gear in all experiments. During execution of the field experimental studies, soil moisture and bulk density were measured five times.

The former was determined by means of well-known thermostat-weight method. The latter was defined utilizing the special densitometer (Nadykto and Kotov, 2015). The peculiarity of this device lies in the fact that its electronic scale immediately shows the soil bulk density in g·cm^{-3}.

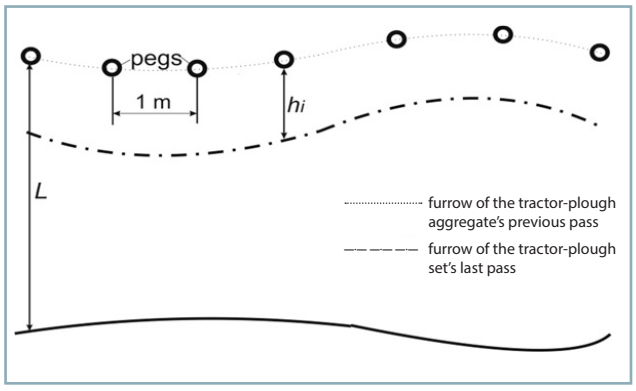

Fig. 4 Measuring scheme of the working width of tractor-plough aggregate

Fig. 5 Steel mouldboards with soil sticking

The fuel consumption was measured by means of a DFM-50C meter with 1% error margin.

Results and discussion

Typical soil type for southern Ukraine is sod-podzolic humus. Testing of the tractor-plough aggregate was carried out after winter wheat harvest. Stubble cleaning of this agricultural crop was completed a month before ploughing. The tillage depth was 5–7 cm. During the period since the stubble cleaning up to ploughing test, there was a rainfall of 10 mm. During the tractor-plough aggregate testing, winter wheat remnants and small weeds did not exceed 15 g·m^{-2}.

The soil bulk density arithmetic mean for the 0–25 cm layer was 1.21 g·cm^{-3} and the soil moisture equalled to 22.8%.

Considering the experimental conditions, wet soil was constantly being stuck to the plough steel mouldboards (Fig. 5). However, this phenomenon was not observed in terms of Tekrone mouldboards (Fig. 6).

Observation of the ploughs showed that, in case of soil sticking to the plough mouldboards, there occurs a "soil moves over soil" process, which always results in the plough draft resistance increase. Analysis of experimental data showed that utilization of the Tekrone mouldboards and landsides instead of steel ones facilitated a decrease in the

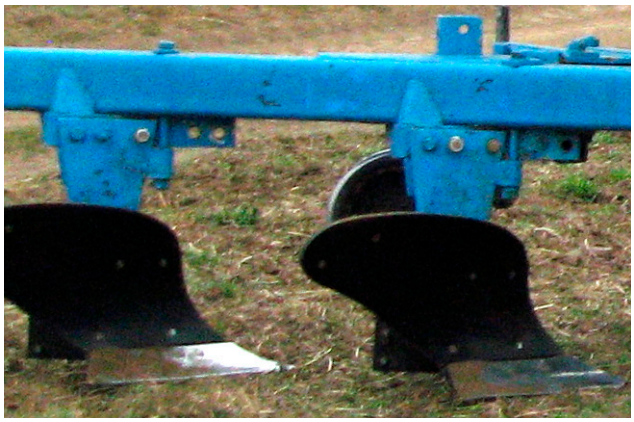

Fig. 6 Tekrone mouldboards without soil sticking

plough draft resistance. Consequently, if the plough draft resistance for the equipment made of steel 60 is 34.5 kN, it is 29.8 kN for the equipment made of Tekrone. The difference between the plough draft resistances was 4.7 kN, accounting to 13.6%. With the confidence level of 95%, it is possible to argue that this difference is significant, because it is larger than the least significant difference ($LSD_{0.5}$). In this case, the latter equals to 0.21 kN.

The draft resistance fluctuation variance of the plough with Tekrone mouldboards and landsides was equal to 6.40 kN^2; it was 8.7 kN^2 for the plough with steel equipment. However, this difference (i.e. 2.3 kN^2) is insignificant according to the *F*-test.

The variation coefficient of the draft resistance fluctuations for each plough did not exceed 9%. The plough average width of both tractor-plough aggregates was practically the same and equalled to 1.76 ±0.01 m.

In regard to the experimental data analysis, it was observed that the frequency spectrum of ploughing width oscillations was approximately the same for both tractor-plough aggregates (Fig. 7).

Therefore, the main part of the variances of these processes is concentrated in the frequency range 0–1 m^{-1}. The cut-off frequency for both normalized spectral densities was also approximately the same. The maximum of these functions took place at frequency 0.2 m^{-1}. Aforementioned observations indicate that the plough width indicators do not show any deterioration by replacing the steel mouldboards and landsides with equipment made of Tekrone.

The real ploughing depth of the plough with Tekrone equipment was changing within the 24.5 ±0.3 cm range (Table 2). The ploughing depth for the plough with steel equipment was changing within the 23.9 ±0.3 cm range.

As it is obvious from Table 2, the difference between ploughing widths is 0.6 cm, and least significant difference ($LSD_{0.5}$, cm) between these parameters is merely 0.4 cm. Consequently, the real ploughing depth of the plough with Tekrone equipment was greater.

The oscillation frequency of ploughing depth for both ploughs was estimated by normalized correlation functions of these processes. Their analysis showed (Fig. 8) that correlation length of the ploughing depth oscillations of the compared ploughs is almost the same and equals to approx. 0.9 m.

At the same time, the process of the ploughing depth oscillations produced by the plough with steel mouldboards and landsides showed a periodic component (Fig. 8). This function is described by the following equation:

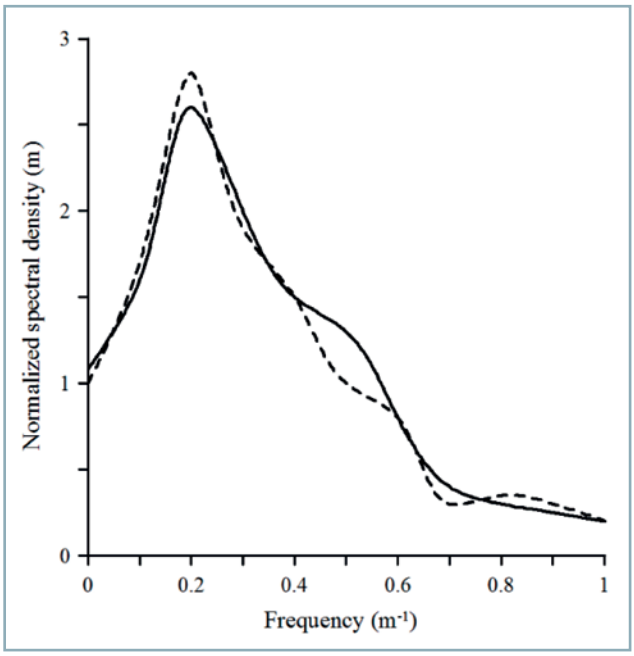

Fig. 7 Normalized spectral densities of the ploughing width oscillations of the ploughs with steel 60 (– – –) and Tekrone (—) equipments

$$R = \exp(-0.47X) \times (\cos 2X + 0.24 \sin 2X) \quad (2)$$

On the contrary, the process of the ploughing depth oscillations produced by the plough with Tekrone mouldboards and landsides did not show a periodic component and can be described as follows:

$$R = \exp(-2.05X) \times (\cos 2.5X + 0.82 \sin 2.5X) \quad (3)$$

The former is a more high-frequency process. The normalized spectral densities of the compared processes confirm this fact (Fig. 9).

The analysis of these figures showed that ploughing depth oscillation variance of the plough with steel mouldboards and landsides is distributed over a wider frequency range in contrast to the plough with Tekrone equipment. Simultaneously, in accordance with the *F*-test,

Table 2 Statistical parameters of the ploughing depth

Parameter	Plough with mouldboards and landsides made of	
	Steel	Tekrone
Average (cm)	23.9	24.5
Confidence interval (95%, cm)	23.9 ±0.3	24.5 ±0.3
Variance (cm^2)	1.80	1.51
Standard deviation (±cm)	1.34	1.23
Coefficient of variation (%)	5.6	5.0
Least significant difference ($LSD_{0.5}$, cm)	0.4	

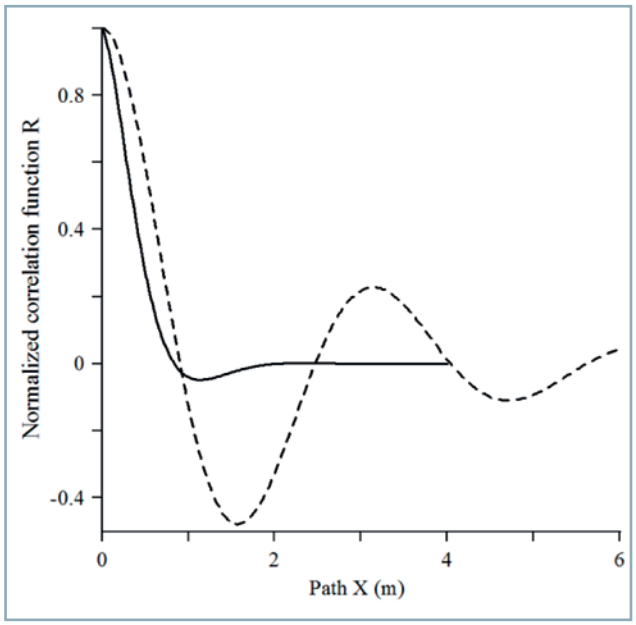

Fig. 8 Normalized correlation functions of oscillations of ploughing depth of the ploughs with steel (– – –) and Tekrone (—) equipments

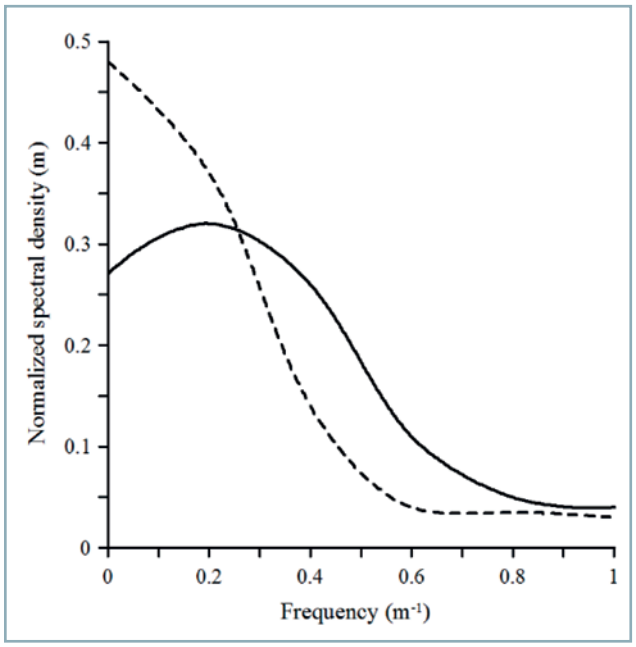

Fig. 9 Normalized spectral densities of ploughing depth oscillations of ploughs with steel (– – –) and Tekrone (—) equipments

both variances (1.80 cm^2 and 1.51 cm^2 – Table 2) represent the same random sample.

In Ukraine, the agrotechnical tolerance (Δ) of the ploughing depth oscillation equals to ±2 cm. Ploughing depth exit frequency beyond this agrotechnical tolerance can be calculated from the following formula (Panov, 2015):

$$\omega = \sqrt{\alpha^2 + \beta^2} \times \frac{1}{2\pi} \exp\left(\frac{-\Delta^2}{2D}\right) \quad (4)$$

where:

α, β – normalized spectral density approximation constants of the ploughing depth oscillations

D – variance of the ploughing depth oscillations

Considering the plough with steel mouldboards and landsides, α = 2.05, β = 2.5, and D = 1.80 cm^2. In this case, ω = 0.169 m^{-1} and the probability (P_{at}) of the maintaining agrotechnical tolerance Δ = ±2 cm amounts to 88%.

For plough with Tekrone mouldboards and landsides, α = 0.47, β = 2.0, and D = 1.45 cm^2. Consequently, ω = 0.084 m^{-1} and P_{at} = 93%.

On the basis of field results, the speed of the tractor-plough aggregate with plough Tekrone mouldboards and landsides was equal to 8.1 $km \cdot h^{-1}$. The analogical quantity for the tractor-plough aggregate steel equipment was equal to 7.2 $km \cdot h^{-1}$.

It is quite clear that such a positive difference in the work speed of the tractor-plough aggregate with Tekrone equipment results from its lower draft resistance. As a result, both tractor-plough aggregates have approximately the same plough width (1.76 m); however, they show different performance. Namely, the modernized tractor-plough aggregate was more productive in contrast to aggregate with traditional steel equipment – by 12.6% (1.43 $ha \cdot h^{-1}$ vs 1.27 $ha \cdot h^{-1}$).

The fuel consumption of the tractor-plough aggregate with the steel mouldboards and landsides was equal to 22.86 $l \cdot h^{-1}$. Simultaneously, the fuel consumption of the modernized tractor-plough aggregate was lower – 22.69 $l \cdot h^{-1}$. In regards to this, fuel consumption per hectare of the aggregate with steel equipment was equal to 22.86/1.27 = 18.00 $l \cdot ha^{-1}$ fuel consumption per hectare of the aggregate with Tekrone equipment was 22.69/1.43 = 15.87 $l \cdot ha^{-1}$.

Obviously, employment of the plough with Tekrone mouldboards and landsides instead of steel ones allowed the reduction of the specific fuel consumption by 11.8%.

Conclusion

Field experiment conducted showed that the Tekrone friction coefficient is 2.6 times lower in contrast to the friction coefficient of steel; Tekrone shows the prerequisites for employment of this composite material in the agricultural machinery, namely in production of the plough mouldboards and landsides.

The analysis of the experimental data showed that utilization of the plough with Tekrone equipment instead of steel one excludes sticking of the wet soil to it. Thereby, there occurs a process of "soil moves over plough mouldboard surface" instead of the "soil moves over soil" process.

The draft resistance of plough with Tekrone equipment decreased by 13.6%. Consequently, the performance of the novel tractor-plough aggregate increased by 12.6% and its specific fuel consumption decreased by 11.8%. At the ploughing depth (±2cm), the preserving probability of the agrotechnical tolerance increased from 88% to 93% for the plough with Tekrone equipment.

References

ABBASPOUR-GILANDEH, Y. – HASANKHANI-GHAVAM, F. – SHAHGOLI, G. – SHRABIAN, V. R. – ABBASPOUR-GILANDEH, M. 2018. Investigation of the effect of soil moisture content, contact surface material and soil texture on soil friction and soil adhesion coefficients. In Acta Technologica Agriculturae, vol. 21, no. 2, pp. 44–50.

ARAYA, K. – KAWANISHI, K. 1985. Soil failure by introducing air under pressure. In Transactions of the ASAE, vol. 27, no. 5, pp. 1292–1298.

BELOUSOV, S. V. – TRUBILIN, E. I. 2013. The development of a reversible plough design for heavy soil treatment. In Science of Kuban, no. 1, pp. 31–37. (In Russian: Razrabotka konstruktsii lemeshnogo plugadly a obrabotkity azholikh pochv)

BULGAKOV, V. – PASCUZZI, S.–ADAMCHUK, V. – IVANOVS, S. – PYLYPAKA, S. 2019. A theoretical study of the limit path of the movement of a layer of soil along the plough mouldboard. In Soil & Tillage Research, vol. 195, pp. 1–11.

GODWIN, R. J. 2007. A review of the effect of implement geometry on soil failure and implement forces. In Soil & Tillage Research, vol. 97, no. 2, pp. 331–340.

KIRYUKHIN, V. G. – CHIRKOV, G. N. – MILTSEV, A. I. 1974. Test results of plow with plastic moldboards. In Tractors and Agricultural Machines, vol. 12, pp. 19–20. (In Russian: Rezultaty i spytaniy pluzhnykh korpusov s plastmassovymi otvalami)

LOVEYKIN, V. – DYACHENKO, L. 2012. Methods of experimental investigation into parameters of vibroploughs with hydraulic vibrators. In Vestnik KHNADU, vol. 57, pp. 161–165. (In Ukrainian: Metodika eksperementalnogo doslidzhennia parametria vibropluga z gidravlichnimi vibratorami)

LUKASHOK, M. A. – KORNEV, D. V. 2009. Method of friction decrease on plow's bottom. In Almanac of Modern Research and Education, vol. 25, no.6, pp. 113–115. (In Russian: Metodsnizheniya treniya, voznika y ushegona korpusr pluga)

NADYKTO, V. – KOTOV, O. 2015. UA 97828, G 01 N/00. Method for Determining Soil Density. Ukraine.

NIYAMAPA, T. – SALOKHE, V.M. 2000. Force and pressure distribution under vibratory tillage tool. In Journal of Terramechanics, vol. 37, no. 3, pp. 139–150.

NKAKINI, S. O. – AKOR, A. J. 2012. Modeling tractive force requirements of wheel tractors for disc ploughing in sandy loam soil. In International Journal of Engineering and Technology, vol. 2, no. 10, pp. 1707–1716.

OWEN, R. R. – CYCLER, J. E. – TRIBBLE, R. T. 1959. Patent no. 2,913,060. Moldboard Plow with Plastic Resin Covering.

PANOV, A. 2015. Statistical evaluation of quality of rotary tiller performance. In VESTNIK of Federal State Educational Institution of Higher Professional Education "Moscow State Agroengineering University named after V.P. Goryachkin", vol. 66, no. 2, pp. 14–27.

PAVLYUK, A. S. – SOTNIKOV, D. V. 2014. Decreasing methods of agricultural machines draft resistance. In Polzunov Vestnik, vol. 1, no. 4, pp. 7–13 (In Russian: Metody snizheniyaty a govogosoprotivleniy a pchvo obrabatyvayuchikh mashin)

POLÁKOVÁ, N. – DOSTÁL, P. 2019. Titanium and stainless steel MIG LSC welding. In Acta Technologica Agriculturae, vol. 22, no. 2, pp. 56–59.

ROMANUK, N. N. – AGEYCHIK, V. A. – NUKESHEV, S. O. – KONDRATENYA, V. N. 2016. Original construction of mounted vibrating plow. In Actual Problems of Formation of Personnel Potential for the Innovation Development of AIC. Minsk: BSATU, pp. 353–357. Available at http://rep.bsatu.by/handle/doc/1090

SHMULEVICH, I. – ASAF, Z. – RUBINSTEIN, D. 2007. Interaction between soil and a wide cutting blade using the discrete element method. In Soil & Tillage Research, vol. 97, no. 1, pp. 37–50.

UTKIN, L. A. 1986. Electro-hydraulic effect and its application in industry. Leningrad: Mashinostroenie, 253 pp. (In Russian: Elektro-gidravlicheskiieffekt I ego primenenie v promishlennosti).

DOI: 10.2478/ata-2020-0008

Acta Technologica Agriculturae 1
Nitra, Slovaca Universitas Agriculturae Nitriae, 2020, pp. 46–52

MONITORING OF SELECTED PHYSICAL AND CHEMICAL PARAMETERS OF TEST OIL IN THE WET DISC BRAKE SYSTEM

Juraj JABLONICKÝ[1], Mirko SIMIKIĆ[2], Juraj TULÍK[1]*, Milan TOMIĆ[2], Ľubomír HUJO[1], Ján KOSIBA[1]

[1]Slovak University of Agriculture in Nitra, Slovak Republic
[2]University of Novi Sad, Serbia

Paper presented is focused on the operating measurements of a tractor wet disc brake system. Operating measurements were evaluated after tractor's operation at 500 Mth on the 3rd, 4th and 5th gear. Reference fluid and ecological fluid were tested during operation. In addition, work results include the evaluation of the fluid samples taken during the operational tests to monitor the tractor braking performance with wet disc brakes. Fluid samples were also tested in order to determine the changes in their physico-chemical properties. Chemical analysis was performed for both oil samples by means of X-ray fluorescence analysis according to the DIN 51829 and DIN 51399-2. Observed physical properties of the tested oils – density, viscosity, acid number, water content – were within the appropriate ranges after the end of test. Further analysis was focused on an amount of abrasive metals, contaminants, additives, and other important elements. On the basis of analyses conducted, it can be concluded that majority of elements preserved their original level showed at the 0 reference hour sample. In terms of the abrasion metals, an increase in their presence was not found. Furthermore, analysis of the physical properties of tested fluids did not prove their negative impact on the tractor wet disc brake system. Results of the operating measurements suggest that neither the applied conference fluid nor the ecological fluid showed negative effect on the minimum braking value. The minimum braking deceleration was implemented in accordance with the Law no. 106/2018.

Keywords: agricultural tractor; deceleration; ecological oil; physical analysis, chemical analysis

Agricultural technology has a negative impact on all elements of the environment (Kučera et al., 2016). The ever-increasing number of mobile transport devices causes air pollution and soil and water contamination with pollutants that burden the environment. It was reported that more than 60% of all lubricants end up in soil and water (Majdan et al., 2013). Together with oil and lubricant manufacturers, producers of mobile transport devices develop special products that are environmentally friendly. Application of suitable ecological oils significantly reduces the damages to the environment, sewer network and communications in case of oil leakage (Janoško et al., 2014; 2010).

Environmental protection has been topical for several years, and it becomes a preferred issue in the established trend of economic development (Majdan et al., 2018; Tóth et al., 2014; Kosiba et al., 2013). According to Janoško et al. (2016) and Čedík et al. (2018), ecological technologies and corresponding technique will become an essential part of everyday life. In addition to acceleration, there is deceleration – braking with specific type of braking system – during the movement of mobile energetic devices. Kamiński and Czaban (2012) stated that an efficient vehicle breaking system is necessary for road safety and in regards to road safety, the braking system of agricultural vehicles has to meet several requirements, including the required braking performance.

One type of brake systems that use oil fillings is called wet disc brake. Friction elements and applied oil fillings are important parts of wet disc brakes (Jablonický et al., 2019). According to Mang et al. (2010), friction is a passive resistance with the opposite direction of action as the relative movement of the friction surfaces. Merely the oil filling in disc wet brake influences the durability of friction elements, as well as the heat dissipation and factors associated with brake efficiency. As it was reported by Tkáč et al. (2014), in practice, mineral oils, synthetic fluids and ecological fluids are the most used for the purposes of gear lubrication and energy transfer. According to Hujo (2017), Hujo et al. (2015), Tulík (2013), Dostál et al. (2019), Hlaváč et al. (2019), the viscosity, viscosity index, stability, oxidation, compressibility and shear stability are key physical properties of fluid in terms of lubrication and energy transfer. The viscosity may decrease or increase during the oil utilization. Helebrant et al. (2001) reported that an increase in viscosity may be caused mainly by oxidation of products or oil contamination. On the contrary, its decrease is mainly caused by mechanical and thermal degradation of the additives. In relation to viscosity, Stopka (2018) pointed out that low viscosity in oils provides a thin lubricating film, resulting in limited lubrication conditions. This leads to metal-to-metal contact and damage of the system components. When two moving metal surfaces get into contact due to insufficient lubrication, excessive wear can occur due to cold

Contact address: Juraj Tulík, Slovak University of Agriculture in Nitra, Faculty of Engineering, Department of Transport and Handling, Slovakia, e-mail: juraj.tulik@uniag.sk

welding and thus damage of the components. Aim of this paper was to provide the operating measurement of the wet braking system of tractor Zetor Super 5321. Furthermore, a reference oil sample and ecological oil were also tested. The results were compared in accordance with the established methodological procedure. Subsequently, the braking effect of the tractor's wet disc brakes was evaluated, and the physical properties of the oil fillings used were tested. Testing of these oils was to demonstrate whether it is possible to fully replace the reference oil sample with ecological oil and what impact the wet brakes have on the tractor in terms of the degradation processes in the tested oils.

Material and methods

Characteristics of the reference fluid

The reference fluid was mineral oil with additives for increasing of the load-carrying of lubricating film. Basic parameters of the reference fluid are shown in Table 1. It guarantees good lubrication properties, high resistance to oxidation and high load-carrying capacity. The reference fluid is intended for lubrication of mechanical transmissions in vehicles and drive axles requiring properties like SAE 80W – 90 with performance level API GL. It is intended for lubrication of vehicles working under demanding operational conditions and suitable for lubrication of mechanical gearboxes and axle drives of vehicles and trucks, construction machines, agricultural machinery, and other gear applications.

Table 1 Basic parameters of the reference fluid

Properties	Units	Values
Density at 40 °C	$kg \cdot m^{-3}$	878
Kinematic viscosity at 40 °C	$mm^2 \cdot s^{-1}$	146
Kinematic viscosity at 100 °C	$mm^2 \cdot s^{-1}$	15
Viscosity index	–	103
Freezing point	°C	-27

Characteristics of the ecological fluid

Ecological fluid was ecological universal synthetic tractor oil. Basic parameters of the ecological fluid are shown in Table 2. It is intended for manual gearboxes, axle drives transmission and gear power take-off shafts, steering gears, hydraulic systems of tractors and their equipment, wet brakes, clutches and hydrodynamic gears.

Table 2 Basic parameters of the ecological fluid*

Properties	Units	Values
Density at 40 °C	$kg \cdot m^{-3}$	899
Kinematic viscosity at 40 °C	$mm^2 \cdot s^{-1}$	80
Kinematic viscosity at 100 °C	$mm^2 \cdot s^{-1}$	15
Viscosity index	–	202
Freezing point	°C	-48

* The physico-chemical analysis was carried out in accredited laboratory of Klüber Lubrication

Methodology of service brake measurement

The service brake was controlled according to the Methodological Instruction of the Slovak Republic Act. No 106/2018, which states the inspection operations related to the vehicle braking system. The measurement purpose was to determine the maximum deceleration of the tractor's oil brakes. Under the prescribed conditions, the tractor-type vehicle must be capable of achieving the minimum braking effect prescribed by the brake deceleration (z_{min}). Evaluation of the set of measured values on the basis of the service brake measurement on the tractor Zetor 5321 was performed by means of mathematical and statistical analysis and software STATISTICA version 12. Mathematical and statistical data for oils fillings included:

- determination of the number of required experiment repetitions;
- extreme value test;
- conformity test of the sample with constant;
- conformity test of the sample – Pearson χ^2 test;
- determination of hypotheses to assess the impact of tested oils on the system of wet disc brakes.

Values of braking deceleration were monitored by XL-meter. The XL-meter measures with accuracy of ±1%. The expanded uncertainty for XL-meter was determined for expansion coefficient $k = 2$ with 95% probability. Statistical methods were considered with a significance level $\alpha = 0.05$.

For a comprehensive assessment of the test oil and for the purpose of assessing the effect of ecological oil on the service brake efficiency, the measurements were performed after operation at 500 Mth with three gears engaged.

Therefore, the value of deceleration was monitored during sequential shifting of the 3rd, 4th and 5th gears in the Zetor Super 5321 tractor. As a brake oil filling, the reference oil filling was used, which was replaced by ecological fluid on the service interval.

On the basis of reference measurements of the braking effect of the service brake with the original oil filling, it was possible to make comparisons with data obtained from ecological oil filling measurements.

Considering the 3rd and 4th gears, the tractor did not exceed 25 $km \cdot h^{-1}$ and thus the deceleration results were compared with the minimum deceleration $z_{min} = 23\%$.

By shifting to the 5th gear, according to the manufacturer, Zetor Super 5321 achieves a maximum speed of 30 $km \cdot h^{-1}$; therefore, the deceleration results were compared with a minimum deceleration of $z_{min} = 28\%$.

Sampling of the tested hydraulic fluid was performed in accordance with the standard STN 65 6207. After the operational test, the physical properties and chemical analyses of the tested oils were evaluated. The evaluation focused on changes in the amount of water content, total acid number, density and kinematic viscosity after operation at 0, 250 and 500 Mth. Oil viscosity and density measurements were performed by means of the Stabinger viscometer "Anton Paar" STN EN 16896. The total acid number (TAN) is used to determine the quantity of acidic components in the oil sample. Specification of changes in TAN was performed according to the ASTM D644 A. The water content in oils was measured according to Karl Fischer titration (KF). Monitoring of chemical elements in the tested oils was performed by

means of X-ray fluorescence analysis according to DIN 51829 and DIN 51399-2. The physico-chemical analysis was carried out at accredited laboratory of Klüber Lubrication by means of test devices that are regularly calibrated and have the required measurement accuracy.

Results and discussion

Values of minimum braking deceleration using reference fluid

On the basis of achieved results, it can be stated that the minimum values of deceleration at 500 Mth given by the legislation were exceed by 2.70% at the 3rd gear and by 10% at the 4th gear. With the 5th gear engaged, the tractor exceeds the deceleration value determined by the legislation by 6.50%. The average results of three consecutive measurements at each gear after 500 Mth are shown in Table 3.

Values of minimum deceleration using ecological fluid

On the basis of obtained results shown in Table 4, it can be stated that, in contrast to deceleration values specified by legislation, the minimum deceleration values after 500 Mth were exceed by 9.60% at the 3rd gear and by 9.10% at the 4th gear. Considering the 5th gear, the tractor exceeded the minimum deceleration value by 1.35%. The average results of three consecutive measurements at each gear after 500 Mth are shown in Table 4.

Values of braking deceleration were measured at 0; 250; and 500 Mth; however, paper presented takes into account only braking deceleration values at 500 Mth, because the oil change interval of tractor Zetor 5321 is 500 Mth.

In relation to the physico-chemical analyses of reference and ecological oil, oils samples were taken at 0; 250; and 500 Mth in order to determine trends and potential oil degradation.

Average braking deceleration was calculated on the basis of EHK Regulation no. 13 as follows:

$$MFDD = \frac{v_b^2 - v_e^2}{25.92(s_e - s_b)} \quad \text{m·s}^{-2} \tag{1}$$

where:
v_o – initial vehicle speed, km·h^{-1}
v_b – vehicle speed at 0.8 v_0, km·h^{-1}
v_e – vehicle speed at 0.1 v_0, km·h^{-1}
s_b – distance travelled between v_0 and v_b, m
s_e – distance travelled between v_0 and v_e, m

Evaluation and analysis of physical properties of tested oils – changes in density at 40 °C and 100 °C

Fig. 1 shows the course of the density of tested oils at 40 °C depending on the tractor hours worked; Fig. 3 shows the course of the density of tested oils at 100 °C depending on the tractor hours worked.

Evaluation and analysis of physical properties of tested oils – kinematic viscosity change

The values of kinematic viscosity (Figs. 2 and 4) are translated by linear function. For the reference sample, linear function of kinematic viscosity at 40 °C can be calculated using Eq. 2 and at 100 °C using Eq. 3:

$$v_{40} = -0.0237t + 145.28 \quad \text{mm}^2\text{·s}^{-1} \tag{2}$$

$$v_{100} = -0.0045t + 15.154 \quad \text{mm}^2\text{·s}^{-1} \tag{3}$$

where:
t – number of tractor hours worked, Mth

Table 3 Measured values of the braking deceleration using reference

	3rd gear	4th gear	5th gear	Units
Braking path, s_0	3.59	5.12	11.26	m
Initial speed, v_0	12.11	19.52	29.94	km·h^{-1}
Braking time, T_{br}	1.75	1.81	3.30	s
Braking deceleration, *MFDD	2.52	3.24	3.39	m·s^{-2}
Deceleration, *z*	25.70	33.00	34.50	%

* *MFDD* – average values of braking deceleration

Table 4 Measured values of the braking deceleration using ecological oil

	3rd gear	4th gear	5th gear	Units
Braking path, s_0	2.50	6.67	18.10	m
Initial speed, v_0	12.47	19.96	29.97	km·h^{-1}
Braking time, T_{br}	1.30	2.10	3.26	s
Braking deceleration, *MFDD	3.20	3.15	2.88	m·s^{-2}
Deceleration, *z*	32.60	32.10	29.35	%

* *MFDD* – average values of braking deceleration

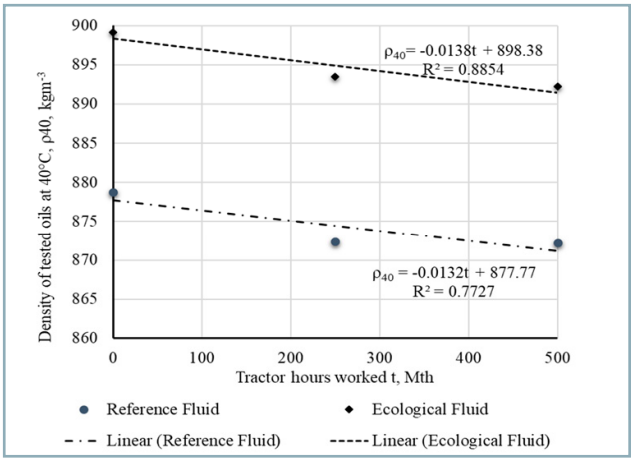

Fig. 1 Density course of tested fluids at 40 °C depending on the number of tractor hours worked

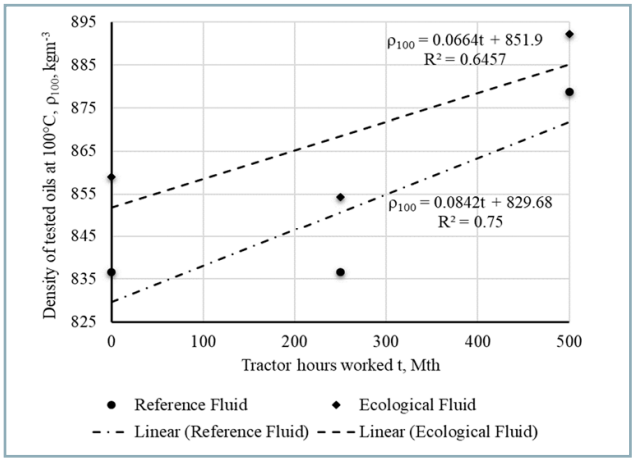

Fig. 3 Density course of tested fluids at 100 °C depending on the number of tractor hours worked

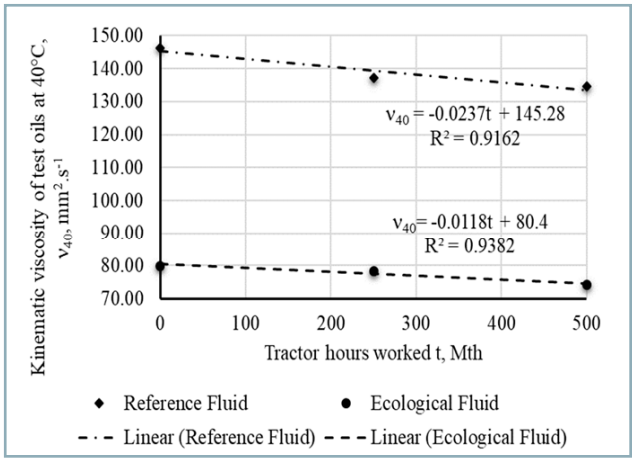

Fig. 2 Kinematic viscosity course of tested fluids at 40 °C depending on the number of tractor hours worked

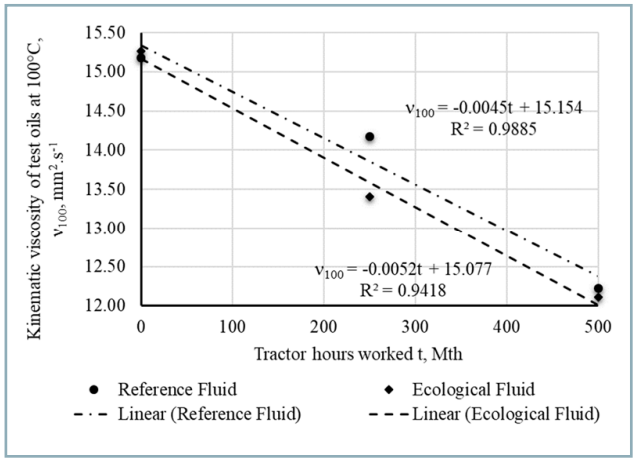

Fig. 4 Kinematic viscosity course of tested fluids at 100 °C depending on the number of tractor hours worked

For the ecological sample, linear function of kinematic viscosity at 40 °C can be calculated by means of Eq. 4 and at 100 °C by means of Eq. 5:

$$\nu_{40} = -0.0118t + 80.4 \quad mm^2 \cdot s^{-1} \tag{4}$$

$$\nu_{100} = -0052t + 15.077 \quad mm^2 \cdot s^{-1} \tag{5}:$$

where:
t – number of tractor hours worked, Mth

The course of viscosity at 100 °C is due to the activation of specific elements, which are contained in the organic oil, caused by increased temperature.

Evaluation and analysis of physical properties of tested oils – acid number change

Fig. 5 shows the dependence of the acid number of tested oils on the number of tractor hours worked. The values of acid number are translated by linear function. Linear function of acid number for the reference sample can be calculated by equation Eq. 6, and by Eq. 7 for the ecological fluid:

$$tan = -0.0004t + 0.36 \quad mm^2 \cdot s^{-1} \tag{6}$$

$$tan = -0.0002t + 0.5667 \quad mm^2 \cdot s^{-1} \tag{7}$$

where:
t – number of tractor hours worked, Mth

For the purpose of observation of changes in acid number, the samples were collected with weight ranging from 0.35 g to 0.55 g for both oils, with weighing accuracy of 0.10 g. The values correspond to the acid number range from 0.05 to <1.0 mg·KOH·g^{-1}. Both oils showed results within the tolerance given by legislation a thus it can be concluded that no degradation process occurred after 500 Mth operation.

Evaluation and analysis of physical properties of tested oils – change in water content

The water content values (Fig. 6) are translated by linear function, which can be calculated by Eq. 8 for the reference sample, and by Eq. 9 for the ecological sample:

$$S_{H_2O} = -2 \times 10^{-6}t + 0.0038 \quad \% \tag{8}$$

$$S_{H_2O} = -2 \times 10^{-6}t + 0.0212 \quad \% \tag{9}$$

where:
t – number of tractor hours worked, Mth

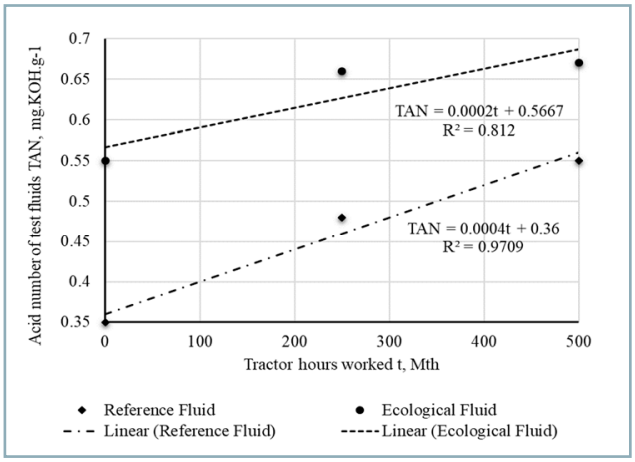

Fig. 5 Acid number course of tested fluids depending on the number of tractor hours worked

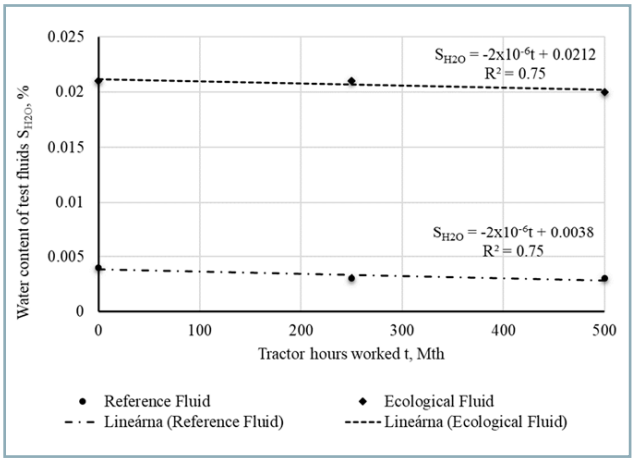

Fig. 6 Water content course of tested fluids depending on the number of tractor hours worked

Fig. 6 shows dependence of the changes in water content in tested oils on the number of engine hours worked. On the basis of laboratory analysis of tested oil, it is possible to conclude that the upper limit of water content in oils was not exceeded. The water content coefficient for both oils tested is $R^2 = 0.75$. The maximum permissible water content is 0.1% in hydraulic oils and 0.3% in gear oils.

The sampling and evaluation of oil samples were carried out by an employee from an accredited laboratory of Klüber Lubrication. Samples were taken from the system of wet

Table 5 X-ray fluorescence analysis (Oilquant.) – analysis of basic particles for reference and ecological oils

	Chemical element	Symbol	Units	Sampling interval					
				reference oil			ecological oil		
				0 h	250 h	500 h	0 h	250 h	500 h
Wear metals	aluminium	Al	mg·kg^{-1}	<10.0	<10.0	<10.0	<10.0	<10.0	<10.0
	molybdenum*	Mo	mg·kg^{-1}	<10.0	<10.0	<10.0	<10.0	<10.0	<10.0
	tin	Sn	mg·kg^{-1}	<10.0	<10.0	<10.0	<10.0	<10.0	<10.0
	titan	Ti	mg·kg^{-1}	<10.0	<10.0	<10.0	<10.0	<10.0	<10.0
	nickel	Ni	mg·kg^{-1}	<10.0	<10.0	<10.0	<10.0	<10.0	<10.0
	chrome	Cr	mg·kg^{-1}	<10.0	<10.0	<10.0	<10.0	<10.0	<10.0
	cooper	Cu	mg·kg^{-1}	<10.0	<10.0	<10.0	<10.0	10	10
	iron	Fe	mg·kg^{-1}	<10.0	<10.0	<10.0	<10.0	<10.0	10
	lead	Pb	mg·kg^{-1}	<10.0	<10.0	<10.0	<10.0	<10.0	<10.0
	zinc*	Zn	mg·kg^{-1}	<10.0	<10.0	<10.0	22	<10.0	<10.0
Contaminants	silicon*	Si	mg·kg^{-1}	<10.0	<10.0	<10.0	62	48	52
	sodium	Na	mg·kg^{-1}	<50.0	<50.0	<50.0	<50.0	<50.0	<50.0
	potassium	K	mg·kg^{-1}	<10.0	<10.0	<10.0	<10.0	<10.0	<10.0
Additives	barium	Ba	mg·kg^{-1}	<10.0	<10.0	<10.0	<10.0	<10.0	<10.0
	magnesium	Mg	mg·kg^{-1}	<10.0	<10.0	<10.0	<10.0	<10.0	<10.0
	phosphorus	P	mg·kg^{-1}	129	226	253	143	187	198
	zircon	Zr	mg·kg^{-1}	<10.0	<10.0	<10.0	<10.0	<10.0	<10.0
	calcium	Ca	mg·kg^{-1}	<10.0	<10.0	<10.0	<10.0	<10.0	<10.0
Others important elements	manganese	Mn	mg·kg^{-1}	<10.0	<10.0	<10.0	<10.0	<10.0	<10.0
	chlorine	Cl	mg·kg^{-1}	<20.0	<20.0	<20.0	<20.0	<20.0	<20.0
	sulphur	S	mg·kg^{-1}	14,460	18,170	18,336	825	4,190	4,230

* Element that can serve also as an additive

disc brakes of tractor Zetor 5321 after specified number of tractor hours worked. Sampling was performed only once in accordance with the methodological procedure of STN 65 6207. The laboratory performed three consecutive measurements of the physico-chemical properties of tested oils, on the basis of which the arithmetic means were calculated. Evaluated samples were translated by linear function with an appropriate coefficient R^2, which is shown in Figs. 1–6. On the basis of the coefficient of determination R^2, it would be possible to state that the linear functions are not suitably selected and if the individual measurement points were translated by polynomial function, the coefficient of determination would reach the value R^2 = 1.00. Due to the scarcity of data, utilization of a polynomial function of the first degree would by physically inaccurate. The polynomial would pass through all points with the determination coefficient R^2 = 1.00, which might seem like a suitable function; however, the linear function has a greater informative value in this case.

Both oils showed only minor changes in their physical properties. The connection of points would not be appropriate, because there would be no trend of increasing or decreasing in observed physical and chemical properties of tested oils after oil change interval.

Evaluation of chemical analysis of tested oils in wet disc brake system

In addition to the monitoring of physical properties, an X-ray fluorescence analysis was performed. During operation, mechanical wear occurs in the tractor's hydraulic system and thus the abrasive particles are produced. Their production is a natural effect, which is unavoidable under practical conditions. A certain small amount of wear particles can also be found in a new oil, since additives may contain these in this case. However, if the particle size increases significantly, it may indicate an issue or malfunction of any part of the hydraulic system or – as in this case – wet brake system. The X-ray fluorescence analysis (Oilquant.) according to the DIN 51829 and DIN 51399-2 was aimed at the concentration determination of important chemical elements in the reference and ecological oils (Table 5).

The samples collected in operational tests were also subjected to X-ray fluorescence analysis. The analysis was focused on testing of reference oil and ecological oil in terms of the content of abrasive metals, contamination, additives and others important elements (Table 5). On the basis of performed analysis, it is possible to conclude that the majority of elements remained at original level of the reference sample (0 tractor hours worked). Considering the content of abrasive metals, increase in their occurrence was not observed. In terms of contaminants, only silicon was activated as additive, and in terms of additives, only a negligible increase in phosphorus was observed. Sulphur was a significant element that was activated, which also serves as protection against wear and abrasion, as well as a source of base oil.

Conclusion

Operational measurements of the wet disc brake system in Zetor Super 5321 were determined.

Two types of oil fillings were tested – a reference oil sample and an ecological oil.

Results of the operational measurements evidence that neither the reference fluid nor the ecological fluid had negative impact on the minimum braking value. Test results in form of graphical dependencies described the changes in physical properties of tested oils. The courses of the individual curves were translated by linear functions with specification of the determination coefficient. Values of the determination coefficient and calculated mean error of the correlation coefficient sr confirmed the reliability of the correlation coefficient, which is a purity measure of tested oils. The correlation coefficient – which characterizes the degree of contamination of the tested oils in this case – confirms the results of analyses in terms of the physical oil properties. At the end of test, both oils showed only minor changes in their physical properties; they did not show any corrosion and negative impacts on the wet brake system of Zetor Super 5321. This was confirmed by the chemical analysis of tested oils according to the DIN 51829 and DIN 51399-2. Furthermore, oil samples were also subjected to X-ray fluorescence analysis, which was carried out at an accredited laboratory Klüber Lubrication. The analysis was aimed at testing of both oils in terms of content determination of abrasive metals, contaminants, additives and other important elements. On the basis of performed analysis, it can be concluded that majority of the elements remained at the original level of the reference 0 hour sample. Considering the abrasive metals, no increase in their values was not observed. In terms of contamination, only silicon was activated as additive. In regards to additives, only the increase in phosphorus in a negligible amount was observed. Considering the important elements, only sulphur was activated; it serves as a protection against wear and abrasion, as well as a source for the base of ecological oil. Experiment conducted confirmed that the ecological oil shows comparable properties to reference oil. Both oils showed only minor changes in their physical properties after completion of operational and laboratory tests. They did not cause corrosion and had no negative impact on the wet brakes system used in tractor Zetor 5321. The results of operational tests and subsequent physico-chemical analysis of samples may serve as a background material for design and development of friction materials used in wet disc brakes system and oil fillings for this type of brakes system. Tested ecological oil is a suitable substitute for conventionally made oils, especially when tractor works in environmentally sensitive areas. The issue of practical measurement of the wet disc brakes system in tractors with application of ecological oil are new and no authors have dealt with it yet. In terms of approving the technical condition of braking systems, merely the braking deceleration is evaluated according to Law no. 106/2018 and the impact of applied oils on properties, such as friction materials, contamination of oil fillings and their influence on values of braking deceleration, are not taken into account. From this point of view, the results can be considered original. The research was focused on potential negative effects of used ecological oil on the wet disc brakes system. Considering the ecological oil application, attention was focused on safety in terms of the minimum braking

deceleration and degradation of friction materials, which was monitored by physico-chemical analyses.

Acknowledgment

This work was supported by AgroBioTech Research Centre built in accordance with the project "Building the AgroBioTech Research Centre" ITMS 26220220180.

This work was supported by the project VEGA 1/0155/18 "Applied Research of the Use of Ecological Energy Carriers in Agricultural, Forestry and Transport Technology".

References

ASTM D644. 2015. Standard test method for acid number of petroleum products by potentiometric titration. Hach Company/ Hach Lange GmbH.

ČEDÍK, J. – PEXA, M. – PETERKA, B. – HOLUBEK, M. – MADER, D. – PRAŽAN, R. 2018. Effect of biobutanol-sunflower oil-diesel fuel blends on combustion characteristics of compression ignition engine. In Acta Technologica Agriculturae, vol. 21, no. 4, pp. 130–135.

DIN 51399-2. 2010. Testing of lubricants – Determination of elements content of additives, wear and other contaminations. Part 2: Wavelength dispersive X-ray fluorescence spectrometry (XRF).

DIN 51829. 2010. Petroleum products – Determination of additive and wear elements in greases – Analysis by wavelength dispersive X-ray fluorescence spectrometry.

DOSTÁL, P. – ROZLIVKA, J. – KUMBÁR, V. 2019. Operational degradation of engine oil in agricultural technology. In Acta Technologica Agriculturae, vol. 21, no. 1, pp. 17–21.

EHK Regulation No 13 of the Economic Commission for Europe of the United Nations (UN/ECE). 2015. Uniform provisions concerning the approval of vehicles of categories M, N and O with regard to braking, [2016/194], 2015.

HELEBRANT, F. – ZIEGLER, J. – MARASOVÁ, D. 2001. Technical Diagnostic and Reliability I. Tribodiagnostic. Ostrava : VŠB – Technical University of Ostrava. (In Czech: Diagnostika a spolehlivost I. Tribodiagnostika)

HLAVÁČ, P. – BOŽIKOVÁ, M. – PETROVIĆ, A. 2019. Selected physical properties assessment of sunflower and olive oils. In. Acta Technologica Agriculturae, vol. 21, no. 3, pp. 86–91.

HUJO, Ľ. – KANGALOV, P. G. – KOSIBA, J. 2015. Laboratory test devices for evaluating the lifetime of tractor hydraulic components: proceedings, methods and applications. Ruse : Angel Kanchev University of Ruse, 69 pp. (scientific monograph)

HUJO, Ľ. 2017. Design of Laboratory Test Device for Testing of Hydrostatic Transducers and Hydraulic Fluids Used in Mobile Energy Devices. Nitra : Slovak University of Agriculture in Nitra, 158 pp. (In Slovak: Návrh laboratórneho zariadenia pre skúšanie hydrostatických prevodníkov a hydraulických kvapalín využívaných v mobilních energetických prostriedkoch)

JABLONICKÝ, J. – OPÁLENÝ, P. – UHRINOVÁ, D. – TULÍK, J. – SAVIN, L. 2019. Influence of ecological fluid on the wet disc brake system of the tractor. In 7th International Conferencie on Trends in Agricultural Engineering 2019, Prague, pp. 218–224.

JANOŠKO, I. – ČERNECKÝ, J. – BRODNIANSKA, Z. – HUJO, Ľ. 2016. Environmental Technologies and Engineering. Nitra : Slovak University of Agriculture in Nitra, 306 pp. (In Slovak: Environmentálne technológie a technika)

JANOŠKO, I. – POLONEC, T. – LINDÁK, S. 2014. Performance parameters monitoring of the hydraulic system with bio-oil. In Research in Agricultural Engineering, vol. 60, special issue, pp. 37–43.

JANOŠKO, I. – ŠIMOR, R. – CHRASTINA, J. 2010. The bio-oil testing used in the hydraulic system of the vehicle for waste collection. In Acta Technologica Agriculturae, vol. 13, no. 4, pp. 103–108.

KAMIŃSKI, Z. – CZABAN, J. 2012. Diagnosing of the agricultural tractor braking system within approval tests. In Eksploatacja i Niezawodnosc – Maintenance and Reliability, vol. 14, no. 4, pp. 319–326.

KOSIBA, J. – TKÁČ, Z. – HUJO, Ľ. – STANČÍK, B. – ŠTULAJTER, I. 2013. The operation of agricultural tractor with universal ecological oil. In Research in Agricultural Engineering, vol. 59, special issue, pp. 27–33.

KUČERA, M. – ALEŠ, Z. – PEXA, M. 2016. Detection and characterization of wear particles of universal tractor oil using a particles size analyser. In Agronomy Research, vol. 14, no. 4, pp. 1351–1360.

Law No. 106/2018. Law on the operation of vehicles in road traffic and on amendments to certain Acts.

MAJDAN, R. – OLEJÁR, M. – ABRAHÁM, R. – ŠAREA, V. – UHRINOVÁ, D. – JÁNOŠOVÁ, M. – NOSIAN, J. 2018. Pressure source analysis of a test bench for biodegradable hydraulic oils. In Tribology in Industry, vol. 40, no. 2, pp. 183–194.

MAJDAN, R. – TKÁČ, Z. – KANGALOV, P. G. 2013. Research of Ecological Oil-Based Fluids Properties and New Test Methods for Lubrication Oils. Ruse : Angel Kanchev University of Ruse, 98 pp. (scientific monograph)

MANG, T. – BOBZIN, K. – BARTELS, T. 2010. Industrial Tribology: Tribosystems, Friction, Wear and Surface Engineering, Lubrication. Wiley, 672 pp. ISBN: 978-3-527-32057-8.

STN 65 6207. 1986. Hydraulic oils and liquids. Sampling for determination of mechanic impurities.

STN EN 16896. 2017. Petroleum products and related products – Determination of kinematic viscosity – Method by Stabinger type viscosimeter.

STOPKA, J. 2018. Lubrications and environment. In Tribotechnika, pp. 46–49. (In Slovak: Mazivá a životné prostredie)

TKÁČ, Z. – MAJDAN, R. – KOSIBA, J. 2014. Research of Properties of Ecological Fluids and New Testing Method of Lubricating Oils. Nitra : Slovak University of Agriculture in Nitra., 94 pp. (In Slovak: Výskum vlastností ekologických kvapalín a nových testovacích metód mazacích olejov)

TÓTH, F. – RUSNÁK, J. – KADNÁR, M. – VÁLIKOVÁ, V. 2014. Study of tribological properties of chosen types of environmentally friendly oils in combined friction conditions. In Journal of Central European Agriculture, vol. 15, no. 1, pp. 185–192.

TULÍK, J. 2013. Analysis of hydraulic fluids properties used in hydraulic systems of transport and handling technics. Nitra : Slovak University of Agriculture in Nitra. (In Slovak: Analýza vlastností hydraulických kvapalín používaných v hydraulických systémech dopravnej a manipulačnej techniky) (PhD thesis)